

https://dspace.org/

Elucidating the Role of Cholesterol Pathways in the Epithelial-to Mesenchymal Transition in Breast Cancer Cells

Perumal, Shanen

2023-10
University of the Witwatersrand, Johannesburg
https://hdl.handle.net/10539/48730
Perumal, Shanen. (2023). Elucidating the Role of Cholesterol Pathways in the Epithelial-to Mesenchymal Transition in Breast Cancer Cells. [PhD thesis, University of the Witwatersrand, Johannesburg]. WIReDSpace. https://hdl.handle.net/10539/48730

Downloaded from a DSpace repository. https://dspace.org/



UNIVERSITY OF THE
WITWATERSRAND,
JOHANNESBURG

Elucidating the Role of Cholesterol Pathways in the Epithelial-to-Mesenchymal Transition in Breast Cancer Cells

by

Shanen Perumal

(705672)

Thesis

Submitted in fulfilment of the requirements for the degree

Doctor of Philosophy

in

Molecular and Cell Biology

in the Faculty of Science, University of the Witwatersrand, Johannesburg, South Africa

Supervisor: Professor Mandeep Kaur

October 2023

Table of Contents

DECLARATION vi

ACKNOWLEDGEMENTS vii

LIST OF FIGURES viii

LIST OF TABLES ix

LIST OF ABBREVIATIONS x

LIST OF SYMBOLS xiii

RESEARCH OUTPUTS xiv

ABSTRACT 1

Chapter 1: INTRODUCTION AND LITERATURE REVIEW 2

1.1 Breast Cancer 2

1.1.1 Epidemiology 2

1.1.2 The Hallmarks of Cancer 2

1.1.3 Breast Cancer Classification 3

1.1.4 Detection and Diagnosis of Breast Cancer 5

1.1.5 Breast Cancer Treatment Strategies 5

1.1.6 Metastasis 7

1.2 The Epithelial to Mesenchymal Transition 8

1.2.1 The EMT Regulatory Network 9

1.2.2 The TGFβ Signalling Pathway 11

1.2.3 Wnt signalling 13

1.2.4 Notch signalling 14

1.2.5 EMT in Invasion and Metastasis 15

1.2.6 EMT in Drug Resistance 16

1.3 Cholesterol and its Role in Cancer 18

1.3.1 Cholesterol Synthesis 19

1.3.2 Cholesterol Transport and Homeostasis 21
1.3.3 The Link Between Cholesterol and Cancer 23
1.3.4 Cholesterol in EMT and Metastasis 26
1.3.5 Statins and Their Use in Cancer Treatment 27
1.3.6 Alternatives to Statins for Lowering Cholesterol 29
1.4 Problem Statement 32
1.5 Aims and Objectives 33
2.1 Aims 33
2.2 Objectives 33
Chapter 2: MATERIALS AND METHODS 34
2.1 Cell Culture 34
2.2 EMT Induction 34
2.3 Cell Counting 34
2.4 Cholesterol-Lowering Treatment 35
2.5 Microscopy Sample Preparation 36
2.6 Immunocytochemistry 36
2.7 Filipin Staining 39
2.8 BODIPY Lipid Droplet Staining 40
2.9 Vybrant Alexa Fluor 594 Lipid Raft Staining 40
2.10 Quantification of Fluorescence Intensity 41
2.11 Cholesterol Quantitation Assay 41
2.12 Invasion Assay 42
2.13 Cell Viability Assay 43
2.14 RNA Extraction 44
2.15 Assessing RNA Purity and Integrity 45
2.16 cDNA synthesis 46
2.17 Reverse Transcriptase Quantitative Polymerase Chain Reaction 47

2.18 Protein Extraction and Quantification 50
2.19 SDS-PAGE 51
2.20 Western Blotting 53
2.21 Statistics and Data Analysis 55
Chapter 3: RESULTS 56
3.1 TGFβ treatment induces a mesenchymal-like morphology in NMuMG cells 56
3.2 Qualitative changes in EMT marker protein expression in NMuMG cells following TGFβ treatment 56
3.3 Quantitative changes in EMT marker protein expression in NMuMG cells following TGFβ treatment 58
3.4 Evaluation of Ki-67 fluorescence in response to EMT induction 59
3.5 Changes in cholesterol levels in NMuMG cells following TGFβ treatment 60
3.6 Changes in cell viability in response to treatment with cholesterol-lowering compounds 62
3.7 Changes in free cholesterol following treatment with cholesterol-lowering compounds 63
3.8 Changes in CEs following treatment with cholesterol-lowering compounds 64
3.9 Changes in lipid raft cholesterol following treatment with cholesterol-lowering compounds 67
3.10 Cholesterol-lowering compounds reduce invasive potential of TGFβ-treated cells 67
3.11 Cholesterol-lowering compounds increase E-cadherin and reduce Vimentin post-EMT 69
3.12 Cholesterol-lowering compounds reduce N-cadherin fluorescence post-EMT. 72
3.13 Changes in EMT pathway gene expression in response to cholesterol depletion 73
3.14 Changes in cholesterol pathway gene expression in response to cholesterol depletion 76
Chapter 4: DISCUSSION 78

4.1 TGFβ-mediated induction of EMT in NMuMG cells 79
4.2 Changes in cholesterol levels in NMuMG cells following EMT induction 83
4.3 The effects of cholesterol depletion on the EMT phenotype 86
CONCLUSIONS 93
LIMITATIONS 94
FUTURE STUDIES 95
REFERENCES 96
SUPPLEMENTARY MATERIAL 115

DECLARATION

I, Shanen Perumal (705672), am a student registered for the degree of Doctor of Philosophy in Science (Molecular and Cell Biology) in the academic years 2019-2023.

I hereby declare the following:

- I am aware that plagiarism (the use of someone else's work without their permission and/or without acknowledging the original source) is wrong.
- I confirm that the work submitted for assessment for the above degree is my own unaided work except where explicitly indicated otherwise and acknowledged. In this context, I understand that the use of editing services is considered aided work and must be declared.
- I have not submitted this work before for any other degree or examination at this or any other University.
- The information used in the Thesis has not been obtained by me while employed by, or working under the aegis of, any person or organization other than the University.
- I have followed the required conventions in referencing the thoughts and ideas of others.
- I understand that the University of the Witwatersrand may take disciplinary action against me if there is a belief that this is not my own unaided work or that I have failed to acknowledge the source of the ideas or words in my writing.

NRF Declaration

The financial assistance of the National Research Foundation (NRF) (grant number: 118425) towards this research is hereby acknowledged.

Opinions expressed and conclusions arrived at, are those of the author and are not necessarily to be contributed to the NRF.

Signed:  on the 10th day of October 2023

ACKNOWLEDGEMENTS

I would like to thank the following people and institutions for providing support during the process of my research:

To Professor Mandeep Kaur: Thank you for your support, patience, and guidance throughout my Master's degree and PhD. I have been under your supervision for 6 years and have learnt countless valuable lessons.

To Dr Theresa Vincent, Dr Varsha Prakash, colleagues, and friends at Uppsala University: Thank you for welcoming me to your country and lab. I appreciate the guidance and training that I received while working in Uppsala. I am also grateful to all the friend I made inside the lab and out, who made my visit both productive and fun.

To my family and friends, thank you for your support throughout the years. I would not be where I am without you. A special thank you to my mother, who has encouraged and supported me without question for as long as I can remember.

A special thank you goes to the most understanding and supportive girlfriend. Gabriella Bianca Henriques Palma, you have been there for me whenever I needed it. You have been my colleague, my best friend and companion, and my source of motivation throughout the past few years. I am proud of you and everything you have achieved, and I appreciate that you always push me to be a better person.

Thank you for past and present colleagues in Gate House 519 (or 527 for those of us old enough to remember those days). I truly appreciate the input and assistance I have received, as well as the friends I have made in the lab.

Finally, I would like to acknowledge the University of the Witwatersrand (Postgraduate Merit Award) and the NRF for financial assistance during my study period (2019-2022) (grant number: 118425). In addition, I acknowledge the NRF-STINT collaboration (grant number: 118720) for enabling the invaluable collaboration with the Uppsala lab, without which this project would not have been possible.

LIST OF FIGURES

Figure 1: Illustration of the signalling pathways driving EMT induction. 11
Figure 2: The cholesterol biosynthesis pathway.....20
Figure 3: An overview of cellular cholesterol homeostasis.....23
Figure 4: Basic structure of a β-cyclodextrin and formation of a complex with a guest compound.....29
Figure 5: Morphological changes in NMuMG cells in response to 10 ng/mL TGFβ treatment. 56
Figure 6: Changes in E-cadherin and Vimentin fluorescence in response to EMT induction. 57
Figure 7: Changes in EMT marker expression in response to TGFβ treatment 59
Figure 8: Changes in Ki-67 fluorescence in response to EMT induction.....60
Figure 9: Changes in cellular cholesterol levels in response to EMT induction. 61
Figure 10: Changes in cell viability after cholesterol-lowering treatment.. 63
Figure 11: Filipin staining of free cholesterol after cholesterol depletion......65
Figure 12: BODIPY staining of CEs after cholesterol depletion.....66
Figure 13: Vybrant Alexa Fluor® Lipid Raft staining after cholesterol depletion.....68
Figure 14: Invasive potential of NMuMG cells following EMT induction and cholesterol depletion.....69
Figure 15: Changes in E-cadherin and Vimentin fluorescence in response to cholesterol depletion.....71
Figure 16: Changes in N-cadherin fluorescence in response to EMT induction and cholesterol depletion.....73
Figure 17: Changes in EMT-related gene expression in response to cholesterol depletion.. ..75
Figure 18: Changes in cholesterol-related gene expression in response to cholesterol depletion.....78
Figure 19: Illustration of the role of cholesterol regulation in EMT and metastasis.. 92

LIST OF TABLES

Table 1: Primary antibodies 38
Table 2: Secondary antibodies 39
Table 3: TBE buffer components 46
Table 4: Components of cDNA synthesis reaction 47
Table 5: Components of SensiFAST™ Probe No-ROX PCR reaction 47
Table 6: qPCR cycling conditions 48
Table 7: Primer Sequences 48
Table 8: RIPA Lysis Buffer Components 50
Table 9: SDS-PAGE Buffer Components 52
Table 10: SDS-PAGE Stacking and Resolving Gel Components (10%; 1 mm) 53
Table 11: Western Blot Running Buffer Components 53
Table 12: Transfer Buffer Components 54
Table 13: TBST Buffer Components 55

LIST OF ABBREVIATIONS

27HC	27-hydroxycholesterol
ABC	ATP-binding cassette
ACAT	Acyl-CoA cholesterol acyltransferase
AI	Aromatase inhibitors
ANOVA	Analysis of variance
AP	Acetyl Plumbagin
BCA	Bicinchoninic
bFGF	Basic fibroblast growth factor
bHLH	Basic helix-loop-helix
BMP	Bone morphogenetic protein
BSA	Bovine serum albumin
CDK	Cyclin-dependent kinase
CE	Cholesteryl ester
CETP	Cholesteryl ester transfer protein
CO2	Carbon dioxide
co-SMAD	Common SMAD
CSC	Cancer stem cell
CSL	C protein binding factor 1
C-SREBP	Cytoplasmic SREBP
CT	Computed tomography
CTCF	Corrected total cell fluorescence
DAAM1	Disheveled-associated activator of morphogenesis 1
DAPI	4′,6-diamidino-2-phenylindole
DMEM	Dulbecco Modified Eagle’s media
Dsh	Disheveled
ECM	Extracellular matrix
ECM	Extracellular matrix
EDTA	Ethylenediaminetetraacetic acid
EGFR	EGF receptor
EGFR	Epidermal growth factor receptor
EMT	Epithelial-to-mesenchymal transition
ERC	Endocytic recycling compartment
ERα	Estrogen receptor alpha

FDA	Food and Drug Administration
FSH	Follicle stimulating hormone
FZD	Frizzled
GnRH	Gonadotropin-releasing hormone
GRAS	Generally Recognized as Safe
HDL	High-density lipoprotein
HER2	Human epidermal growth factor receptor
Hh	Hedgehog
HIF1α	Hypoxia Inducible Factor 1 Subunit Alpha
HMG-CoA	3-hydroxy-3-methylglutaryl-CoA
HMGCR	HMG-CoA reductase
HPβCD	Hydroxypropyl-beta-cyclodextrin
HRP	Horseradish peroxidase
IDL	Intermediate-density lipoprotein
IDOL	Inducible degrader of LDLR
LCAT	Lecithin-cholesterol acyltransferase
LDL	Low-density lipoprotein
LDLR	LDL receptor
LH	Luteinizing hormone
LRP	Low-density lipoprotein receptor related protein
LTED	Long-term estrogen deprived
LXR	Liver X receptor
MAML1	Mastermind-like 1
MDR1	Multidrug resistance protein 1
MET	Mesenchymal-to-epithelial transition
miRNA	Micro RNA
MMP	Matrix Metalloproteinase
MMTV-PyMT	Mouse mammary tumour virus-polyoma middle tumour-antigen
MRI	Magnetic resonance imaging
MβCD	Methyl-β-cyclodextrin
NF-κB	Nuclear factor kappa B
NICD	Notch intracellular domain
NMuMG	Namru Mus musculus Mammary Gland

N-SREBP	Nuclear SREBP
PAGE	Polyacrylamide gel electrophoresis
PARP	Poly(ADP-ribose) polymerase
PBS	Phosphate-buffered saline
PCP	Planar cell polarity
PCSK9	Proprotein convertase subtilisin/kexin type-9
PDGFRα	Platelet-derived growth factor receptor alpha
PET	Positron emission tomography
PP	Pyrophosphate
PR	Progesterone receptor
PVDF	Polyvinylidene difluoride
RIPA	Radioimmunoprecipitation assay
ROCK	Rho-associated kinases
R-SMAD	Receptor-regulated SMAD
SARA	SMAD anchor for receptor activation
SCAP	SREBP cleavage activating protein
SDS	Sodium dodecyl sulfate
SERM	Selective estrogen receptor modulators
siRNA	Small interfering ribonucleic acid
SREBP	Sterol regulatory element binding protein
TACE	Tumour necrosis factor α-converting enzyme
TBE	Tris-borate-EDTA
TBST	TBS with Tween 20
TCF/LEF	DNA-bound T-cell factor/lymphoid enhancing factor
TF	Transcription factor
TGFβ	Transforming growth factor-β
TGFβRI	TGFβ receptor type I
TGFβRII	TGFβ receptor type II
TKI	Tyrosine kinase inhibitors
TNBC	Triple-negative breast cancer
UV	Ultraviolet
VEGF	Vascular endothelial growth factor
VLDL	Very low-density lipoprotein

LIST OF SYMBOLS

α	Alpha
β	Beta
©	Copyright
°C	Degrees Celsius
g	Grams
κ	Kappa
kDa	Kilodaltons
µ	Micro
µg	Micrograms
µL	Microlitres
µM	Micromolar
mg	Milligrams
mL	Millilitres
nm	Nanometres
nM	Nanomolar
pg	Picograms
®	Registered
™	Trademark
g	Relative centrifugal force
%	Percent

RESEARCH OUTPUTS

Conferences:

- Perumal, S. and Kaur, M. Elucidating the role of cholesterol pathways in the epithelial to mesenchymal transition in breast cancer cells.
    - New Zealand Breast Cancer Symposium (NZBCS-2021)
    - Type: Oral presentation
    - Date: 19/11/2021
    - Venue: Virtual
- Perumal, S. and Kaur, M. Investigating the Effect of Cholesterol Depletion on the Epithelial to Mesenchymal Transition of Breast Cancer Cells.
    - South African Society of Biochemistry and Molecular Biology (SASBMB-2022)
    - Type: Oral presentation
    - Date: 26/01/2022
    - Venue: Virtual
- Perumal, S. and Kaur, M. Elucidating the role of cholesterol pathways in the epithelial to mesenchymal transition in breast cancer cells
    - Molecular Biosciences Research Thrust Postgraduate Symposium (MBRT-2022)
    - Type: Oral presentation
    - Date: 01/12/2022
    - Venue: Adler Museum at Wits Medical School, Johannesburg, South Africa
    - Prize: Bronze prize for oral presentation

Provisional patent:

- Kaur M, Abdulla N, Aronson A, Perumal S, Pillay R. KS-01 as a cancer therapy neoadjuvant or adjuvant. PCT patent no: PCT/IB2023/057400, filed 20th July 2023.

Research article:

- Perumal S., Abdulla N., Aronson A., Kaur M. Cholesterol-lowering treatment reverses markers of the epithelial-to-mesenchymal phenotype in cancer cells

ABSTRACT

Breast cancer is the most prevalent cancer affecting women, globally. Metastasis, which is the spread of tumour cells from the primary tumour to a secondary site, accounts for approximately 75.6% of cancer-related mortalities. The epithelial-to-mesenchymal transition (EMT) is a critical cellular program underlying the metastatic spread of cancer cells. The role of cholesterol in EMT and metastasis has not yet been established; however, there is a link between cholesterol and cancer cell growth and proliferation. This study serves to determine the role of cholesterol in the induction of EMT and metastasis and delineate the cholesterol - related pathways affected by EMT induction. This study also aimed to assess the efficacy of cholesterol-lowering treatment on cells undergoing EMT. An *in vitro* model of EMT was established using the NMuMG cell line, a well-established model for studying EMT, treated with recombinant TGFβ. Induction of EMT was confirmed by assessing the expression of pre- and post-EMT markers. Cholesterol levels were measured using the Cholesterol Quantitation Kit (Sigma Aldrich, UK) and immunocytochemical lipid stains. Cellular cholesterol was lowered using cholesterol depleting agents: methyl-β-cyclodextrin (MβCD), 2-hydroxypropyl-β-cyclodextrin (HPβCD), and simvastatin treatment. Changes in proliferative capacity after EMT induction and treatment with cholesterol depleting agents were measured using the 2,5-diphenyl-2H-tetrazolium bromide (MTT) cell viability assay and immunocytochemistry. Changes in gene expression were measured using Western blotting and RT-qPCR. Invasive potential was measured using a Transwell assay. The induction of EMT in NMuMG cells resulted in a change from epithelial to mesenchymal morphology, along with an increase in expression of EMT-associated proteins, such as Vimentin and N-cadherin, and a decrease in E-cadherin expression. EMT induction resulted in an increase in invasive potential and an overall decrease in cellular cholesterol content. Cholesterol depletion with MβCD, HPβCD, and simvastatin treatment reversed EMT-related expression changes and restored expression of epithelial marker E-cadherin. In addition, cholesterol-lowering treatment reduced the invasive potential of cells after EMT induction. Due to its ability to reverse EMT-related phenotype changes, cholesterol depletion may serve as a therapeutic strategy for metastatic cancer.

Chapter 1: INTRODUCTION AND LITERATURE REVIEW

1.1 Breast Cancer

Cancer is a group of diseases in which control mechanisms governing the normal growth and proliferation of cells is altered. Cancer progression is a multi-faceted process, influenced by genetic predisposition, lifestyle, biological sex, and repeated exposure to carcinogenic agents. Cancer can affect different tissues in the body, resulting from a loss of cellular homeostasis. Breast cancer is a complex disease that exhibits uncontrolled cellular growth in the breast tissue.

1.1.1 Epidemiology

With approximately 2.26 million new cases and 684 996 deaths reported in the year 2022, breast cancer has exceeded lung cancer as the most diagnosed cancer globally and is a leading cause of cancer-related mortality [1]. In South Africa, breast cancer is the most diagnosed cancer in women, accounting for 23.22% of cancer diagnoses in the year 2019 (National Cancer Registry, 2019). Breast cancer incidence rates have increased by 3-4% per year in South Africa and mortality rates have followed, reflecting the lack of medical infrastructure necessary to address the increasing need for treatment [2]. Breast cancer risk is associated with lifestyle and hereditary factors, affecting women in both rural and urban areas. The increasing prevalence and high mortality risk of breast cancer globally necessitates urgent development and improvement of diagnostic and treatment strategies. This development begins with expanding our understanding of this complex neoplastic disease.

1.1.2 The Hallmarks of Cancer

Our understanding of cancer continuously evolves with the growing publication of diverse and novel research. The predominant characteristics of neoplastic disease were presented by Hanahan and Weinberg in their “Hallmarks of Cancer” review, initially published in the year 2000, later revised over a decade later, and then recently revised again in 2022 [3-5]. The additions made to this review demonstrate the advancement of our understanding of the fundamentals of tumorigenesis.

In these articles, Hanahan and Weinberg detail the properties that cells acquire to enable tumorigenesis. These properties include chronic proliferation, evading growth suppression and immune detection, and avoiding senescence and cell death, which enables tumour cells to accumulate and form a solid tumour [4]. Tumour cells alter their energy metabolism and tumour microenvironment to provide a favourable growth environment [5]. Enabling

angiogenesis and metastasis allows for tumour dissemination throughout the body. These alterations from normal cellular behaviour are made possible by the genetic instability, epigenetic reprogramming, and phenotypic plasticity observed in tumours [3]. These hallmarks are present in all cancer types, but the pathways controlling them differ between cancer types.

1.1.3 Breast Cancer Classification

The molecular mechanisms of tumorigenesis in breast cancer differ from other cancer types and can vary depending on subtype. The breast is primarily made up of glandular and adipose tissues. Alveoli, which contain the lactocytes, cluster to form lobules. The lobules form lobes, connecting to a network of lactiferous ducts, which function to transport milk toward the nipple [6]. Breast tumours most commonly develop in the ducts and lobules, called ductal and lobular carcinoma, respectively. While each case of breast cancer differs in its prognosis and pathway aberrations, similar cases can be grouped into subtypes with patient outcome and response to therapeutic agents.

Breast cancer subtypes are classified based on the expression of the progesterone receptor (PR), the oestrogen receptor alpha (ERα), and the human epidermal growth factor receptor 2 (HER2) proteins [7]. Utilising the expression of these receptor proteins as biomarkers, breast cancer is can be classified into five major intrinsic subtypes: luminal A, luminal B, HER2-expressing, normal-like, and triple-negative breast cancer [7]. Each subtype requires different treatment targeting pathways known to be active in each case.

Luminal A and B are the most prevalent breast cancer subtypes [8]. Luminal tumours overexpress ERα and PR and are sensitive to hormone-based therapies, but respond poorly to common chemotherapies [9]. Luminal A subtypes do not express HER2 and express low levels of the Ki-67 protein, indicating a low rate of proliferation and a good prognosis. Luminal B breast cancers have a worse prognosis due to the expression of HER2 and higher expression of Ki-67, indicating a faster growth and proliferation rate of cancer cells [10]. HER2-expressing tumours overexpress the cell-surface receptor HER2 which promotes cell growth and proliferation [8]. Due to their lack of ERα and PR expression, they do not respond to hormone therapy and generally have a poor prognosis in patients. They are, however, more responsive than luminal subtypes to taxane and anthracycline-based chemotherapeutic agents, such as doxorubicin [9]. HER2-expressing tumours can also be treated with HER2-targeting compounds, such as trastuzumab, but the effectiveness of this

treatment is limited in PTEN-deficient breast cancers, as it relies on increasing PTEN membrane localization and phosphorylation [11]. The basal subtype includes triple-negative breast cancer (TNBC), named for its lack of ERα, PR, and HER2 expression. These tumours express basal markers, such as the epidermal growth factor receptor (EGFR), keratins, and genes involved in proliferation, such as components of PI3K/Akt/mTOR signalling [12]. Basal tumours are generally aggressive and lack targeted therapeutic options. Patients diagnosed with TNBC have a poor prognosis and high relapse rate [13]. The differences in breast cancer subtype affect patient outcome and the treatment prescribed by physicians; however, it is important to note that breast cancer cases diagnosed at an early stage are more responsive to treatment and have better patient outcome regardless of subtype [14].

Breast cancer progression is measured in stages, which estimate how advanced the tumour is. Stage 0 describes both malignant and benign tumours which are non-invasive and easily treatable. Stage 0 is often associated with ductal carcinoma *in situ*, which has a low risk of becoming invasive [15]. Stage 1 tumours increase in size up to 2 cm and are able to invade [16]. Stage 1 of breast cancer is divided into stage 1A and 1B. Stage 1A exhibits no spread of tumour cells to lymph nodes. In stage 1B of breast cancer, groups of tumorigenic cells ≥0.2 mm in size are present in the lymph nodes [16]. In stage 2A, tumours between 2 and 5 cm in size are detected in the sentinel or axillary lymph nodes. Stage 2B tumours may be ≥5 cm, but are generally absent in the axillary lymph nodes [17].

Stage 3 of breast cancer is separated into three categories. Stage 3A tumour cells are not detected in the breast tissue, but are present in between four and nine axillary or sentinel lymph nodes [18]. Stage 3B indicates tumour spread to up to nine lymph nodes, as well as swelling of the skin of the breast, which indicates breast tissue inflammation. Stage 3C tumours are detected in ≥10 lymph nodes and are present in tissue surrounding the clavicle [18]. Stage 4 is the most advanced and metastatic form of breast cancer. At this stage, tumour metastases are detected in distant organs, such as the lungs, brain, or liver. Patients with stage 4 breast cancer respond poorly to treatment and generally have poor prognoses [19]. Advanced breast cancer cases are often fatal due to limited treatment options and high relapse rates. While earlier detection is priority, treatment options for late-stage cancer should be explored to improve patient outcome.

1.1.4 Detection and Diagnosis of Breast Cancer

There are several conventional techniques used to detect and diagnose breast cancer, each having strengths and limitations. Mammography is the most common test for breast cancer, which allows for early detection of tissue abnormalities using X-ray examination [20]. While mammograms are quick and allow for early detection of breast cancer, they have relatively high false-negative and false-positive rates, cause significant discomfort, have limited diagnostic utility for women with dense breast tissue, and make use of ionizing radiation [21]. Ultrasound is used as a supplement to mammography, which evaluates lumps detected during the mammogram. Magnetic resonance imaging (MRI) can be used to create an image of cross sections of the breast [20]. MRI has high sensitivity, allowing for detection of small tumours. It is, however, only recommended for patients with a high risk of breast cancer due to the high cost and high false-positive rate. Computed tomography (CT) and positron emission tomography (PET) are both used to image metastases, allowing for breast cancer staging and evaluation of treatment response [20]. These methods carry a radiation risk due to the use of ionizing radiation and radioactive tracer injections but allow for the progression of the disease to be tracked.

Apart from imaging, a breast biopsy is commonly performed for analysis of abnormal tissue detected in previously mentioned tests. Effort has been made to reduce the invasive nature of breast biopsies by using image guidance and biopsy markers to reduce the time of the surgery and the volume of resected tissue [22]. Resected tissue and blood are used for histological analysis and detection of biomarkers associated with tumour progression. This gives physicians information about tumour stage, subtype, and the treatment strategy.

1.1.5 Breast Cancer Treatment Strategies

The goal of treatment for non-metastatic breast cancer is the eradication of tumours from breast and lymph nodes and preventing metastasis and relapse. The first line of treatment of non-metastatic cases is surgical removal of the tumour and radiation therapy. For metastatic breast cancer, which is virtually incurable, therapy aims to alleviate symptoms and prolong survival. Therapy depends on subtype and may be administered preoperatively (neoadjuvant), postoperatively (adjuvant), or both. When hormone receptors ERα and PR are present, endocrine therapy is administered to counteract estrogen-induced tumour growth [23]. Endocrine therapy is orally administered daily for 5 years, and the type depends on menopausal status. Selective estrogen receptor modulators (SERMs), such as tamoxifen, are effective in premenopausal women, whereas aromatase inhibitors (AIs), such as anastrozole,

letrozole, and exemestane, are effective in postmenopausal women, including women subject to oophorectomy or medical ovarian suppression. SERMs competitively bind to the ER with high affinity, acting as an antagonist to the function of ER in the breast [24]. AIs suppress the activity of aromatase enzymes, preventing the conversion of androgens to estrogen and decreasing circulating estrogen [25]. Endocrine therapy is shown to reduce 5-year recurrence rates by 50% [26]. Clinicians may decide to combine endocrine therapy with oophorectomy or ovarian suppression with gonadotropin-releasing hormone (GnRH) agonists, such as leuprolide acetate [27]. GnRH agonists bind to GnRH receptors, which decreases luteinizing hormone (LH) and follicle stimulating hormone (FSH) through desensitisation. A decrease in LH and FSH inhibits estrogen and progesterone production [28]. Endocrine therapy can be combined with various chemotherapy regimens if necessary.

HER2-expressing tumours are treated using HER2-targeted therapy. Trastuzumab is a monoclonal antibody that targets the extracellular domain of HER2 [23]. It is administered in combination with chemotherapy regimens, commonly docetaxel/carboplatin or adriamycin/cyclophosphamide-paclitaxel, as a neoadjuvant and adjuvant therapy for approximately 1 year [29]. In high-risk patients with advanced disease, novel agents such as neratinib, an oral tyrosine kinase inhibitor of HER family proteins, can be administered following trastuzumab-chemotherapy regimens to improve disease-free survival over 5 years [30].

In the unfavourable case of TNBC diagnosis, chemotherapy is the only approved option for treatment for tumours larger than 5 mm [23]. Due to the lack of DNA damage repair in TNBC, platinum chemotherapies that crosslink DNA are being evaluated to improve current treatment strategies. A randomized phase II clinical trial evaluating the combination of neoadjuvant chemotherapy with carboplatin demonstrated a significant improvement in the pathologic complete response, compared to chemotherapy alone [31].

Metastasis poses a significant clinical challenge in both treatment availability and severity of the disease. In particular, brain metastases, which occur in 10 to 20% of cases of metastatic breast cancer, include the challenge of poor permeability of systemic therapies due to the presence of the blood-brain barrier [32]. In the case of metastatic breast cancer without germline *BRCA1/2* mutation, the only therapeutic option available is sequential single-agent chemotherapy [33]. While chemotherapy may be effective in prolonging overall survival, it is associated with notable toxicity, side effects, and an overall decrease in quality of life. In the

approximately 5% of patients presenting a germline mutation in *BRCA1/2* – which are tumour suppressor genes functioning in DNA repair – PARP (poly(ADP-ribose) polymerase) enzyme inhibitors talazoparib and olaparib have been approved by the United States Food and Drug Administration (FDA) for treating refractory metastatic breast cancer [34]. However, these compounds carry the same toxicities as conventional chemotherapeutic agents with high risk of severe side effects.

In addition to the treatment strategies mentioned above, numerous novel strategies in development due to the failure of current treatment regimens to completely prevent relapse and treatment resistance, and the severe side effects of chemotherapeutic agents [23]. The lack of treatment options for metastatic breast cancer combined with the poor patient outcome highlight an urgent need for the development of therapeutic agents targeting metastatic breast cancer. The treatment and prevention of metastasis is a priority for improving patient survival.

1.1.6 Metastasis

Metastasis is the process whereby tumour cells disseminate from the primary tumour to distant sites. Metastasis accounts for approximately 75.6% of breast cancer-related mortality [35]. The process of metastasis involves local invasion, intravasation, circulation, extravasation, and establishment of a secondary tumour [36]. Tumour cells lose adherence to the primary tumour and enter circulation by invading surrounding parenchyma tissue and infiltrating blood or lymphatic systems. They circulate through the blood or lymphatic systems until they exit from circulation and colonise distant tissue, forming a secondary tumour [36]. Tumour cells in circulation have a survival rate of approximately 0.2% and require adaptations for successful metastasis [37]. The heterogeneity and genetic instability of tumours allows for the high frequency of genetic alterations required to for cancer cells to successfully metastasize. Beneficial adaptations include the downregulation of cohesive molecules, increased motility, angiogenesis, the epithelial-to-mesenchymal transition (EMT), and modification of the tumour microenvironment [38].

The cellular microenvironment influences cell function and phenotype through biochemical and physical mechanisms. In mammary ducts, epithelial cells are surrounded by stroma, a layer of connective tissue containing fibroblasts and other structural support components. The stroma and epithelial layers are separated by the extracellular matrix (ECM) [38]. The interaction between epithelial cells, stroma, and the ECM controls the proliferation and

function of the cells [39]. Gap junctions, desmosomes, adherens junctions, and tight junctions are responsible for maintenance of the epithelial layer [39]. These connections limit cell motility and proliferation. During tumour formation and metastasis, these connections are broken down and epithelial cells alternatively attach to and detach from the ECM and stroma to aid in locomotion [40].

With increased tumour size, it becomes necessary to generate new blood vessels through angiogenesis. Several growth factors are required to induce blood vessel growth, including basic fibroblast growth factor (bFGF) and vascular endothelial growth factor (VEGF) [41]. The formation of new blood vessels provides a route for tumour cells to detach from the primary tumour and enter circulation [42]. The ECM acts as a physical barrier, preventing tumour cells from entering circulation. The process of invasion involves proteolysis of the ECM [43]. Matrix metalloproteinases (MMPs) degrade the ECM and are overexpressed in metastatic cells [40].

Once in circulation, tumour cells are exposed to fluid sheer forces generated by blood flow and leukocytes, both of which can lead to cell destruction. Matrix stiffness is the resistance to cellular deformation by mechanical forces such as sheer stress. In breast tumours, increased matrix stiffness is caused by the presence of dense collagen fibrils [44]. An increase in matrix stiffness promotes invasion, metastasis and EMT by promoting nuclear translocation of the Twist-related protein 1 (TWIST1) transcription factor (TF) [44]. Tumour cells may be able to resist leukocyte-mediated destruction by adhering to endothelium or forming a thrombus by interacting with platelets [45].

Circulating cancer cells eventually arrest at a secondary site. Arrest occurs when a thrombus forms due to the large size of tumour cells compared to the lumen of capillaries through which they flow, or through adherence to the endothelium [46]. After the tumour cell attaches to the vessel wall, extravasation occurs whereby cells penetrate the blood vessel wall and adapt to the new environment, forming a secondary tumour.

1.2 **The Epithelial-to-Mesenchymal Transition**

EMT is a critical cellular program underlying invasive and metastatic cellular behaviour. EMT is the biological process by which polarised epithelial cells undergo biochemical changes to assume a mesenchymal phenotype [47]. Epithelial cells are immobile and adhere to each other and the basement membrane [47]. EMT promotes a mesenchymal phenotype in which cells lose cell-to-cell contacts and apical-basal polarity, and gain migratory and

invasive properties and an increased resistance to apoptosis [48]. The process of EMT is important in many non-tumorigenic processes. EMT is classified into three subtypes, each contributing to the development and maintenance of an organism.

The first type of EMT is associated with embryogenesis and organogenesis. It plays a role in embryonic gastrulation, which gives rise to mesodermal and ectodermal tissue layers [49]. The primary epithelial cells in the epiblast undergo EMT to give rise to the primary mesenchyme, which forms secondary epithelial cells by undergoing a mesenchymal to epithelial transition (MET), which has the opposite effect of EMT [50]. These cells differentiate to form different types of epithelial tissues during embryo and organ formation.

The second type of EMT is associated with organ fibrosis, wound healing and regeneration [49]. This form of EMT is responsible for generating fibroblasts and other cells involved in tissue reconstruction after inflammatory injury and trauma. Molecules secreted by fibroblasts and inflammatory cells degrade the basement membrane, causing epithelial cells to either undergo apoptosis or EMT, accumulating in the interstitial tissue, where they gain a fibroblastic phenotype [51]. The accumulation connective tissue in fibrosis is associated with wound healing, repair of damaged epithelial structures and scar formation.

The third type of EMT occurs in neoplastic cells in response to altered oncogene and tumour suppressor expression [49]. EMT is a critical step in the acquisition of invasive properties in metastatic tumours [52]. Metastatic cells undergoing EMT express mesenchymal markers, such as desmin, vimentin, FSP1 and α-SMA [53]. These cells acquire a mesenchymal phenotype and are usually on the invasive front of the primary tumour, where they initiate invasion and metastasis [52]. EMT induces a stem cell-like phenotype in cancer cells, which is essential for the formation of a secondary tumour in the process of metastasis [54].

1.2.1 The EMT Regulatory Network

EMT is a complex process orchestrated by a range of proteins, microRNAs (miRNAs) and changes to the cellular microenvironment. The EMT-TFs, most studied of which are the Snail, Twist, and Zeb families, are not expressed in adult epithelial cells under normal circumstances but are expressed in tumours and are associated with higher risk of metastasis and poor patient outcome. The Snail family of transcriptional repressors includes Snail1, Snail2 (Slug), and Snail3 (Smuc), each sharing highly conserved C-terminal zinc finger domains and binding to a 5’-CANNTG-3’ E-box motif in the promoters of target genes [55]. Snail expression is regulated by numerous signalling pathways, including the transforming

growth factor beta (TGFβ), Wnt, and Notch pathways [56]. Snail expression is important for EMT induction and its expression is associated with cancer metastasis [57]. One of the main mechanisms of EMT initiation by the Snail family of TFs is the repression of E-cadherin expression, reducing cellular adhesion and promoting cell migration [58].

The Twist family of proteins are basic helix-loop-helix (bHLH) TFs that plays a critical role in embryonic development. The aberrant expression of TWIST1 in cancer induces EMT and promotes invasion and metastasis [59]. High expression of TWIST1 and other EMT-TFs inhibits p53-dependent senescence and apoptosis in cancer cells [60]. Activation of TWIST1 is shown to promote EMT and enhance cell dissemination, and repression of TWIST1 is required for cell proliferation and colonization once tumour cells have reached a secondary metastatic site [61]. TWIST1 expression acts not only by altering expression of proteins such as E-cadherin, but also by changing cellular structure and behaviour. TWIST1 promotes the formation of invadopodia, which are membrane protrusions which enhance ECM degradation and invasion [62]. It is also associated with the vascular mimicry observed in hypoxic conditions in solid tumours, which gives tumours access to circulatory networks [63].

The Zeb TF family is characterized by a central homeodomain, and two zinc finger clusters, which are involved in DNA binding. ZEB1 is regulated by numerous signalling pathways, including TGFβ, Wnt, and HIF1α (Hypoxia Inducible Factor 1 Subunit Alpha) signalling, and contains protein binding domains that allow it to interact with Smads, CtBP, and p300 [64]. ZEB1 is specifically expressed in mesodermal and nerve tissues during embryogenesis and plays a role in developmental EMT [65]. Its expression in adult humans varies between tissues with high expression observed in the bladder and uterus, moderate levels of expression in the ovaries and mammary glands, and low expression in the liver and pancreas [66]. Its function in these adult tissues is largely unknown. In cancer, ZEB1 drives EMT by directly repressing E-cadherin expression and promoting cell plasticity [67]. Its aberrant expression has been observed in numerous cancers and is associated with advanced tumour progression and metastasis [67-72]. In addition to E-cadherin repression, ZEB1 represses genes involved in epithelial polarity and adhesion, promoting an invasive phenotype in tumour cells [73]. It mediates the conversion of tumour cells to cancer stem cells in basal subtypes of breast cancer and regulates cancer cell response to both drug treatment and radiation therapy [74-76]. The expression changes observed in EMT leading to changes in morphology and cell behaviour are driven by the activation of various key signalling

pathways. These include the TGFβ, Wnt, and Notch signalling pathways, illustrated in Figure 1 [77].

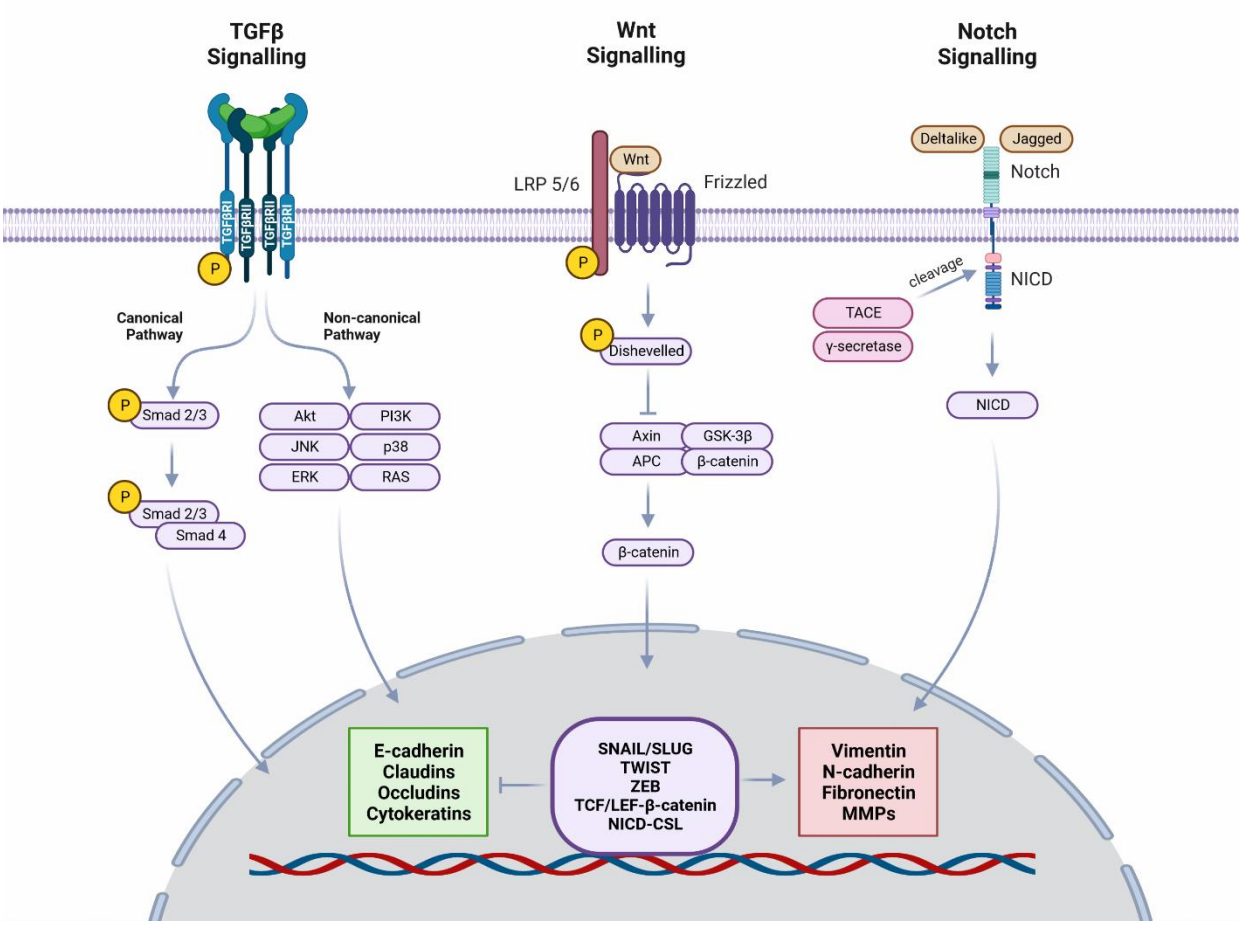

Figure 1: Illustration of the signalling pathways driving EMT induction. A summary of receptor activated signalling pathways involved in EMT induction. The TGFβ pathway is activated by the binding of the TGFβ ligand to the transmembrane heterotrimeric complex of TGFβRI and TGFβRII, resulting in signal transduction through Smad and non-Smad pathways. Wnt signalling relies on the activation of the Frizzled receptor by the Wnt ligand, resulting in the release and stabilization of β-catenin. Notch signalling begins with the binding of Deltalike or Jagged ligands on adjacent cells to the extracellular domain of the Notch receptor, resulting in the cleavage of NICD, which forms a transcriptionally active complex with CSL. EMT-TFs are activated, which activate the expression of mesenchymal genes and repress epithelial genes. Figure created with BioRender.com

1.2.2 The TGFβ Signalling Pathway

TGFβ proteins are cytokines belonging to the transforming growth factor β superfamily and are highly conserved in multicellular organisms. TGFβ is a principal regulator of EMT and is involved in several cellular processes including proliferation, differentiation, migration,

invasion and cell survival [78]. Physiologically, TGFβ is involved in embryonic development, wound healing, angiogenesis, immunosuppression, and remodelling of the ECM [78]. In cancer, TGFβ signalling plays a dual role, acting as both a tumour suppressor and an oncogene depending on cellular context. During the early stages of tumour development, TGFβ acts as a tumour suppressor by inhibiting proliferation and promoting apoptosis. At later stages, it enables advanced tumour progression by activating EMT, enhancing invasive and metastatic potential [79]. In addition, TGFβ signalling suppresses immune surveillance and promotes angiogenesis and inflammation, leading to a more advanced and aggressive cancer [80].

The TGFβ superfamily consists of more than 30 members in humans, which act as ligands to the TGFβ receptors [81]. There are two types of TGFβ receptors in humans – type I (TGFβRI) and type II (TGFβRII) receptors – which are both transmembrane serine/threonine kinase receptors. These receptors contain an extracellular N-terminal ligand-binding domain and a cytoplasmic C-terminal serine/threonine kinase domain [82]. Binding of the TGFβ ligand to the TGFβRII dimer leads to the recruitment of the TGFβRI dimer, forming a hetero-tetrameric complex with the bound ligand and catalysing the phosphorylation of the GS domain of TGFβRI, activating the TGFβ signalling pathway [83].

TGFβ signalling occurs through the canonical pathway or the non-canonical pathway, both of which can occur simultaneously [82]. The canonical pathway begins with receptor-regulated SMAD (R-SMAD) proteins (SMAD1, 2, 3, 5, and 9) phosphorylation by TGFβRI. SMAD2 and 3 are initially immobilized by the SMAD anchor for receptor activation (SARA) near the cell surface [84]. SMAD phosphorylation destabilizes its interaction with SARA, allowing it to dissociate from the SARA-SMAD complex. Additionally, phosphorylation of the R-SMADS increases their affinity for the common SMAD (co-SMAD), SMAD4, allowing for the formation of a transcriptional regulation complex, which translocates to the nucleus, activating or repressing gene expression [82]. The interaction between R-SMADS and SMAD4 can be competitively inhibited by antagonistic signalling through inhibitory SMADS (I-SMADS), SMAD6/7, which suppresses TGFβ signalling [85]. In addition to the canonical pathway, TGFβ signalling can occur independently of SMAD activation through the non-canonical pathway. This occurs when the TGFβ-receptor complex interacts with the interleukin-1 receptor-effector module, leading to the activation of PI3K-AKT, p38, JNK, and RAS/ERK signalling, which also play a role in EMT and tumorigenesis [86].

1.2.3 Wnt signalling

The Wnt signalling pathway regulates a variety of cellular processes including cell motility, polarity, differentiation, organogenesis, and stem cell renewal and maintenance [87] It is a key regulator of embryogenesis and is tightly regulated under normal conditions. Deregulation of Wnt signalling during development is linked to birth defect disorders and its deregulation after birth is linked to skeletal defects and breast, colon, and skin cancers [88].

WNTs are secreted glycoproteins involved in signalling through the canonical β-catenin-dependent pathway, or the non-canonical pathway, which does not depend on β-catenin [89]. WNT proteins act as ligands for Frizzled (FZD) receptors on the cell surface. The interaction between WNT and FZD relies on many co-receptors, including the low-density lipoprotein receptor related protein (LRP) [90]. Upon activation of Wnt signalling, the protein Disheveled (Dsh) transduces the signal to downstream pathways depending on which of its domains is activated [91].

The canonical pathway regulates cell proliferation, homeostasis, and embryogenesis and relies on β-catenin – a subunit of the cadherin protein complex that acts as a signal transducer in the Wnt pathway – present in the cytoplasm and adherens junctions of the cytoskeleton [90]. Without WNT ligands present, β-catenin is phosphorylated by a multimeric protein complex known as the destruction complex, composed of Axin, GSK-3β, CK1, and APC proteins, followed by ubiquitination and proteasomal degradation [90]. When WNT ligands bind FZD and LRP5/6, cytoplasmic Dsh interacts with FZD and binds to Axin, inhibiting the GSK-3-mediated phosphorylation and degradation of β-catenin. β-catenin then accumulates in the cytoplasm and moves to the nucleus, where it complexes with the TF DNA-bound T-cell factor/lymphoid enhancing factor (TCF/LEF), allowing for the regulation of Wnt target genes [92].

The non-canonical pathway branches into two distinct sub-pathways, each independent of β-catenin. The planar cell polarity (PCP) pathway regulated cell polarity, motility during gastrulation, and migration of neural crest cells [93]. This pathway is activated when WNT ligands bind to FZD in the absence of LRP co-receptors [91]. WNT-bound FZD interacts with Dsh and the Disheveled-associated activator of morphogenesis 1 (DAAM1), which interact with Rho GTPases, activating Rho-associated kinases (ROCK), which leads to cytoplasmic reorganization [94]. The PCP pathway regulates cellular organization and plays an important role in cell polarity and adhesion. The second type of non-canonical Wnt

signalling is the WNT/Ca^{2+} pathway, which regulates intracellular Ca^{2+} release from the endoplasmic reticulum [95]. Like all Wnt signalling, this pathway relies on WNT ligands binding to FZD, which in this case activates heterotrimeric G-proteins, increasing the concentration of intracellular Ca^{2+}, which activates protein kinase C, calcineurin, or calcium/calmodulin-dependent kinase II, modulating dorsal axis formation and PCP signalling required for cell motility, adhesion, and migration during gastrulation [87, 95].

As Wnt signalling regulates a wide range of cellular processes, its dysregulation is associated with diseases including cancer. Most well-known is the mutation of the APC protein, preventing the regulation of β-catenin in hereditary familial adenomatous polyposis, leading to cancer progression [96]. Mutation or dysregulation of components of Wnt signalling influence cancer development by altering cell proliferation, EMT, and metastasis. Induction of the canonical Wnt pathway has been correlated with poor prognosis in breast cancer [97]. Blocking the canonical pathway through LRP5 knockdown is shown to block EMT in cancer cells, as well as reduce invasive potential [98]. Additionally, β-catenin-mediated transcription induces Snail2 and Twist1 expression, contributing to the induction of EMT [99, 100]. The activation of non-canonical Wnt signalling through WNT5A expression induces EMT and promotes invasiveness and stem-like properties in cancer [101, 102]. In contrast, Wnt signalling has a tumour suppressing role, depending on cellular context. Activation of non-canonical Wnt signalling can have a tumour suppressive role and is downregulated in certain cases of breast cancer [103]. Furthermore, TCF4, a member of the TCF/LEF TF family that regulate Wnt target genes, acts as both a tumour promoter and suppressor depending on isoform variation [104-106]. The role of Wnt signalling in EMT and cancer is complex and its manipulation in therapeutic strategies should be used with caution until its role in tumorigenesis is better understood.

1.2.4 Notch signalling

The Notch signalling pathway is active in many organ systems, regulating cell proliferation, differentiation, and apoptosis [107]. Notch signalling in mammals utilizes four Notch transmembrane receptors (Notch1-4), and five ligands (Deltalike1-3, and Jagged1/2). The Notch pathway initiates with the binding of one of these ligands to a Notch receptor on the surface of an adjacent cell. This results in Notch cleavage by the complex of the metalloprotease tumour necrosis factor α-converting enzyme (TACE) and γ-secretase, releasing the intracellular domain of Notch (NICD) [108]. When the NICD enters the nucleus, it forms a transcriptionally active complex with C protein binding factor 1 (CSL)

and co-activators p300-CBP and mastermind-like 1 (MAML1) [109]. This complex regulates the expression of target genes including nuclear factor-kappa B (NF-κB), c-myc, cyclin D1, Akt, mTOR, and VEGF [110].

Aberrant Notch signalling is associated with many aspects of tumorigenesis. High expression levels of Notch-1 and Jagged-1 correlate with poorer patient prognosis in breast, prostate, and bladder cancers and leukaemia [111-114]. Notch plays a role in proliferation, apoptosis, and angiogenesis in tumour cells [110, 115]. In addition, dysregulation of the Notch pathway drives EMT in cancer. In a hypoxic cellular environment, the expression of HIF-1α increases, which stabilizes NICD, resulting in Snail1 expression and the induction of EMT [116]. Moreover, the EMT-TF Slug is a downstream target of Notch signalling and upregulation of Notch signalling induces Slug expression and EMT in breast cancer [117]. There is also crosstalk between Notch and TGFβ signalling in which the TGFβ induces Notch ligand expression, which contributes to cell cycle inhibition and EMT [118].

1.2.5 EMT in Invasion and Metastasis

EMT has become implicated in the process of epithelial cells acquiring the ability to invade and disseminate during metastasis [77]. This is orchestrated by the activation of a set of EMT-TFs, including Snail, Twist, Slug, and Zeb1/2. These TFs are associated with migratory processes activated during embryogenesis and are ectopically expressed in different combinations during tumour invasion and metastasis [119, 120]. The expression of these TFs lead to a loss of adherens junctions and the conversion of cells undergoing EMT from a rectangular morphology characteristic of epithelial cells to an elongated fibroblastic morphology [5]. The additional expression of matrix-degrading enzymes and repression of E-cadherin promotes an increase in cell motility and invasiveness [121].

One of the key characteristics of EMT is the loss of epithelial cell-cell adhesion, largely caused by the loss of E-cadherin expression [77]. E-cadherin is a transmembrane glycoprotein that mediates cell-cell adhesion through calcium-dependent interactions with E-cadherins on surrounding cells. Reduced E-cadherin expression correlates with the development of invasive cancer with poor prognosis [122]. Transcriptional repression of the *CDH1* gene that encodes the E-cadherin protein is mediated by EMT-TFs Snail1/2, Zeb1/2, and Twist [123]. The loss of E-cadherin expression and the concomitant gain of N-cadherin expression changes the adhesive properties of the cell. N-cadherin is a transmembrane glycoprotein that mediates cell-cell adhesion in a similar manner to E-cadherin [124]. N-

cadherin is rarely expressed in epithelial cells and its ectopic expression in epithelial cancers correlates with increased tumour aggression and invasion [125]. Cells lose affinity for surrounding epithelial cells and gain an affinity for mesenchymal cells including vascular endothelial cells. This change in cadherin expression is accompanied by increased migratory and invasive capacity [125]. In addition, when EMT is induced, vimentin expression increases. Vimentin is a type III intermediate filament with high expression in mesenchymal cells, responsible for the maintenance of cellular integrity. Its expression in cancer cells drives cell migration, aiding in metastasis and leading to a poor clinical outcome [126].

Proteins involved in EMT induction have been linked to invasion and metastasis. Repression of Snail1 was found to inhibit metastasis in a breast cancer model [127]. In pancreatic cancer, inhibition of the *Zeb1* gene suppresses plasticity and metastatic potential [128]. Knockdown of the *TWIST1* gene inhibits cell migration and invasion in a mouse model of breast cancer, but has no effect on tumour growth [129]. TWIST1 plays a further role in metastasis by inducing the expression of platelet-derived growth factor receptor alpha (PDGFRα), which activates Src, promoting the formation of invadopodia [62]. These studies demonstrate a link between EMT-related gene expression and metastasis in cancer.

The induction of EMT changes the expression of both cell surface and secreted proteins. One key change is the loss of E-cadherin expression, which is responsible for cell-cell anchoring. The loss of E-cadherin observed in EMT disrupts cell-cell contacts and promotes metastasis by increasing the ability of the tumour cell to migrate, invade, and resist anoikis, which is the induction of apoptosis observed when cells lose contact with neighboring cells and the ECM [100]. While the loss of E-cadherin is commonly associated with EMT, some aggressive carcinomas maintain E-cadherin expression. Evidence suggests that in these cases, the proteolysis of E-cadherin, mediated by MMPs, results in a soluble E-cadherin fragment, sE-CAD, which inhibits the function of E-cadherin and promotes invasion [130].

1.2.6 EMT in Drug Resistance

Along with metastasis, drug resistance is one of the most important challenges in cancer treatment. EMT has been implicated in drug resistance, contributing to the ongoing challenge of cancer therapy [131]. The link between EMT and drug resistance was first identified in the study of adriamycin-resistant MCF7 cells and vinblastine-resistant ZR-75-B cells [132]. In both cases, cells showed a loss of E-cadherin expression and an increase of vimentin expression, accompanied by reduced desmosome and tight junction formation, characteristic

of cells undergoing EMT [132]. EMT has also been correlated with drug resistance in pancreatic cancer, breast cancer, and bladder cancers [76, 133, 134]. A causal link between EMT and chemoresistance was established in the study of cyclophosphamide treatment resistance in murine breast-to-lung metastasis model in which EMT inhibition abrogated treatment resistance [135]. This was confirmed by the deletion of EMT-TFs Snail and Twist in a murine model, which suppressed EMT induction, leading to enhanced response to gemcitabine treatment and an improvement in overall survival [136].

A key regulator of the EMT phenotype, the TGFβ pathway, is associated with drug resistance in cancer. This relationship was first established in 1996, when Teicher *el al.* discovered that the use of anti-TGFβ antibodies in animal tumour models significantly increased sensitivity to chemotherapeutic agents [137]. Furthermore, inhibition of TGFβ/Smad4 signalling reversed EMT induced by doxorubicin treatment in a human colorectal carcinoma cell line, HCT116 [138]. This reversed the acquired resistance to doxorubicin and increased the chemosensitivity of the cells. The EMT-TFs are also linked to drug resistance. Twist expression induces EMT, invasion and migration, and promotes oxaliplatin resistance in colorectal cancer by increasing the expression of multidrug resistance protein 1 (MDR1) [139]. Upregulation of *Snail* and *Slug* correlates with cisplatin resistance in ovarian cancer and reducing their expression reversed the mesenchymal phenotype and restored sensitivity to cisplatin treatment [140]. Finally, ZEB1 is preferentially expressed in invasive glioblastoma cells, influencing invasion and chemoresistance and acting as a predictor of a poor response to Temozolomide treatment and poor survival in general [141].

Wnt and Hedgehog (Hh) pathways are also closely linked to EMT and contribute to drug resistance. Trastuzumab resistance in HER2-positive breast cancer is accompanied by the activation of the Wnt/β-catenin signalling pathway [142]. Wnt3 expression in trastuzumab-resistant cells increased the nuclear expression of β-catenin and induced partial EMT, whereby E-cadherin expression was reduced and N-cadherin, Slug, and Twist expression was increased [142]. siRNA-mediated knockdown of Wnt3 reversed EMT-related expression changes, inhibited cell invasion, and sensitivity to trastuzumab [142]. The Hh pathway, which is an important mediator of EMT, is activated in lung cancer cells resistant to tyrosine kinase inhibitors (TKI) of the EGF receptor (EGFR), a targeted treatment of non-small cell lung cancer [143]. Inhibition of components of Hh signalling showed antitumoral activity and sensitized cells to chemotherapy.

While EMT has been linked to drug resistance through numerous studies, the mechanisms of EMT-mediated drug resistance are not fully elucidated. Cells undergoing EMT have stem-like properties and share key signalling pathways with cancer stem cells (CSCs) [144]. A mechanism of drug resistance thought to be shared between CSCs and cells undergoing EMT is the overexpression of drug efflux proteins, such as the ATP-binding cassette (ABC) transporter proteins. These transmembrane proteins form ATP-dependent pumps that efflux drugs from the cell, lowering intracellular drug concentrations. In particular, P-glycoprotein (ABCB1), MDR-associated protein 1 (ABCC1), and the breast cancer resistance protein (ABCG2) have been linked to drug resistance in cancer [145]. Induction of EMT directly increases expression of ABC proteins associated with drug resistance with EMT-TFs binding to promoters and activating expression of these proteins, increasing resistance to doxorubicin treatment [146]. Reversal of EMT in this study reduced expression of ABC proteins, reducing migration, invasion, and restoring chemosensitivity. The ABC proteins are also the primary mediators of cholesterol efflux pathways, responsible for transporting cholesterol out of the cell, where it is converted to high-density lipoprotein (HDL) particles and transported to the liver for excretion [147].

1.3 **Cholesterol and its Role in Cancer**

Cholesterol is a polycyclic molecule containing four ring structures fused in a planar conformation [148]. It is a type of lipid called a sterol and is an integral component of the membranes of all animal cells, making up approximately 30% of the lipid bilayer [149]. As a structural component of the lipid membrane, cholesterol maintains membrane fluidity and permeability [150]. Its role in membrane biogenesis makes cholesterol essential for cell proliferation. Cholesterol also plays a part in the structure and organization of the lipid rafts. Lipid rafts are plasma membrane microdomains that contain components of cell signalling cascades and regulate signal transduction [151]. In addition to a structural role, cholesterol also plays a role in molecular and vesicular trafficking and in modulating the functions of receptor proteins [152]. It is also the precursor to steroid hormones including estrogens, androgens, and glucocorticoids, which are involved in cell signalling [153]. Furthermore, cholesterol can regulate signalling pathways, demonstrated by its ability to covalently modify Hh and Smoothened proteins during embryonic development [154]. Cholesterol homeostasis in the cell is maintained by a complex network of molecular processes and signalling pathways. Cellular cholesterol levels are regulated by a balance between cholesterol synthesis, uptake, and efflux.

1.3.1 Cholesterol Synthesis

Cholesterol can be synthesized in almost all cells, but approximately 50% of cholesterol is made in the liver [155]. Cholesterol synthesis occurs through a series of biochemical reactions known as the mevalonate pathway [156], illustrated in Figure 2. The mevalonate pathway is initiated by the Claisen condensation of acetyl-CoA with the enolate of a second acetyl-CoA molecule, catalysed by acetoacetyl-CoA thiolase, to form acetoacetyl-CoA. 3-hydroxy-3-methylglutaryl-CoA (HMG-CoA) synthase then catalyses the condensation of acetoacetyl-CoA with another acetyl-CoA molecule to form HMG-CoA. HMG-CoA is converted to mevalonate by HMG-CoA reductase (HMGCR), which is the rate-limiting step of the mevalonate pathway [157]. Mevalonate is phosphorylated by mevalonate-5-kinase, followed by further phosphorylation by phosphomevalonate kinase, yielding mevalonate-pyrophosphate (PP) [158]. Mevalonate-PP is converted to isopentenyl-5-PP by mevalonate-PP decarboxylase, followed by conversion to geranyl-PP by geranyl-PP synthase, which is then converted to farnesyl-PP by farnesyl-PP synthase [156].

The first step of the mevalonate pathway that is specifically committed to hepatic cholesterol biosynthesis is the conversion of farnesyl-PP to squalene by squalene synthase [156]. Squalene is converted to lanosterol by squalene epoxidase, followed by the conversion of lanosterol to cholesterol. The conversion of lanosterol to cholesterol is a 19-step anabolic reaction requiring nine different enzymes [159]. Among these enzymes is a member of the cytochrome P450 family, a protein family also involved in drug metabolism [160]. The first step of the mevalonate pathway that is specifically committed to hepatic cholesterol biosynthesis is the conversion of farnesyl-PP to squalene by squalene synthase [156]. Squalene is converted to lanosterol by squalene epoxidase, followed by the conversion of lanosterol to cholesterol. The conversion of lanosterol to cholesterol is a 19-step anabolic reaction requiring nine different enzymes [159]. Among these enzymes is a member of the cytochrome P450 family, a protein family also involved in drug metabolism [160].

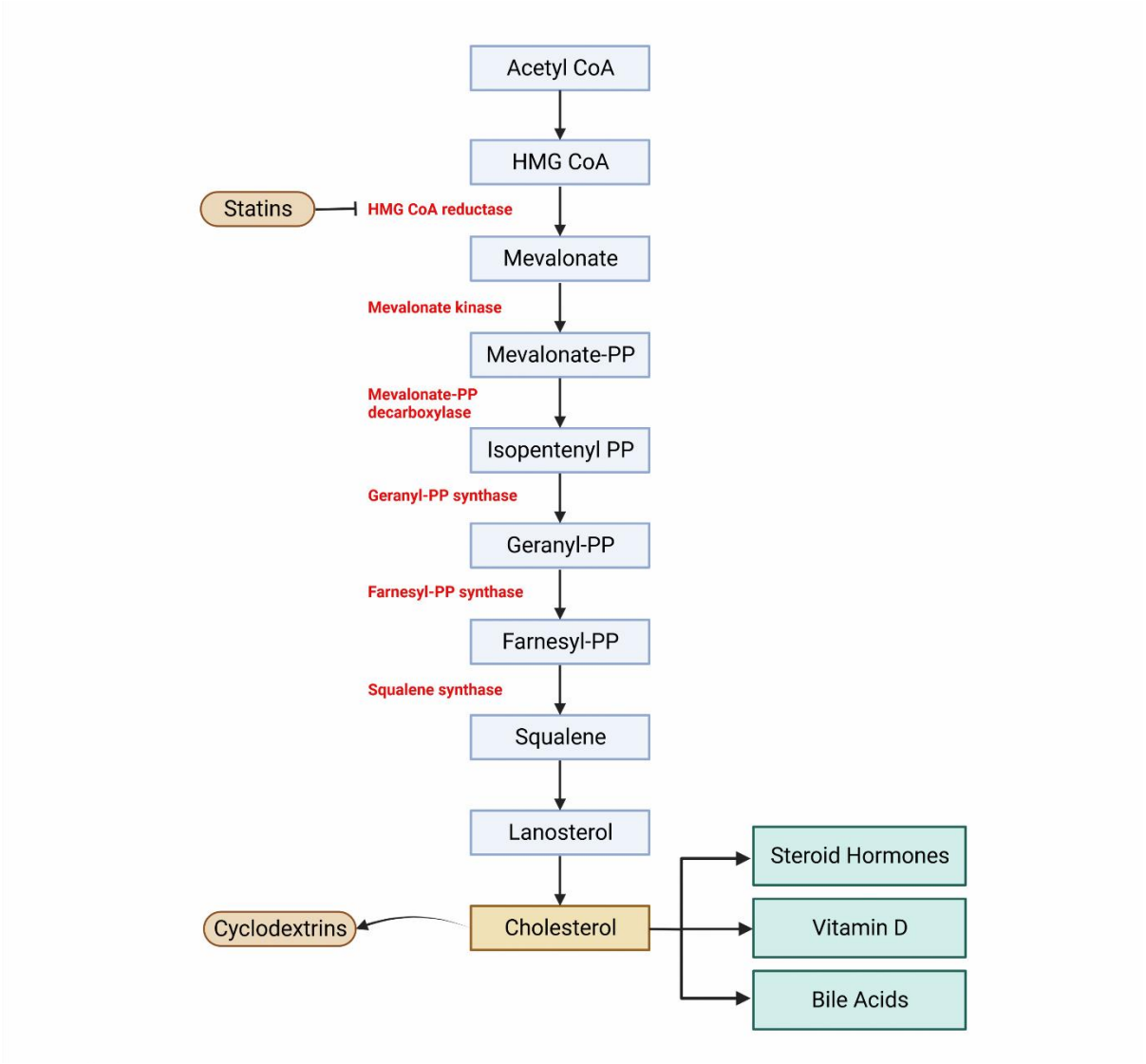

Figure 2: The cholesterol biosynthesis pathway. An illustration of the mevalonate pathway in which cholesterol is synthesized starting with the conversion of acetyl-CoA to mevalonate. Enzymes catalysing the conversion between pathway intermediates are shown in red. Statins inhibit the conversion of HMG-CoA to mevalonate and cyclodextrins absorb and solubilize cholesterol after it has been synthesized. Cholesterol is used in the synthesis of steroid hormones, vitamin D, and bile acids after it is synthesized. Figure created with BioRender.com. [Source: Buhaescu and Izzedine, 2007; accessed 20 February 2022].

1.3.2 Cholesterol Transport and Homeostasis

Due to its hydrophobic nature, cholesterol is found in lipid membranes or in complex with lipids or proteins. The transport of cholesterol is facilitated by lipoproteins, which are amphipathic assemblies of phospholipids, cholesterol, and apolipoproteins, allowing for the emulsification and transport of cholesterol in the blood [161]. The five major classes of lipoproteins are: HDL, intermediate-density lipoprotein (IDL), low-density lipoprotein (LDL), very low-density lipoprotein (VLDL), and chylomicrons. Cholesterol transport begins in the liver where synthesised or absorbed cholesterol is packaged into VLDL. VLDL enters into circulation and is converted to IDL and then to LDL by cholesterol ester transfer protein (CETP) and lipoprotein lipase [161]. LDL particles transport cholesterol to peripheral tissues and bind to the LDL-receptor (LDLR), where they undergo endocytosis and are internalised by the tissue. Excess cholesterol is removed from peripheral tissue as HDL particles and transported to the liver, where it is converted to bile salts and excreted [162].

Cholesterol homeostasis in the body is tightly regulated by several proteins, summarised in Figure 3. A key regulator of intracellular cholesterol levels is the Sterol Regulatory Element Binding Protein-2 (SREBP2) [163]. The activity of this TF is negatively regulated by the presence of free cholesterol in the cell. SREBP2 exists in an inactive state attached to the endoplasmic reticulum, where it acts as a sensor for intracellular cholesterol levels. When cholesterol levels are reduced, SREBP cleavage activating protein (SCAP) facilitates the migration of SREBP2 to the Golgi, where it is activated. SREBP2 then enters the nucleus, where it induces the expression of genes such as HMGCR, which is involved in cholesterol synthesis, and LDLR, which is involved in cholesterol import into the cell [164]. When cholesterol levels increase, SREBP2 remains inactive, decreasing cholesterol biosynthesis pathways in the cell.

In addition to cholesterol biosynthesis, cholesterol uptake from the blood can increase cellular cholesterol levels. This cholesterol may be absorbed dietary cholesterol or cholesterol effluxed by other cells. The main mechanism of dietary cholesterol uptake is mediated by NPC1L1 – a transmembrane protein expressed on the surface of intestinal cells [165]. NPC1L1 is normally found in the endocytic recycling compartment (ERC) and rapidly translocates to the membrane when cholesterol levels are reduced, where it mediates intestinal cholesterol absorption [166]. When cholesterol is absorbed, NPC1L1 and absorbed cholesterol are transported from the membrane to the ERC [167]. Uptake of cholesterol in the form of LDLs from circulation is mediated by the cell surface glycoprotein LDLR. The

extracellular ligand binding domain of cell surface LDLR captures circulating LDLs, enabling the endocytosis of LDL [168]. LDLs carrying cholesteryl esters (CEs) are processed through the endo-lysosomal system, yielding cholesterol which is delivered to cellular compartments, such as the endoplasmic reticulum [169].

Cholesterol uptake is halted by the degradation of LDLR. One mechanism of LDLR degradation is through activation of liver X receptor (LXR) TFs. LXR binds to the promoter of the inducible degrader of LDLR (IDOL), upregulating its expression [170]. IDOL is an E3 ubiquitin ligase protein that induces the ubiquitination of LDLR, leading to its degradation. Additionally, proprotein convertase subtilisin/kexin type-9 (PCSK9), a proprotein convertase, forms a complex with LDLR which is internalized in clathrin-coated pits and delivered to endosomes, where the complex eventually undergoes lysosomal degradation [171]. Degradation of LDLR is a response to excess cellular cholesterol levels and is required to maintain cholesterol homeostasis.

Due to the inability of most mammalian cells to catabolize cholesterol, excess cholesterol needs to be either stored as CEs in lipid droplets or removed from the cell through reverse cholesterol transport or efflux mechanisms. Cholesterol efflux is mediated by members of the ABC superfamily of transporter proteins: mainly ABCA1, ABCG1, ABCG5, and ABCG8. ABCA1 facilitates cellular cholesterol export to its extracellular acceptor, apolipoprotein-A1 (apoA-1) [172]. This export generates nascent HDL molecules that require the action of lecithin-cholesterol acyltransferase (LCAT) to mature into HDL molecules which are exported by ABCG1 [173]. The expression of both ABCA1 and ABCG1 is upregulated by LXR binding to their promoters [164]. Exported HDL is transported to the liver. ABCG5 and ABCG8 are expressed on the surface of hepatocytes, where they mediate the excretion of cholesterol from the liver into the bile [174]. The esterification process required for cholesterol storage, secretion, and absorption is mediated by acyl-CoA cholesterol acyltransferase (ACAT) proteins. ACAT1 is present throughout the body and catalyses the esterification of free cholesterol to CEs [175]. ACAT2 functions in a similar manner, but is expressed primarily in enterocytes and facilitates intestinal absorption of cholesterol [176]. Stringent regulation of cholesterol is required to maintain cellular homeostasis. Aberrations in cholesterol regulatory pathways result in loss of homeostasis and changes in cell behaviour that lead to disease.

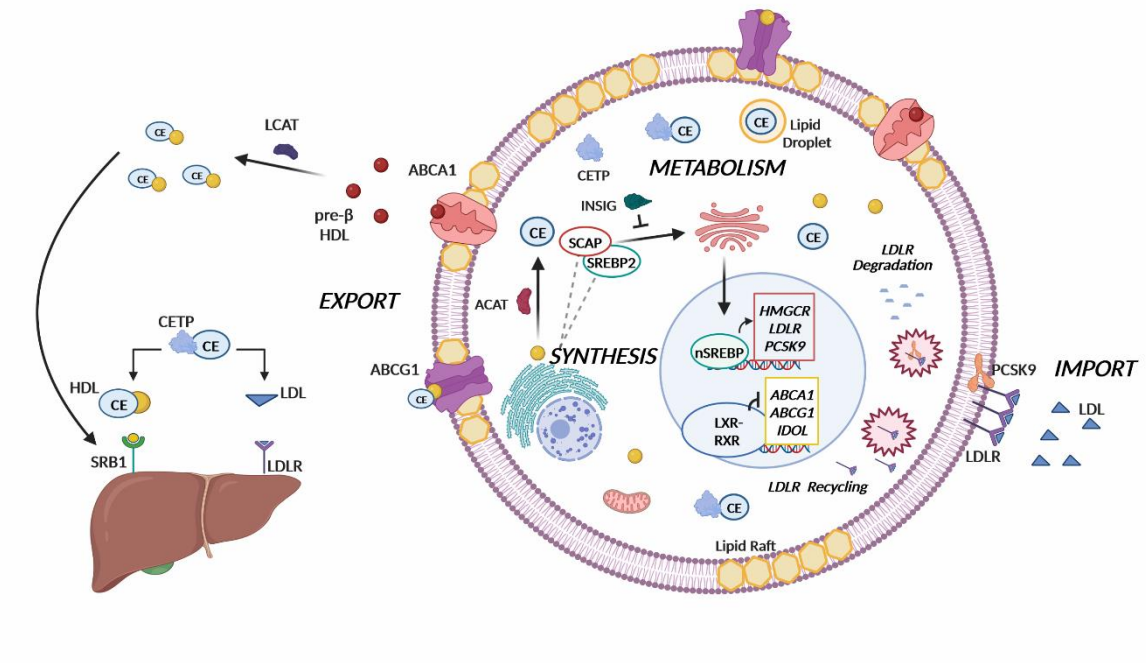

Figure 3: An overview of cellular cholesterol homeostasis. Cellular cholesterol homeostasis is maintained by a balance of cholesterol synthesis, metabolism, import, and export. Cholesterol import is mediated by the sterol regulatory element binding proteins (SREBP), leading to cholesterol synthesis through activation of the mevalonate pathway in the endoplasmic reticulum (ER). Import of cholesterol into the cell is mediated by proprotein convertase subtilisin/kexin type-9 (PCSK9) and low density lipoprotein receptor (LDLR). Acyl-CoA cholesterol acyltransferase (ACAT) mediates the conversion of free cholesterol to cholesteryl esters (CEs), which are transported by cholesteryl ester transfer proteins (CETP) to lipid droplets for storage. Excess cholesterol is exported from the cell in a process mediated by the Liver-X-Receptor (LXR) and the Retinoid-X-Receptor (RXR), which activate the expression of ATP-binding cassette efflux proteins ABCA1 and ABCG1. Exported cholesterol is converted to high density lipoprotein (HDL) and eventually transported to the liver for excretion. [Source: Abdulla *et al.*, 2021, accessed 25 February 2023].

1.3.3 The Link Between Cholesterol and Cancer

Cholesterol is a key structural component of cells and is involved in several signalling pathways. Loss of normal cholesterol metabolism has the potential to alter cellular behaviour, resulting in diseases such as cancer. Increased serum cholesterol levels are correlated with a higher risk of developing cancers of the prostate, breast, colon, rectum, and testicles [177]. However, the molecular mechanisms associated with this correlation are complex and are not fully understood. Several studies, including the present study, aim to elucidate the role cholesterol plays, if any, in the development and progression of cancer.

A correlation between increased cholesterol levels and cancer risk has been observed in many different cancer types. A high-cholesterol diet is shown to be a risk factor for developing

breast cancer [178]. Additionally, the REDUCE clinical trial reported an association between increased serum cholesterol and a higher risk of developing advanced prostate cancer [179]. Furthermore, low serum levels of the HDL-bound cholesterol – indicating a reduction of efflux of cholesterol from cells – is associated with increased breast cancer risk [180]. Higher levels of LDL-bound cholesterol were observed in breast cancer patients compared to women without breast cancer, suggesting that an increase in cellular cholesterol uptake contributes to breast cancer risk [181]. Llaverias *et al.* demontrated that elevated plasma cholesterol accelerated breast tumour formation in a mouse model [182]. Interestingly, this study also showed reduced plasma cholesterol levels after tumour initiation, suggesting an increase in cholesterol utilization by tumour cells.

In addition to serum cholesterol, intracellular cholesterol is increased in cancer cells compared to untransformed cells [183]. In breast cancer, increased cholesterol synthesis mediated by the activation of the SREBP pathway induced cancer cell proliferation and self-renewal [184]. As previously mentioned, the SREBP pathway induces the expression of HMGCR, which increases cholesterol synthesis. SREBP also enhances the expression of squalene epoxidase, which is involved in cholesterol biosynthesis and is shown to be overexpressed in high grade, aggressive subtypes of breast cancer [185]. Intracellular cholesterol is also increased through the uptake of cholesterol. Cholesterol uptake is achieved through increased LDLR activity, which is associated with increased proliferation in TNBC cell lines [186]. In addition, repression of NPC1L1-mediated cholesterol uptake reduces β-catenin expression, inflammation, and protects against tumorigenesis in mice [187]. A reduction of cholesterol efflux increases cellular cholesterol levels by allowing cholesterol to accumulate in the cell. Inhibition of ABCA1 efflux protein caused by the overexpression of Ras and mutant p53 led to increased mitochondrial cholesterol levels in tumour xenografts, which decreased mitochondrial release of molecules that promote cell death, leading to increased cancer cell survival [188]. Furthermore, the cholesterol accumulation associated with ABCA1 knockdown contributes to aggressive prostate cancer progression [189].

The presence of cholesterol in the cell membrane and lipid rafts suggests that cholesterol may be closely associated with the function of membrane receptors, thereby affecting oncogenic signalling. An example of this is the direct activation of the Smoothened protein by cholesterol, activating the Hh signalling pathway, which is known to contribute to tumorigenesis [190]. Additionally, the binding of cholesterol to NHERF1/EBP50 activates the signal complex, contributing to the assembly of proteins of the PI3K/Akt and Wnt/β-

catenin pathways related to cancer cell proliferation and tumour formation [152]. Precursors and derivatives of cholesterol may also play a role in cancer progression. Mevalonic acid, a precursor to cholesterol, can activate PI3K, resulting in mTOR and NFκB activation in cancer [191]. 27-hydroxycholesterol (27HC), a primary metabolite of cholesterol, is shown to be a ligand for both ER and LXR, leading to ER-dependent growth and LXR-dependent metastasis in breast cancer [192]. 27HC also acts as an endogenous SERM, modulating the activity of ERα and Erβ and altering the expression of their target genes to promote cell growth [193]. 27HC is produced by the action of the sterol 27-hydroxylase CYP27A1, which is a target of endocrine treatment in breast cancer [194].

In addition to its role in cancer cell proliferation, elevated cholesterol may also be involved in drug resistance in cancer. Breast cancer cells that are long-term estrogen deprived (LTED), commonly observed during menopause, display resistance to AIs. LTED breast cancer cells that maintain ER expression are shown to have elevated expression of enzymes in the cholesterol biosynthesis pathway, as well as elevated 27HC levels, implicating cholesterol biosynthesis in the acquired resistance to endocrine therapy [195]. Furthermore, exposure to 27HC leads to the expression of genes associated with tamoxifen resistance in ERα-positive breast cancer [192]. Intracellular cholesterol accumulation leads to the expression of efflux pump proteins including ABCA1 and ABCG1. Overexpression of ABCA1 is observed in breast cancer cells resistant to curcumin-induced apoptosis [196]. ABCA1 expression is also associated with acquired chemotherapy resistance in ovarian cancer [197]. In hepatocellular carcinoma, failure to respond to oxaliplatin and saracatinib treatment is attributed to the upregulation of ABCG1 and the activation of Wnt signalling [198]. ABCG1 expression is also upregulated in aggressive, metastatic colon cancer cells and its depletion reduced tumorigenesis [199]. Accumulation of the cholesterol metabolite, 7-ketocholesterol, stimulated the efflux function of ABCB1 (also known as P-glycoprotein), resulting in doxorubicin resistance in MCF7 breast cancer cells [200]. The difference in expression levels of cholesterol-regulatory proteins in different tumour cell contexts emphasizes the complexity of the role cholesterol plays in cancer progression. Cholesterol accumulation plays a key role in the context of cancer cell proliferation, while the expression changes observed in cholesterol efflux pathways may be important in the context of drug resistance and metastasis.

1.3.4 Cholesterol in EMT and Metastasis

The exact mechanisms cholesterol plays in the initiation and maintenance of EMT, and metastasis is not yet established; however, emerging evidence suggests that a link may exist. The use of lovastatin is shown to reduces tumour growth and metastasis to the lungs in a mouse model of mammary carcinoma [201]. Additionally, pravastatin and fluvastatin have also been shown to prevent metastasis in hepatocellular carcinoma and renal cancer respectively [202, 203]. These studies demonstrate that lowering cholesterol synthesis reduces metastatic potential in different cancer types.

Increased cellular cholesterol may contribute to a metastatic phenotype in some cancer types. In a mouse model of melanoma, loss of function of PCSK9 in the liver lead to an increase in liver expression of LDLR, allowing more cholesterol to be removed from the bloodstream and excreted by the liver. This led to a reduction in liver metastasis, whereas increasing dietary cholesterol consumption resulted in increased metastasis, suggesting that increased cholesterol levels are associated with cancer metastasis [204]. Additionally, the downregulation of LDLR in hepatocellular carcinoma cells, while decreasing cellular cholesterol uptake, upregulated cholesterol biosynthesis in the cell, resulting in increased metastatic potential [205].

The cholesterol metabolite, 27HC is also implicated in enhancing metastatic potential of cancer cells. As mentioned previously, 27HC promotes LXR-dependent metastasis in breast cancer cells [192]. This coincided with the expression of EMT-related proteins and the induction of EMT-associated changes of morphology in breast cancer cells, suggesting that LXR activation by 27-HC may induce EMT and cause metastasis [192]. *In vitro,* exposure of MCF7 breast cancer cells to 27HC induced EMT [206]. In ERα-positive breast cancer patients, more 27HC is observed in tumour tissue compared to healthy tissue, and the growth and metastasis of these tumours is directly correlated with 27HC concentration [207].

Cholesterol is involved in numerous pathways linked to EMT induction. Cholesterol is shown to activate canonical Wnt signalling by facilitating the recruitment of the PZD domain of Dsh to the membrane [208]. The use of drugs that disrupt the cholesterol-rich lipid rafts reduced Wnt/β-catenin signalling [209]. As previously mentioned, cholesterol activates Hh signalling by modifying the Smoothened protein [190]. Hh signalling is active during embryogenesis and regulates EMT [210]. Additionally, TGFβ signalling seems to depend on the integrity of lipid rafts and the depletion of cholesterol from cells, which results in lipid raft disruption, is

shown to prevent the association of TGFβRI and TGFβRII, impeding TGFβ signalling and consequently, EMT induction [211]. In contrast, lowering cholesterol can enhance TGFβ signalling by increasing c-Jun expression and activation, which increases the expression of Smad2/3 [212]. In addition, statin use promotes TGFβ expression through SREBP1 activation, inducing EMT and poor patient prognosis in pancreatic cancer [213]. Furthermore, the CtBP transcriptional corepressor is shown to form a complex with ZEB1 and repress the transcription of *SREBF2*, which encodes SREBP2 [214]. This reduces intracellular cholesterol levels, which stabilize membrane TGFβ receptors, promoting TGFβ signalling and EMT. The ectopic expression of CtBP in breast cancer cells is correlated with increased lung metastasis [214]. The contradictory information regarding the role of cholesterol in EMT and metastasis necessitates further investigation to determine whether cholesterol depletion provides benefit or increased risk to in cancer treatment.

1.3.5 Statins and Their Use in Cancer Treatment

Cellular cholesterol levels can be reduced in several ways. Statins are the most used cholesterol-lowering drug in clinical practice. They are commonly used in the treatment of hypercholesterolemia. They function by competitively inhibiting HMGCR, preventing the conversion of HMG-CoA to mevalonate in the sterol biosynthetic pathway, thus inhibiting cholesterol synthesis [215]. By reducing cholesterol synthesis, statins have been effective in the treatment of cardiovascular disease and atherosclerosis, lowering the risk of heart attacks, strokes, and angina in patients with high cholesterol levels [215]. There are different types of statins, each differing slightly in structure and chemistry. Simvastatin, pravastatin, and lovastatin are fungal-derived, while pitavastatin, storvastatin, rosuvastatin, and cerivastatin are synthetically produced [216]. The addition of hydroxyl groups to statins such as pravastatin increases their hydrophilicity, whereas simvastatin and lovastatin remain lipophilic. Lipophilic statins have a greater ability to enter the cell membrane through passive diffusion, resulting in a higher cytotoxic potential, which may be beneficial in cancer treatment [217].

Due to the high cholesterol requirements of proliferating tumours, statins may be useful as a part of cancer therapeutic strategies. The anticancer properties of statins have gained attention, leading to research into their efficacy in cancer treatment [218]. *In vitro,* statins are shown to cause cell cycle arrest and inhibit the growth of cancer cells [219]. Statin use is also shown to induce apoptosis in cancer cells, as well as decrease metastatic properties [220, 221]. Notably, cancer cells undergoing EMT seem to be more sensitive to the apoptotic effect

of statins, demonstrated by the observed resistance in E-cadherin-expressing cells and the sensitivity of mesenchymal cells to statins [222]. The anticancer properties of statins are validated *in vivo* through a study that determined that statins inhibit breast tumour growth and proliferation in a mouse model [223]. Furthermore, a clinical trial evaluating the effect of statins on breast cancer risk found that statins may be associated with a lower incidence of breast cancer [224].

In addition to their cholesterol-lowering properties, statins exhibit additional effects that may aid in cancer treatment. One such effect is their ability to act as DNA methyltransferase inhibitors, demethylating the promoter of bone morphogenetic protein 2 (BMP2), activating the BMP signalling pathway, which is shown to induce differentiation of colorectal cancer cells [225]. This increases the chemosensitivity of colorectal cancer cells to 5 -fluorouracil treatment, demonstrating the utility of statins in combination with chemotherapy. In addition, the ability of statins to inhibit the mevalonate pathway prevents the nuclear localization of transcriptional regulators YAP and TAZ, which have been implicated in cancer growth, drug resistance, and metastasis, inhibiting their role in cancer cell proliferation and self-renewal [184].

Despite the potential of statins in cancer therapy, there are limitations in their use as a therapeutic drug. Statin use is limited by the associated side effects. Several musculoskeletal side effects have been reported following statin use including myositis, rhabdomyolysis, and other myopathies, for which the only treatment is discontinuation of statin use [226]. Additionally, the use of lipid lowering drugs including statins correlates with an increased risk of acute memory impairment [227]. Further, statins selectively localize to the liver and less than 5% of an orally administered statin dose enters the circulatory system, resulting in a low systemic availability and little chance that statins will act on tumour cells (Boudreau et al., 2010). Even though some clinical studies determined that statins are beneficial in cancer therapy, contradictory studies find no protective effect of statins in lung, breast, or colorectal cancers [228, 229], while other studies find that statin use correlates with a slightly increased risk of colorectal, bladder, and lung cancers [230]. Efficacy and safety of statin use may also differ depending on age, sex, and race. A recent meta-analysis suggested that people of older age, female sex, and African and Asian races had a higher risk of being intolerant to statin treatment, showing a greater risk of developing severe side effects [231]. Based on the available evidence, there is no clear answer as to whether statin use is beneficial or

detrimental to cancer risk; however, there is enough promising evidence of the benefits of lowering cholesterol levels in cancer treatment to warrant further investigation.

1.3.6 Alternatives to Statins for Lowering Cholesterol

While statins are the most prescribed cholesterol-lowering drug, other compounds exist that deplete cholesterol levels without inhibiting its synthesis, such as cyclodextrins. Cyclodextrins are cyclic oligosaccharides produced by enzymatically treating starch. The 3 main types of cyclodextrins, α-, β-, and γ-cyclodextrins, are produced in a mixture consisting of all three types in a ratio that depends on the specific cyclodextrin glycosyltransferase enzyme used [232]. This is followed by purification of each cyclodextrin, which makes use of their different solubilities. Cyclodextrins can be chemically modified through methylation, acetylation, or hydroxypropylation.

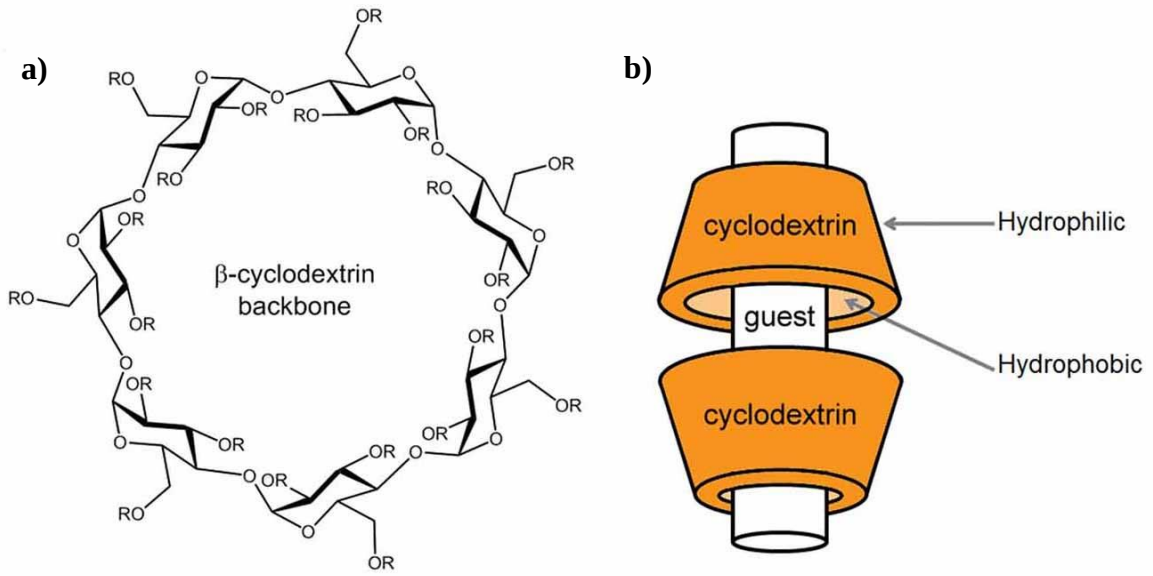

Figure 4: Basic structure of a β-cyclodextrin and formation of a complex with a guest compound. (a) The chemical structure of a β-cyclodextrin backbone with chemical substitution groups depicted as R, which are replaced with different chemical groups during the modification process (b) Illustration of the interaction between cyclodextrins and guest compounds modelled from the interaction between hydroxypropyl-beta-cyclodextrin (HPβCD) and cholesterol. One cholesterol molecule is encapsulated in the hydrophobic interior of a cyclodextrin dimer, and the hydrophilic exterior allows for solubilisation. [Source: Crumline *et al.*, 2017, accessed 20 February 2023].

Cyclodextrins have found use in a diverse range of industries due to their ability to hold guest compounds. They are considered safe for consumption by the FDA, which has given them the "Generally Recognized as Safe" (GRAS) label for consumption by humans (FDA; GRAS Notice No. GRN 000155, 000074, and 000046). The ability of cyclodextrins to form

inclusion complexes gives them utility in pharmaceutical applications in which they can increase the solubility and stability of delivered drugs and act as scavenging compounds to bind and inactivate compounds in the blood [233]. The ability to solubilize compounds is due to the hydrophobic interior of cyclodextrins, which encapsulates guest compounds, and the hydrophilic exterior, which allows the complex to dissolve in aqueous solution, shown in Figure 1.4.

The most studied cyclodextrin in cell biology is methyl-β-cyclodextrin (MβCD). Unlike statins, MβCD does not block the synthesis of cholesterol, but rather binds cholesterol in its hydrophobic cavity, solubilising cholesterol in water [234]. The addition of the methyl group makes MβCD more efficient than unmodified β-cyclodextrins at removing cholesterol from cells [235]. Hydrophobic cholesterol molecules fit inside the cyclodextrin ring, allowing MβCD to disrupt lipid rafts by removing cellular membrane cholesterol [236]. MβCD has demonstrated the ability to deplete up to 100% of membrane cholesterol, depending on treatment time, concentration, and cell type, as well as the ability to influence intracellular cholesterol levels as a response to membrane cholesterol depletion [237]. It has been shown to suppress tumour growth in a mouse model of colorectal cancer [238]. In addition, it has been shown to enhance the efficacy of other cancer drugs, such as carboplatin, tamoxifen, and 5-fluorouracil [239, 240]. One issue concerning the use of MβCD is the potential effects on non-cancer cells, with a study showing significant cytotoxicity on non-tumorigenic cells at higher concentrations [241]. Nevertheless, cyclodextrins provide an alternative to statins for cancer treatment and require further study to formulate an effective treatment strategy.

Like MβCD, hydroxypropyl-beta-cyclodextrin (HPβCD) is a β-cyclodextrin with the ability to solubilize cholesterol in aqueous solution. HPβCD forms a dimer with a hydrophobic cavity in which one cholesterol molecule is encapsulated [233]. It has improved solubility and is more toxicologically benign compared to other cyclodextrins [242]. It has shown potential in the treatment of atherosclerosis, where it reduced the size of atherosclerotic plaques in mice, even with a cholesterol-rich diet [243]. There is also evidence that HPβCD may have use in the treatment of Alzheimer disease, where in cell and mouse models treatment with HPβCD is shown to promote amyloid-β clearance, improve learning and memory deficits in mice, and reduce tau immunoreactive dystrophic neurites [244]. HPβCD has received attention for its potential use in the treatment of Niemann-Pick Type C Disease, which is a disease characterized by intracellular accumulation of unesterified cholesterol and other lipids. In a study evaluating drug combinations, HPβCD alone showed potential to

reduce symptoms and increase the lifespan of mouse models of Niemann-Pick Type C Disease [245]. The FDA has approved the use of HPβCD for the compassionate treatment of Niemann-Pick Type C Disease, which has since shown to reduce the progression of this disease in clinical trials [246]. Recognising its potential in treating cholesterol-related diseases, we proposed that HPβCD may have potential in treating cancer, which involves intracellular cholesterol accumulation. Studies in our lab have demonstrated depletion of intracellular cholesterol from MCF7 and MDA-MB-231 breast cancer cells, as well as significant tumour size reduction in a mouse xenograft model of ER- breast cancer with no toxicity in non-tumorigenic cells, leading to a patent for the preparation of a pharmaceutical composition comprising HPβCD and its use in treating breast cancer (https://patents.justia.com/patent/20220096529). We hypothesize that HPβCD may reverse the effects of EMT and reduce tumour metastasis and drug resistance.

Another cholesterol-depleting agent is Acetyl Plumbagin (AP), a derivative of Plumbagin (PL). Plumbagin is a naphthoquinone derived from the roots of the *Plumbago zeylanica* plant with antiproliferative and anticancer activity [247]. AP displays lower toxicity than Plumbagin in normal cells, but significantly inhibits the breast cancer cell growth [248]. Although the mechanisms of AP are not known, its action as a cholesterol depleting agent has been shown [249]. Cholesterol depletion using AP resulted in an increase in mitochondrial-mediated apoptosis, indicating that AP could be a novel treatment for breast cancer, targeting cholesterol accumulation.

1.4 **Problem Statement**

Metastatic breast cancer is a leading cause of mortality in women globally, with few treatment options and a high risk of treatment failure and relapse. To date, most cancer treatment options target highly proliferative cells with few options specifically targeting the non-proliferative cells implicated in metastasis, drug resistance, and relapse. The shift between a proliferative phenotype and invasive and drug-resistant phenotypes is caused, in part, by the induction of EMT through various signalling pathways. With increasing evidence of the role EMT plays in metastasis and drug resistance, novel research has emerged, demonstrating the efficacy of EMT pathway inhibition in cancer treatment [250]. Preventing the induction of EMT has proved successful in reducing drug resistance and metastatic events in recent research; however, few studies present a viable strategy for the reversal of the EMT phenotype. Furthermore, currently proposed methods of EMT inhibition rely on blocking specific proteins or miRNAs, which may not be effective in all cases of cancer.

In addition to EMT, cholesterol is shown to play a pivotal role in the development and progression of cancer. Several studies have emerged showing the role cholesterol and its metabolites play in cancer cell proliferation, metastasis, and drug resistance [177]. As previously mentioned, studies investigating the effect of cholesterol-lowering drugs in cancer treatment have been conducted. These studies show that cholesterol-lowering drugs have potential in enhancing the effect of currently available cancer therapeutics, as well as reducing drug resistance and metastasis. Although there have been efforts to delineate the role of cholesterol pathways in EMT [251], its role in the induction and maintenance of the EMT phenotype is still not fully understood. Additionally, the effect of cholesterol-lowering drugs in reversing the EMT phenotype has not been fully explored.

It is the aim of the present study to further elucidate the mechanisms of cholesterol-related signalling pathways in the context of EMT and metastasis. This was achieved using the Namru Mus musculus Mammary Gland (NMuMG) *in vitro* model, which was induced to undergo EMT using TGFβ treatment. Changes in cholesterol levels and cholesterol-associated gene expression were compared pre- and post-EMT induction. Cholesterol levels were lowered using simvastatin, MβCD, and HPβCD, followed by analysis of gene expression, cell viability, and invasive potential. This research aims to assess the importance of cholesterol in EMT and evaluate the efficacy of cholesterol depletion treating metastatic cancer.

1.5 Aims and Objectives

1.5.1 Aims

1. To characterize EMT *in vitro.*
2. To assess changes in cellular cholesterol levels during EMT induction.
3. To determine the effects of cholesterol depletion in EMT and metastasis.
4. To elucidate the molecular mechanisms of cholesterol regulatory pathways in EMT.

1.5.2 Objectives

Aim 1

1. To induce and characterise EMT *in vitro* using the NMuMG model of EMT.
2. To confirm EMT induction by assessing EMT-associated gene expression.

Aim 2

1. To visualise the cellular cholesterol, lipid raft cholesterol, and cholesteryl esters levels pre- and post-EMT and in response to treatment with cholesterol-lowering drugs using confocal microscopy.
2. To quantitatively measure cholesterol levels pre- and post-EMT

Aim 3

1. To determine the effect of cholesterol depletion on EMT cell morphology
2. To measure changes in cell viability pre- and post-EMT in response to treatment with cholesterol-lowering drugs.
3. To determine the effect of cholesterol depletion on the invasive potential of cells post-EMT.
4. To determine changes in proliferative potential pre- and post-EMT by measuring expression of Ki67.

Aim 4

1. To determine changes in transcriptional expression of cholesterol and EMT associated genes in cells pre- and post-EMT in response to cholesterol-lowering drugs using RT-qPCR.
2. To determine changes in EMT and cholesterol related protein expression in cells pre- and post-EMT in response to cholesterol-lowering drugs using Western blotting.

Chapter 2: MATERIALS AND METHODS

2.1 Cell Culture

NMuMG cells (ATCC: CRL-1636) were a gift from Theresa Vincent lab at Uppsala University, Sweden. NMuMG cells are nontransformed mouse mammary gland epithelial cells [252]. The cell line was maintained in Dulbecco Modified Eagle's media (DMEM, Gibco/ThermoFisher Scientific, USA), supplemented with 10% foetal bovine serum (Gibco/ThermoFisher Scientific, USA), 1% penicillin-streptomycin (Gibco/ThermoFisher Scientific, USA), 1% GlutaMAX (Gibco/ThermoFisher Scientific, USA), and 10 μg/mL insulin (Sigma-Aldrich, UK) and incubated at 37 °C and 5% carbon dioxide (CO_2). Cells were subcultured using the TrypLE Express (Gibco/ThermoFisher Scientific, USA) cell dissociation reagent. Media was removed from the cell culture flask, followed by the addition of 1X phosphate buffered saline (PBS) to wash the adherent cells. PBS was discarded and TrypLE Express was added to the flask followed by incubation at 37 °C and 5% CO_2 for up to 5 minutes to detach cells from the flask surface. The dissociation reagent was neutralized using an equal volume of cell culture media and the cell suspension was removed for use in experiments and cell culture maintenance. The cell line was maintained at a passage number of between 4 and 10.

2.2 EMT Induction

NMuMG cells were used in this study because they exhibit a well-documented EMT response to TGFβ treatment [252]. NMuMG cells were treated with 10 ng/mL of the recombinant human TGFβ protein (R&D Systems, USA), followed by incubation at 37 °C and 5% CO_2 for 48 hours prior to analysis to induce EMT, as documented in literature [252]. Changes in morphology were observed using a Nikon Phase Contrast microscope (Nikon Imaging, Japan), showing a change in cell shape from a rectangular epithelial shape to a spindle-like mesenchymal shape.

2.3 Cell Counting

To ensure equal and consistent seeding density for experiments, cell counting was performed before each experimental setup. Cells were counted using the Neubauer haemocytometer. Following cell detachment, 100 μL of the cell suspension was removed and combined with 100 μL of 0.4% Trypan Blue (Gibco: Life Technologies, USA). 10 μL of the mixture was added to the chamber of the haemocytometer and cells were viewed and counted using a Nikon Phase Contrast Microscope. Cell viability was estimated using Trypan Blue exclusion

in which the intact membrane of viable cells prevents the entry of the dye into the cell leaving viable cells colourless and inviable cells blue. After counting cells in the four corner squares of the haemocytometer grid, cell counts were added and used to calculate cell concentration in suspension as follows:

$$Concentration\ (cells/mL) = \frac{Total\ Cell\ Count\ \times 10\ 000}{Number\ of\ Squares\ \times Dilution\ Factor}$$

Cell viability was then calculated as follows:

$$Cell\ viability\ (\%) = \frac{Unstained\ Cell\ Count\ \times 100}{Total\ Cell\ Count}$$

The concentration of viable cells was calculated by multiplying the percentage of cell viability by the total cell concentration. This was used to seed culture dishes for further experiments. Cell counts were performed in triplicate and the average of the calculated concentrations was used.

2.4 Cholesterol-Lowering Treatment

After seeding cells at the appropriate density and allowing for attachment overnight, cells were treated with cholesterol-lowering compounds for experimental comparison. To keep the 48-hour EMT induction period consistent, cells were treated during EMT induction with 24-hour treatments added 24 hours after TGFβ addition and 2-hour treatments added 46 hours after TGFβ addition. This ensured that drug treatments were complete at the same time as the 48-hour EMT induction period. MβCD was used at a concentration of 1 mM, HPβCD was used at a concentration of 10 mM, and simvastatin was used at a concentration of 10 μM. The concentrations of MβCD and HPβCD used were determined by previous unpublished experiments to deplete cholesterol in epithelial cells without causing significant cell death. The lowest concentration of simvastatin to induce HMGCR inhibition was selected from literature [253].

2.5 Microscopy Sample Preparation

To fluorescently label molecules of interest in the cell, samples need to be prepared for microscopy and mounted on glass coverslips. Following cell detachment and counting, cells were seeded at a density of 10 000 cells/well on 12 mm circular glass coverslips in a 24-well plate and allowed to attach overnight. EMT induction and cholesterol-lowering treatments were administered as described above. After treatment, media was discarded from the wells and adherent cells were washed three times with 1X PBS. The cells were fixed to the coverslips with 4% formaldehyde (Sigma Aldrich, UK) diluted in PBS for 15 minutes at room temperature. Coverslips were washed three times with 1X PBS and used for staining in future experiments.

Formaldehyde fixing is a method of preserving biological samples, preventing decomposition and terminating biochemical reactions. It preserves the integrity and spatial position of proteins, carbohydrates, and lipids, allowing them to be studied through microscopy [254]. Formaldehyde reacts with the primary amines of proteins, causing covalent bond formation between proteins in a process called crosslinking, which anchors proteins to the cytoskeleton and preserves the structure of the cell [255]. It is not known to cause excessive shrinkage or distortion of organelles in the cell [254]. Fixed samples can be stained using antibodies or targeted dyes, which will be described below.

2.6 Immunocytochemistry

Immunocytochemistry is a technique used to visualize the location and abundance of specific proteins in the cell. The indirect method of immunofluorescent staining was performed, in which an unconjugated primary antibody is used that binds to the target epitope of the protein of interest. This is followed by incubation with a secondary fluorophore-conjugated antibody that binds to the primary antibody. Although more time consuming, indirect immunofluorescence is preferred due to higher sensitivity and signal amplification [256]. To prevent cross-reactivity between antibody and endogenous immunoglobulins, it is preferable to use a primary antibody derived from a different species than the sample tissue or cells. For the same reason, the secondary antibody needs to be derived from a different species than that of the primary antibody. The secondary antibody provides the signal through excitation of the conjugated fluorophore, which emits light at a frequency detectable by fluorescent microscope sensors, allowing for the visualization of specific proteins in sample cells.

Following preparation and fixation, cells were permeabilized using 0.1% Triton X-100 (Sigma Aldrich, UK), diluted in 1X PBS, for 15 minutes at room temperature. Triton X-100 is a non-ionic surfactant capable of breaking lipid-lipid and protein-lipid interactions, while leaving protein-protein interations intact [257]. It disrupts the cell and nuclear membranes, allowing larger molecules such as antibodies to pass through. After permeabilization, Triton X-100 was discarded, and a blocking step was performed in which 1% bovine serum albumin (BSA) in 0.1% PBST (1X PBS with 0.1% Tween-20) was added to the samples for 1 hour at room temperature. Despite the high affinity of the antibody to the target epitopes, intermolecular forces may cause binding to non-specific sites. Blocking prevents non-specific binding by binding to non-specific sites before antibodies are introduced. Tween-20 is a non-ionic detergent used at a low concentration in the blocking buffer and in subsequent wash steps to prevent weak and non-specific protein-protein interactions that could cause non-specific antibody binding or background fluorescence.

After blocking, the primary antibody specific to the protein of interest, diluted in 0.1% BSA in 0.1% PBST, was added to each well and allowed to bind to the target overnight on an orbital shaker at 4°C (primary antibody dilution factors shown in Table 1). The primary antibody was then removed, and cells were washed three times in 0.1% PBST. Cells were stained with secondary antibody diluted in 0.1% PBST for 45 minutes at room temperature (secondary antibody dilution factors shown in Table 2). The secondary antibody solution was removed, and each coverslip was washed three times with 0.1% PBST. Nuclei were stained using 4′,6-diamidino-2-phenylindole (DAPI) (Sigma Aldrich, UK), which binds to the minor groove of double stranded DNA with a strong affinity to adenine-thymine-rich regions. It is detected through its emission spectrum peaking at 461 nm when excited by in the ultraviolet (UV) range peaking at 359 nm. DAPI was diluted in 1X PBS to 0.1 μg/mL and added to each well for 10 minutes at room temperature. Cells were washed three times with 1X PBS and coverslips were mounted on microscope slides using Fluoromount™ Aqueous Mounting Medium (Sigma Aldrich, UK). After drying, cells were visualized with the Floid™ Cell Imaging System (Thermo Fisher Scientific, US) and the LSM 710 confocal microscope (Zeiss, Germany).

Table 1: Primary antibodies

Target	Source	Target Size (kDa)	Vendor	Immunofluorescence Dilution	Western Dilution
β-Tubulin	Mouse monoclonal	50	Sigma-Aldrich, UK		1:1000
E-cadherin	Mouse monoclonal	60	BD Biosciences, US	1:250	1:1000
Vimentin	Rabit monoclonal	54	Abcam, Biocom Africa, SA	1:250	1:1000
N-cadherin	Rabit monoclonal	100	Abcam, Biocom Africa, SA	1:250	1:1000
ABCG1	Rabbit monoclonal	100	Abcam, Biocom Africa, SA		1:1000
SREBP1	Rabbit polyclonal	125 and 68	Novus Biologicals, Whitehead Scientific, SA		1:1000
SREBP2	Rabbit polyclonal	125, 68, and 58	Novus Biologicals, Whitehead Scientific, SA		1:1000
Ki-67	Rabbit monoclonal	359	Novus Biologicals, Whitehead Scientific, SA	1:250	
HMGCR	Rabbit monoclonal	100	Novus Biologicals, Whitehead Scientific, SA		1:1000
LXRα	Rabbit polyclonal	55	Novus Biologicals, Whitehead Scientific, SA		1:1000

Table 2: Secondary antibodies

Antibody name	Source	Vendor	Dilution
Rabbit IgG – Texas Red conjugate	Goat	Thermo Fisher Scientific, USA	1:1000
Mouse IgG – AlexaFluor 488 conjugate	Goat	Thermo Fisher Scientific, USA	1:1000
Mouse IgG (H+L)-HRP conjugate	Goat	Bio-Rad, USA	1:5000
Rabbit IgG (H+L)-HRP conjugate	Goat	Bio-Rad, USA	1:5000

2.7 Filipin Staining

Filipin is a fluorescent polyene antibiotic naturally produced by the bacterium *Streptomyces filipinensis* as an antifungal compound. Filipin binds to free, unesterified cholesterol in cell membranes, where it can be detected by its emission of 480 nm light when excited at 360 nm [258]. Filipin is useful for the detection and quantification of cellular cholesterol, as the brightness of filipin labelling has been correlated with chemically measured cellular cholesterol levels [259]. In this study, filipin was used to detect and estimate cholesterol levels in fixed cell samples pre- and post-EMT and with cholesterol-lowering treatments.

Cells were seeded on glass coverslips in a 24-well plate, underwent EMT induction, and were treated and fixed as described above. A working solution of 0.05 mg/mL of Filipin III (Sigma Aldrich, UK) diluted in 1X PBS was added to each well and incubated in the dark for 2 hours. Coverslips were washed three times with 1X PBS and nuclei were stained red using NucRed™ Dead 647 (Thermo Fisher Scientific, USA) in 1X PBS for 10 minutes at room temperature in the dark. NucRed™ Dead 647 emits light peaking at 661 nm when excited at a range peaking at 642 nm. Cells were washed three times with 1X PBS and coverslips were mounted on microscope slides using Fluoromount™ Aqueous Mounting Medium (Sigma Aldrich, UK). After drying, cells were visualized with the Floid™ Cell Imaging System (Thermo Fisher Scientific, USA) and the LSM 710 confocal microscope (Zeiss, Germany).

2.8 BODIPY Lipid Droplet Staining

BODIPY™ 493/503 (4,4-Difluoro-1,3,5,7,8-Pentamethyl-4-Bora-3a,4a-Diaza-s-Indacene) (Thermo Fisher Scientific, USA) is a non-polar, lipophilic fluorophore that can detect the presence of cholesteryl esters (CEs) in cellular lipid droplets. Excitation at 493 nm causes it to emit a green fluorescence peaking at 503 nm. Cells were seeded on glass coverslips in a 24-well plate, underwent EMT induction, and were treated and fixed as described above. Cells were permeabilized using 0.1% Triton X-100 (Sigma Aldrich, UK), diluted in PBS, for 15 minutes at room temperature to allow for dye uptake. Triton X-100 was removed and 1 μL/mL of BODIPY™ 493/503 diluted in 1X PBS was added to each well, followed by incubation at 37°C for 30 minutes. The BODIPY™ 493/503 solution was removed, and coverslips were washed three times with 1X PBS. Nuclei were stained blue with 0.1 μg/mL DAPI in 1X PBS for 10 minutes at room temperature, followed by three washes with 1X PBS. Coverslips were mounted on microscope slides using Fluoromount™ Aqueous Mounting Medium (Sigma Aldrich, UK). After drying, cells were visualized with the Floid™ Cell Imaging System (Thermo Fisher Scientific, USA).

2.9 Vybrant Alexa Fluor 594 Lipid Raft Staining

The Vybrant Alexa Fluor 594 Lipid Raft Labelling Kit fluorescently labels lipid rafts in both live and fixed cells. It makes use of the Alexa Fluor 594 fluorophore conjugated to cholera toxin subunit B, which binds specifically to the plasma membrane ganglioside GM1 (monosialotetrahexosylganglioside), which selectively partitions into membrane lipid rafts. An antibody specific to cholera toxin subunit B is introduced to crosslink labelled lipid rafts into distinctive patches, which are easily visualized by fluorescent microscopy. The fluorophore, Alexa Fluor 594, has absorbance and emission maxima of 590 nm and 617 nm, respectively.

Cells were seeded on glass coverslips in a 24-well plate, underwent EMT induction, and were treated and fixed as described above. Cells were permeabilized using 0.1% Triton X-100 (Sigma Aldrich, UK), diluted in PBS, for 15 minutes at room temperature to allow for stain uptake. Lipid rafts were stained adding 1 μL/mL Alexa Fluor® 594 CT-B conjugate diluted in 1X PBS to each well and incubating at 37 °C for 30 minutes. The conjugate solution was removed from each well and coverslips were washed three times in 1X PBS. Anti-cholera toxin subunit B antibody was diluted to 1:500 in 1X PBS and added to each well, followed by incubation at 37 °C for 30 minutes. Coverslips were washed three times with 1X PBS and

mounted on microscope slides using Fluoromount™ Aqueous Mounting Medium (Sigma Aldrich, UK). After drying, cells were visualized with the Floid™ Cell Imaging System (Thermo Fisher Scientific, USA).

2.10 Quantification of Fluorescence Intensity

Although fluorescence microscopy is an intrinsically qualitative method of analysis, methods exist that allow for quantification of the fluorescence intensity of micrograph images. While these methods do not replace truly quantitative methods like the enzyme-linked immunosorbent assay (ELISA), they are useful in determining statistical significance of image data and removing unintentional bias in image and cell selection. Quantification of fluorescence intensity was performed using ImageJ image processing software (developed by National Institutes of Health, USA and the Laboratory for Optical and Computational Instrumentation, USA). For each treatment condition, 3 coverslips were plated, acting as technical replicates. For each coverslip, 10 images were captured of random fields on the coverslip. 10 cells were selected at random from each image, meaning the total number of cells quantified per treatment condition per experimental repeat was 300 (n=300). In the ImageJ software, images were separated into their colour channels, allowing the emission spectrum of interest to be quantified. Cells were selected using the drawing tool and analysed, yielding area integrated intensity and mean grey value of the selection. Background fluorescence was corrected for by selecting the area next to each cell without fluorescence and taking the mean of these values. Corrected total cell fluorescence (CTCF) was calculated for each cell as follows:

$$CTCF = Integrated\ Density - (Area\ of\ selected\ cell \times mean\ background\ fluorescence)$$

The mean CTCF was used as the intensity value for each treatment condition with standard deviation and statistical significance calculated on the individual values.

2.11 Cholesterol Quantitation Assay

As a quantitative measure of cellular cholesterol content, the Cholesterol Quantitation Kit (Sigma Aldrich, UK) was used. NMuMG were seeded in a 6-well plate at 3 x 10^5 cells per well, allowed to attach in an incubator at 37 °C overnight, underwent EMT induction. Cholesterol standards were prepared for colorimetric detection to construct a standard curve

using concentrations of 0, 1, 2, 3, 4, and 5 μg/mL of cholesterol. Cell samples were detached and counted, and 1 x 10^6 cells for each condition were transferred to separate tubes and pelleted by centrifugation, discarding the supernatant. Cells were extracted using 200 μL of chloroform:isopropanol:IGEPAL CA-630 mixed to a ratio of 7:11:0.1 and agitating with a vortex mixer. Samples were centrifuged at 13 000 × *g* for 10 minutes to remove insoluble materials. The organic phase was transferred to a new tube and allowed to dry at 50 °C to remove organic solvents. Dried lipids were dissolved in 200 μL of Cholesterol Assay Buffer (Sigma Aldrich, UK). Reactions were set up in a 96-well plate, adding 50 μL of each sample and the standards to each well in triplicate. An equal volume of Reaction Mix, made up of 46 μL Cholesterol Assay Buffer, 2 μL Cholesterol Probe, and 2 μL Cholesterol Enzyme Mix, was mixed with each sample. The plate was incubated at 37 °C for 1 hour and absorbance at 570 nm of each well was measured. Total cholesterol mass was calculated using the absorbance of the sample and the standard curve, correcting for dilution.

2.12 Invasion Assay

The invasive potential of NMuMG cells was measured using a Transwell invasion assay. This measures the ability of the cells to attach to and invade through a basement membrane extract, mimicking the first step of metastasis *in vitro.* Before the experiment, cells were preincubated in a 6-well plate, induced to undergo EMT, treated with cholesterol-lowering compounds, detached, and counted as described above. The invasion assay was prepared by inserting the 24-well plate inserts (0.8 μm pore size; BD Bioscience, USA) and coating them with Geltrex basement membrane mix (Thermo Fisher Scientific, UK) diluted to 2 mg/mL of protein using serum-free growth medium (not containing FBS). The insert has a membrane with 0.8 μm pore that invasive cells can pass through. Geltrex contains components of the extracellular matrix (ECM), laminin, collagen IV, entactin, and heparin sulphate proteoglycans, which act as a basement membrane through which invasive cells are required to pass. The Geltrex was allowed to polymerise at 37 °C for 30 minutes. 500 μL of complete medium (containing 10% FBS) was added to the lower chamber of the plate, acting as a chemoattractant for invasive cells. Cells were pelleted through centrifugation and resuspended in serum-free growth medium at a density of 1 × 10^5 cells/mL. Cell suspension mixture was added to the upper chambers of the plate and incubated at 37 °C for 24 hours. Non-invasive cells were removed from the top of the membrane using a cotton swab and invasive cells were fixed to the bottom of the membrane with 4% formaldehyde at room temperature for 10 minutes. Inserts were washed three times in 1X PBS and nuclei of

attached cells were stained using 0.1 μg/mL DAPI diluted in 1X PBS at room temperature for 10 minutes. The membrane was removed from the insert and mounted to a microscope slide using Fluoromount™ Aqueous Mounting Medium (Sigma Aldrich, UK). After drying, cells were viewed with the Floid™ Cell Imaging System (Thermo Fisher Scientific, USA). Images were captured of 10 fields per treatment condition and all cells were counted in each field. Counts were averaged and used to calculate the percentage invasion relative to experimental control. Each experiment was performed on three biological replicates.

2.13 Cell Viability Assay

The viability of cells after treatment with cholesterol-lowering drugs was measured relative to an untreated control. The cell viability assay used relies on the reduction of the yellow tetrazolium dye 3-(4,5-dimethylthiazol-2-yl)-2,5-diphenyltetrazolium bromide (MTT) to an insoluble purple formazan, catalysed by succinate dehydrogenase in the mitochondria of metabolically active cells [260]. The MTT assay is a colorimetric assay in which spectrophotometric measurement of formazan production is proportional to the viability of cells. In this study, the MTT assay was used to assess cytotoxicity and growth inhibition caused by cholesterol-lowering compounds.

Cells were seeded in a 96-well plate at a density of 5 000 cells per well and allowed to attach overnight in an incubator maintained at 37 °C and 5% CO_2. EMT induction and treatment with cholesterol-lowering compounds were performed as described above. MTT (Sigma-Aldrich, USA) stock solution diluted in 1X PBS was added to each well to a final concentration of 0.5 mg/mL and incubated at 37 °C for 3 hours. Formazan was dissolved in 10% sodium dodecyl sulphate (SDS) (Sigma-Aldrich, UK) with 10 mM hydrochloric acid (HCl) at 37 °C overnight. Formazan formation was measured by spectrophotometrically quantifying the sample absorbance at 570 nm using the Multiskan GO Microplate Reader (Thermo Fisher Scientific, SkanIt™ software). Viability of each treated sample was calculated as a percentage relative to the untreated control. Plumbagin (5-hydroxy-2-methyl-1,4-naphthoquinone), a known cytotoxic compound, was used as a positive control for cell growth inhibition at a concentration of 40 μM. Each experiment was repeated three times with each repeat containing three technical replicates for each treatment condition. To assess the quality of the assay, the Z-prime factor (Z'-factor) was calculated for each experiment, which determines the likelihood of false positives or negatives by describing how well-separated negative and positive controls are, using the following formula:

$$Z'factor = 1 - \frac{3 \times (\sigma_p + \sigma_n)}{|\mu_p - \mu_n|}$$

Where σ_p is the standard deviation of the positive control replicates, σ_n is the standard deviation of the negative control replicates, μ_p is the mean of the positive control replicates, and μ_n is the mean of the negative control replicates. The results of an experimental repeat were used if Z' factor was greater than 0.6, where 0 means that positive and negative values overlap, making the assay unusable, $0 < Z' \leq 0.5$ represents poorly separated negative and positive controls and a Z' value above 0.5 is considered acceptable.

2.14 RNA Extraction

RNA was extracted from cells for quantification using the Direct-zol™ RNA MiniPrep kit (Zymo Research, Inqaba Biotec™, SA). Cells were seeded in a 6-well plate at 3 x 10^5 cells per well, allowed to attach in an incubator at 37 °C overnight, underwent EMT induction and were treated with cholesterol lowering compounds as described above. The cells were detached and pelleted, discarding the supernatant, and washed with 1X PBS, discarding the wash. TRIzol® Reagent (Invitrogen™, Thermo Fisher Scientific, USA) is a solution of guanidium isothiocyanate and phenol that solubilises cell membranes and denatures proteins. This is used to lyse the cells and release nucleic acids for extraction. Each cell pellet was resuspended in 300 µL of TRIzol® Reagent, pipetting up and down to aid the lysing process. An equal amount of 99.9% ethanol was added to precipitate nucleic acids. Samples were transferred to Zymo-Spin™ II CR Columns placed in collection tubes and centrifuged at 12 000 × g for 30 seconds. The flow-through was discarded and columns were washed with 400 µL of Direct-zol™ RNA wash buffer. To degrade genomic DNA, a 1:5 dilution of DNase I in DNA digestion buffer was added to each column matrix for 15 minutes at room temperature. Samples were washed twice using Direct-zol™ RNA PreWash buffer, centrifuging at 12 000 × g for 30 seconds after each wash and discarding flow-through. A final wash was performed using 700 µL of Direct-zol™ RNA wash buffer, followed by centrifugation at 12 000 × g for 2 minutes, discarding the flow-through and the collection tubes. Columns were transferred to new nuclease-free tubes and RNA was eluted by adding nuclease-free water to each column and centrifuging at 12 000 × g for 30 seconds. RNA samples were stored at -80°C when not in use.

2.15 Assessing RNA Purity and Integrity

The concentration and purity of RNA samples were assessed using the NanoDrop™ One/One C Microvolume UV-Vis Spectrophotometer (Thermo Fisher Scientific, USA). Absorbance at wavelengths of 230 nm, 260 nm, and 280 nm were taken, and the concentration (ng/μL) and purity of RNA were calculated. Purity was assessed using the A_{260}/A_{280} ratio to determine the presence of salt, carbohydrates, protein, phenol, and other contaminants, and A_{260}/A_{230} ratio to determine guanidine thiocyanate contamination from the use of TRIzol® Reagent. An A_{260}/A_{280} ratio of ~2.0 and an A_{260}/A_{230} ratio between 2.0 and 2.2 was considered acceptable for use.

RNA integrity was assessed using agarose gel electrophoresis. A 1% (weight/volume) agarose gel was made using agarose powder (BioConcept, Switzerland) in 1X tris-borate-EDTA (ethylenediaminetetraacetic acid) (TBE) buffer and adding 0.5 μg/mL ethidium bromide (Protea Laboratory Solutions, SA). TBE buffer consists of Tris base, boric acid, and EDTA, prepared according to Table S4. Ethidium bromide intercalates double-stranded DNA and RNA, acting as a fluorescent tag for nucleic acids when excited with UV light. After preparing and setting the gel in a gel cast, 500 ng of RNA from each sample mixed with an equal volume of 2X RNA loading dye (Thermo Fisher Scientific, USA) was loaded into the wells of the gel. RiboRuler High Range RNA Ladder (Thermo Fisher Scientific, USA) was loaded into the gel to determine the size of RNA bands. Gel electrophoresis was run at 80 volts for 40 minutes, followed by visualisation on the ChemiDoc XRS+ System (Bio-Rad, USA). RNA integrity was assessed by the presence of sharp 28S and 18S ribosomal RNA (rRNA) bands of sizes approximately 5 000 base pairs and 2 000 base pairs respectively, and a lack of high molecular weight genomic DNA contamination, as well as a lack of smearing caused by RNA degradation.

Table 3: TBE buffer components

	Components for 1 L
10X TBE buffer	108g 1 M Tris base 55g 1 M Boric acid 7.5g 0.02 M EDTA Dissolved in 900 mL of dH_2O Adjusted to pH 8 Made up to 1 L with dH_2O
1X TBE buffer	100 mL 10X TBE buffer 900 mL dH_2O

2.16 cDNA synthesis

cDNA was synthesized from extracted RNA for use in downstream quantitative assays. The RevertAid First Strand cDNA Synthesis Kit (Thermo Fisher Scientific, USA) was used to synthesise cDNA, making use of the RevertAid Reverse Transcriptase (RT), which is a modified version of the reverse transcriptase from the Moloney murine leukaemia virus, which is active at 42°C and can synthesise up to 13 kilobases (kb) of cDNA. The cDNA synthesis reaction was prepared for each RNA sample by mixing the components listed in Table 3.x in microcentrifuge tubes. The concentration of each RNA sample determined above was used to determine the volume needed for 1 µg of RNA (x) and the reaction solution was made up to 20 µL with nuclease-free water. The tubes were placed in a T100™ Thermal Cycler set to 42 °C for 1 hour, followed by 70 °C for 5 min and cDNA was stored at -20 °C.

Table 4: Components of cDNA synthesis reaction

Reaction Components	Volume (µL)
5X Reaction Buffer	4
Template RNA	x
dNTP Mix (10 mM)	2
RevertAid RT (200 U/µL)	1
RiboLock RNase Inhibitor (20 U/µL)	1
Oligo(dT)18 Primer (100 µM)	1
Nuclease-free water	11 - x
Total volume	**20**

2.17 Reverse Transcriptase Quantitative Polymerase Chain Reaction

Reverse transcriptase quantitative polymerase chain reaction (RT-pPCR) was performed to quantify the transcriptional expression of selected genes using cDNA synthesized from RNA samples. RT-qPCR was prepared for each sample and primer pair on ice in white 0.2 mL 8-tube PCR strips according to Table 3.2 using the SensiFAST™ Probe No-ROX Kit (Meridian Bioscience®; Celtic Diagnostics, SA).

Table 5: Components of SensiFAST™ Probe No-ROX PCR reaction

Reaction Components	Volume (µL)
2 X SensiFAST Probe No-ROX Mix	5
Forward primer (10 µM)	0.4
Reverse primer (10 µM)	0.4
Nuclease-free water	2.2
Template cDNA	2
Total volume	**10**

The PCR strips were sealed with optical flat 8-cap and placed in the CFX96 Touch™ Real-Time PCR Detection System (Bio-Rad, USA). Cycling conditions were set according to Table 6, where annealing temperature depends on the annealing temperature of the primer pair used. Primer sequences and annealing temperatures are shown in Table 7. The annealing

temperature of each primer pair was optimized by temperature gradient PCR. Fluorescence intensity data was captured at the extension step of each cycle.

Table 6: qPCR cycling conditions

Step	Number of cycles	Time	Temperature (°C)
Initial Denaturation	1	2 min	95
Denaturation	40	5 s	95
Annealing		10 s	x
Extension		20 s	72
Final extension	1	1 min	72

Table 7: Primer Sequences

Gene	Strand	Annealing temperature (°C)	Primer sequence (5'-3')
CDH1	Forward	58	ATC CTC GCC CTG CTG ATT
CDH1	Reverse	58	ACC ACC GTT CTC CTC CGT A
Vim	Forward	58	TGC GCC AGC AGT ATG AAA
Vim	Reverse	58	GCC TCA GAG AGG TCA GCA AA
SNAI1	Forward	58	CTT GTG TCT GCA CGA CCT GT
SNAI1	Reverse	58	CAG GAG AAT GGC TTC TCA CC
TWIST1	Forward	58	GGA CAA GCT GAG CAA GAT TCA
TWIST1	Reverse	58	CGG AGA AGG CGT AGC TGA G
ZEB1	Forward	56	GCTGGCAAGACAACGTGAAAG
ZEB1	Reverse	56	GCCTCAGGATAAATGACGGC
CTBP1	Forward	56	GTGCCCTGATGTACCATACCA
CTBP1	Reverse	56	TGATGTCGATATTGTCAAACCCG
SMAD4	Forward	56	GAG AAC ATT GGA TGG ACG ACT
SMAD4	Revers	56	CAC AGA CGG GCA TAG ATC AC
ABCA1	Forward	58	GCT TGT TGG CCT CAG TTA AGG
ABCA1	Reverse	58	GTA GCT CAG GCG TAC AGA GAT

ABCG1	Forward	58	GTG GAT GAG GTT GAG ACA GAC C
ABCG1	Reverse	58	CCT CGG GTA CAG AGT AGG AAA G
SREBF2	Forward	56	GCAGCAACGGGACCATTCT
SREBF2	Reverse	56	CCCCATGACTAAGTCCTTCAACT
LXR	Forward	56	CTCAATGCCTGATGTTTCTCCT
LXR	Reverse	56	TCCAACCCTATCCCTAAAGCAA
LDLR	Forward	56	TGA CTC AGA CGA ACA AGG CTG
LDLR	Reverse	56	ATC TAG GCA ATC TCG GTC TCC
HMGCR	Forward	56	TGA TTG ACC TTT CCA GAG CAA G
HMGCR	Reverse	56	CTA AAA TTG CCA TTC CAC GAG C
PCSK9	Forward	56	GAG ACC CAG AGG CTA CAG ATT
PCSK9	Reverse	56	AAT GTA CTC CAC ATG GGG CAA
LCAT	Forward	56	GCT TGG GGA ATC GGC TAG AAG
LCAT	Reverse	56	CCT CTG TCT TAC GGT AGC ACA T
GAPDH	Forward	58	GTA TGA CTC CAC TCA CGG CAA A
GAPDH	Reverse	58	GGT CTC GCT CCT GGA AGA TG

Once complete, the data was analysed and expression was quantified using the delta-delta Ct method ($2^{-\Delta\Delta Ct}$), normalizing expression based on the glyceraldehyde 3-phosphate dehydrogenase (GAPDH) housekeeping gene, shown below:

$$\Delta CT = CT(target\ gene) - CT(reference\ gene)$$
$$\Delta\Delta CT = \Delta CT(target\ sample) - \Delta CT(control\ sample)$$

This method calculates gene expression of a treated sample relative to an untreated control to measure changes in expression resulting from a change in condition. Log_2 fold change was calculated as log_2(calculated fold change) to interpret increases and decreases in fold change on a symmetrical scale.

2.18 Protein Extraction and Quantification

In preparation for Western blotting, cells were seeded in a 6-well plate at a density of 3×10^5 cells, underwent EMT induction and treated with cholesterol-lowering compounds as described previously. Cells were detached and pelleted via centrifugation, removing the supernatant. Cells were resuspended in 100 µL of 1X radioimmunoprecipitation assay (RIPA) lysis buffer per 10^6 cells, which was prepared according to Table S5. RIPA buffer is used to disrupt cell and nuclear membranes and decrease protein-protein interactions, while keeping proteins intact and maintaining their immunoreactivity. The cell suspensions were kept on ice and agitated with a vortex mixer every 5 minutes for 30 minutes. Cell lysates kept on ice and their concentrations were measured using a bicinchoninic acid (BCA) assay.

Table 8: RIPA Lysis Buffer Components

	Components for 100 mL
1X RIPA lysis buffer	1.21g 50mM Tris-HCl (pH 7.4) 0.876g 300 mM NaCl 1 mL 1% Triton X-100 1g 1% Sodium deoxycholate 1mL 10% SDS 1 mL 10 mM EDTA Made up to 100 mL with dH_2O

The BCA assay is a colorimetric assay used to quantify the concentration of total protein in solution. It relies on the reduction of Cu^{2+} ions from copper (II) sulphate to Cu^{+} by peptides containing three or more amino acids in a strong alkaline solution. This is known as the biuret reaction and the amount of Cu^{2+} reduction is proportional to the protein concentration in solution. The second reaction of the BCA assay is the formation of a chelate of two BCA molecules with each Cu^{+} molecule in solution, forming a purple-coloured complex with linear absorbance at 562 nm that is proportional to protein concentration.

BSA (Glentham Life Sciences; Inqaba Biotec™, SA) standards were prepared at concentrations of 0 (blank), 0.2, 0.4, 0.6, 0.8, and 1 mg/mL diluted in 1X RIPA buffer. The first reaction was prepared by mixing 50 parts of BCA solution (Sigma-Aldrich, UK) with 1 part of copper (II) sulfate solution (Sigma-Aldrich, UK) to make a BCA working solution. 25 µL of each BSA standard was added to the wells of a 96-well plate in triplicate. Unknown

protein samples were diluted 1:5 in 1X RIPA buffer and 25 µL of each was added to the same 96-well plate in triplicate. Following this, 200 µL of BCA working solution was mixed with the protein solution in each well and the plate was incubated at 37 °C for 30 minutes, avoiding light exposure. Absorbance at 562 nm was measured using the Multiskan GO Microplate Reader (Thermo Fisher Scientific, SkanIt™ software) for each well. A standard curve was plotted to determine the concentration of each unknown protein lysate using the equation of the line of best fit (y = mx + b) according to the following formula:

$$y = mean\ sample\ absorbance - mean\ blank\ absorbance$$

$$Protein\ concentration\ \ (mg/mL) = x\ \times 5$$

Where y is used to solve for x in y = mx + b and 5 is the sample dilution factor. The protein concentration of each sample was normalized to 10 mg/mL by diluting with 1X RIPA buffer.

2.19 SDS-PAGE

SDS-polyacrylamide gel electrophoresis (PAGE) was run to separate proteins in the sample lysates by molecular weight. SDS denatures protein and masks the intrinsic charge of the amino acids making up the polypeptide chain, giving proteins a proportional charge to mass ratio, allowing them to migrate through the gel matrix based on size. Larger proteins experience more resistance moving through the polyacrylamide gel matrix and will therefore move slower and remain higher on the gel than smaller proteins.

The polyacrylamide slab gel was prepared using components listed in Table S6 and S7. A 10% 1mm resolving gel was prepared first and allowed to set between glass plates attached to a gel casting mould. This layer of the gel separates proteins into bands based on their molecular weights. An overlay of 100% isopropanol was used on top of the gel to ensure an even interface between the two gel layers. The resolving gel was allowed to polymerize for 15 minutes. The overlay was removed, and the stacking gel solution was poured on top of the resolving gel. The stacking gel concentrates proteins of different molecular weight into a horizontal line, allowing them to enter the resolving gel at the same time. The stacking gel was allowed to polymerize for 15 minutes.

The polymerized gel was placed in the Mini-PROTEAN® tetra vertical electrophoresis cell (Bio-Rad, USA), submerged in 1X running buffer (Table S8). The 8-lane comb was removed and wells were flushed using a pipette. Protein lysates were diluted 1:1 in 2X Laemmli buffer (Sigma-Aldrich, UK) and heated to 95°C for 5 minutes in an AccuBlock™ digital dry bath

(Labnet International, USA) to assist in protein denaturation. Laemmli buffer contains β-mercaptoethanol, SDS, bromophenol blue and glycerol. β-mercaptoethanol reduces disulphide bonds in the tertiary and quaternary structure of the protein and SDS denatures the proteins and gives them a negative charge proportional to protein size. Bromophenol blue is used as a tracking dye to monitor the progress of the electrophoresis, and glycerol increases the density of the lysate, allowing it to sink into the wells of the gel.

Table 9: SDS-PAGE Buffer Components

	Components
Resolving gel buffer	36.2 g Tris 0.8 g SDS Dissolved in 150 mL dH_2O Adjusted pH to 8.9 Made up to 200 mL with dH_2O
Stacking gel buffer	5.9 g Tris 0.4 g SDS Dissolved in 70 mL dH_2O Adjusted pH to 6.8 Made up to 100 mL with dH_2O
30% Bis-acrylamide	30 g Acrylamide 0.8 g Bis-acrylamide (Sigma-Aldrich, UK) 0.1 g SDS 100 mL dH_2O
10% Ammonium persulfate (APS) (Sigma-Aldrich, UK)	100 mg APS 1 mL dH_2O

Table 10: SDS-PAGE Stacking and Resolving Gel Components (10%; 1 mm)

Components	Resolving gel	Stacking gel
Resolving gel buffer	3 mL	-
Stacking gel buffer	-	750 µL
30% Bis-acrylamide	3 mL	500 µL
dH_2O	3 mL	1.75 mL
10% APS	100 µL	30 µL
N, N, N′, N′-Tetramethylethylenediamine (TEMED) (Sigma-Aldrich, UK)	10 µL	3 µL

The gel was loaded with 2 µL of Precision Plus Protein™ unstained protein standards (Bio-Rad, USA), which was the molecular weight marker used, and 10 µg of protein from each sample lysate. Electrophoresis was run at 100 V until the dye front reached the bottom of the gel. After completion of electrophoresis, the gel was removed from glass plates and the stacking gel was cut off to prepare for protein transfer.

Table 11: Western Blot Running Buffer Components

	Components for 1 L
10X running buffer	30.2 g Tris 144 g Glycine 10 g SDS 1 L dH_2O
1X running buffer	100 mL 10X running buffer 900 mL dH_2O

2.20 Western Blotting

Western blotting was performed to detect and quantify proteins of interest in sample lysates. The blotting involves the transfer of resolved proteins from the SDS-PAGE gel to a hydrophobic membrane for targeted detection using immunodetection. Following protein separation using SDS-PAGE, a polyvinylidene difluoride (PVDF) membrane with 0.22 µm pore size was activated by soaking in 100% methanol for 15 seconds and then the membrane and gel were equilibrated by soaking in 1X transfer buffer (Table 12) for 5 minutes. PVDF is

hydrophobic, which may interfere with aqueous buffers penetrating through the membrane. Activation with methanol allows the membrane to be hydrated, increasing protein binding capacity. Soaking in transfer buffer removes contaminating buffer salts and SDS from electrophoresis, and reverses heat-induced expansion of the gel from the electrophoresis process. Proteins were transferred from the gel to the PVDF membrane using the semi-dry method at 25 V for 30 minutes, sandwiched between two sheet of filter paper soaked in 1X transfer buffer, in the Trans-Blot®Turbo™ Transfer System (Bio-Rad, USA).

Table 12: Transfer Buffer Components

	Components for 1 L
10X transfer buffer	38 g Tris 144 g Glycine 1 L dH_2O
1X transfer buffer	100 mL 10X transfer buffer 700 mL dH_2O 200 mL methanol

Following transfer, the PVDF membrane was blocked by incubating in 3% BSA blocking solution in 1X tris-buffered saline with 0.1% Tween 20 (TBST) at room temperature for 1 hour. The membrane was then probed using a target-specific primary antibody (Table 1) diluted in 3 % BSA blocking solution, incubating overnight at 4 °C on an orbital shaker. The membrane was washed with 1X TBST (Table 13) 5 times for 5 minutes each time at room temperature. The membrane was incubated with a secondary antibody (Table 2) specific to the primary antibody diluted in 3% BSA blocking solution for 1 hour at room temperature. The secondary antibody is conjugated with horseradish peroxidase (HRP) for detection. StrepTactin-HRP conjugate was added for the detection of the Precision Plus Protein™ unstained protein standards. The membrane was washed with 1X TBST 5 times for 5 minutes each time at room temperature. After removal of TBST, Clarity™ Western ECL Substrates (Bio-Rad, USA) were added for detection of HRP-conjugated secondary antibodies through chemiluminescence. Equal volumes of Peroxidase solution and Luminol/enhancer solution from the Clarity™ Western ECL Substrates (Bio-Rad, USA) were added to the membrane for 2 minutes before visualising with the ChemiDoc XRS+ System (Bio-Rad, USA). β-tubulin was probed as the loading control for Western blots performed in this study. PVDF

membranes were stripped by washing for 30 minutes with TBST, followed by 5 washes of 5 minutes each with TBST. PVDF membrane was then re-probed using the same protocol as above.

Table 13: TBST Buffer Components

	Components for 1 L
10X TBS	60.5 g Tris 87.6 g NaCl Dissolved in 700 mL dH_2O Adjusted pH to 7.5 Made up to 1 L with dH_2O
1X TBST	100 mL 10X TBS buffer 900 mL dH_2O 1 mL TWEEN® 20 (Sigma-Aldrich, UK)

2.21 Statistics and Data Analysis

Statistical analyses and data visualisation were performed using Microsoft Excel©, GraphPad Prism 8, and the Python programming language. A minimum of three independent experimental repeats were performed for each assay and each experiment was performed using three technical replicates. Data was presented as the mean of the replicates ± standard deviation. Comparisons were considered statistically significant if p-value > 0.05 for a given statistical test.

A two-tailed unpaired Student's t-test was performed to determine statistically significant difference between two treatment conditions. The Student's t-test compares the means between two groups with the null hypothesis that states that the means are statistically equal and the alternative hypothesis states that means of the two samples are statistically different. T-test assumes normally distributed, continuous data with equal variance. To test for equal variance, Levene's test is computed and a p-value > 0.05 demonstrates equal variance. A two-way analysis of variance (ANOVA) was used to determine the relationship between two categorical independent variables and a dependent variable. The Bonferroni *post-hoc* test was used to correct for multiple comparisons. P-values < 0.05 are marked with 1 star (*), p-values

< 0.01 are marked with 2 stars (**), and p-values < 0.001 are marked with 3 stars (***). P-values > 0.05 were considered non-significant and labelled ns.

Chapter 3: RESULTS

3.1 TGFβ treatment induces a mesenchymal-like morphology in NMuMG cells

The first validation of EMT induction is the change in cellular morphology in response to EMT-inducing treatment. Figure 5 shows the change from a rectangular cellular morphology which is characteristic of epithelial cells (Figure 5a) to a more spindle-like morphology with fewer cell-cell contacts, characteristic of mesenchymal cells (Figure 5b) following treatment with 10 ng/mL TGFβ for 48 hours. Reduced cell proliferation following EMT induction is also observed.

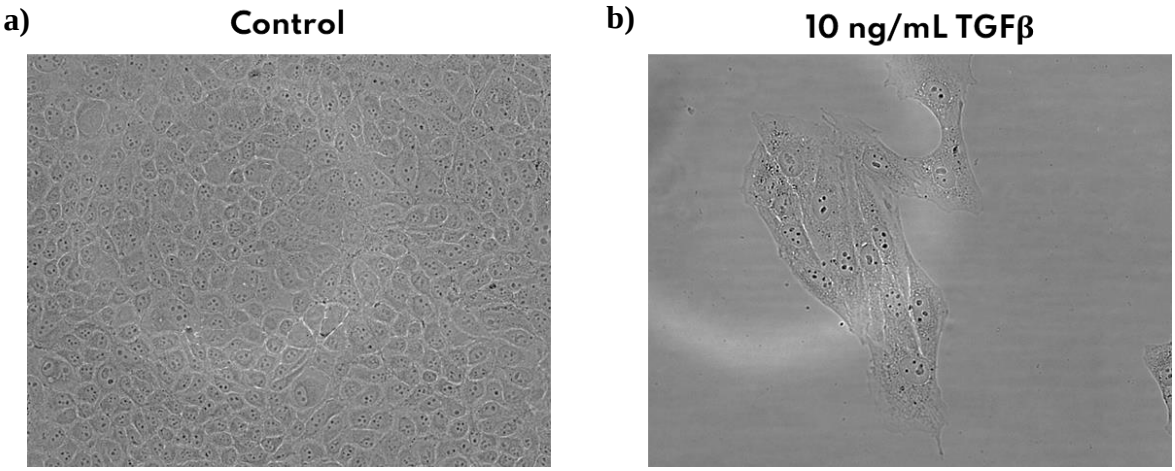

Figure 5: Morphological changes in NMuMG cells in response to 10 ng/mL TGFβ treatment. Micrograph images showing (a) NMuMG cells with a rectangular, cobblestone morphology characteristic of epithelial cells and (b) a change to a spindle-like morphology characteristic of mesenchymal cells following 10 ng/mL TGFβ treatment for 48 hours. Micrographs generated using the Floid™ Cell Imaging System.

3.2 Qualitative changes in EMT marker protein expression in NMuMG cells following TGFβ treatment

Further confirmation of EMT induction was achieved through a qualitative comparison of the expression of E-cadherin and Vimentin in NMuMG cells with and without treatment with 10 ng/mL TGFβ for 48 hours. E-cadherin is expressed in epithelial cells and its expression is used to determine an epithelial phenotype. Vimentin is expressed in mesenchymal cells and

its expression is commonly used to determine EMT induction. Figure 6a depicts representative micrograph images showing the green fluorescence of labelled E-cadherin and Vimentin in NMuMG cells pre- and post-EMT induction. A reduction in E-cadherin fluorescence and an increase in Vimentin fluorescence is observed after TGFβ treatment relative to the control. The graph shown in Figure 6b represents the average corrected total cell fluorescence across 3 technical replicates with 10 micrograph images processed using the ImageJ image processing software for each replicate. Labelled E-cadherin fluorescence intensity was reduced by 70.03% and vimentin fluorescence was increased by 449.86% after TGFβ treatment compared to the control. This confirms EMT-associated expression changes in addition to the morphological changes presented previously, confirming the induction of EMT.

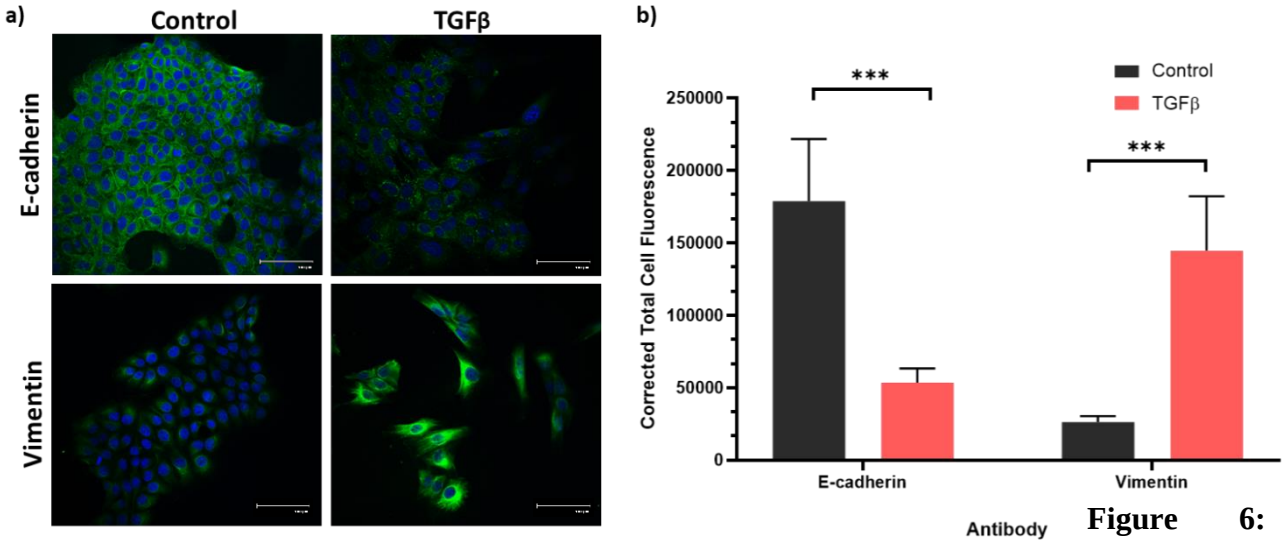

Figure 6: Changes in E-cadherin and Vimentin fluorescence in response to EMT induction. (a) Representative micrograph images showing fluorescent labelling of E-cadherin and Vimentin following 10 ng/mL TGFβ treatment for 48 hours compared to control cells. E-cadherin and Vimentin are stained with a green fluorophore, and nuclei are stained blue with DAPI nuclear stain. Micrographs were generated using the LSM 710 confocal microscope (Zeiss, Germany). (b) Graph representing the corrected total cell fluorescence of E-cadherin and Vimentin in NMuMG cells pre- and post-EMT induction quantified using ImageJ. Data represents the mean CTCF of all cells analysed ± standard deviation. Statistical significance was calculated using a two-tailed unpaired Student's t-test where * $P < 0.05$, ** $P < 0.01$, *** $P < 0.001$; n=300 cells

3.3 Quantitative changes in EMT marker protein expression in NMuMG cells following TGFβ treatment

As further confirmation of EMT induction, RT-qPCR and Western blotting were performed on NMuMG cells with and without treatment with TGFβ as a quantitative measure of expression of EMT marker genes. Figure 7a shows the transcriptional expression of *CDH1, Vim, SNAI1, and TWIST1* genes in post-EMT cells relative to pre-EMT cells. CDH1 expression decreased with a $\log_2$ fold change of -0.97, and the expression of *Vim, SNAI1, and TWIST1* increased with $\log_2$ fold changes of 1.26, 3.17, and 2.37, respectively, relative to pre-EMT cells. This corroborates the expression changes observed in Figure 6 and confirms a decrease in epithelial marker E-cadherin (*CDH1*), an increase in mesenchymal marker Vimentin (*Vim*), and an increase in EMT-TFs Snail1 (*SNAI1*) and TWIST1 (*TWIST1*) expression after TGFβ treatment.

Western blot analysis, shown in Figure 7b, shows a decrease in E-cadherin protein expression after EMT induction, further confirming the loss or epithelial characteristics after TGFβ treatment. An increase in the protein expression of mesenchymal markers Vimentin and N-cadherin is also observed after EMT induction. Together with immunocytochemistry and RT-qPCR analyses of gene expression, these results validate the induction of EMT by TGFβ treatment.

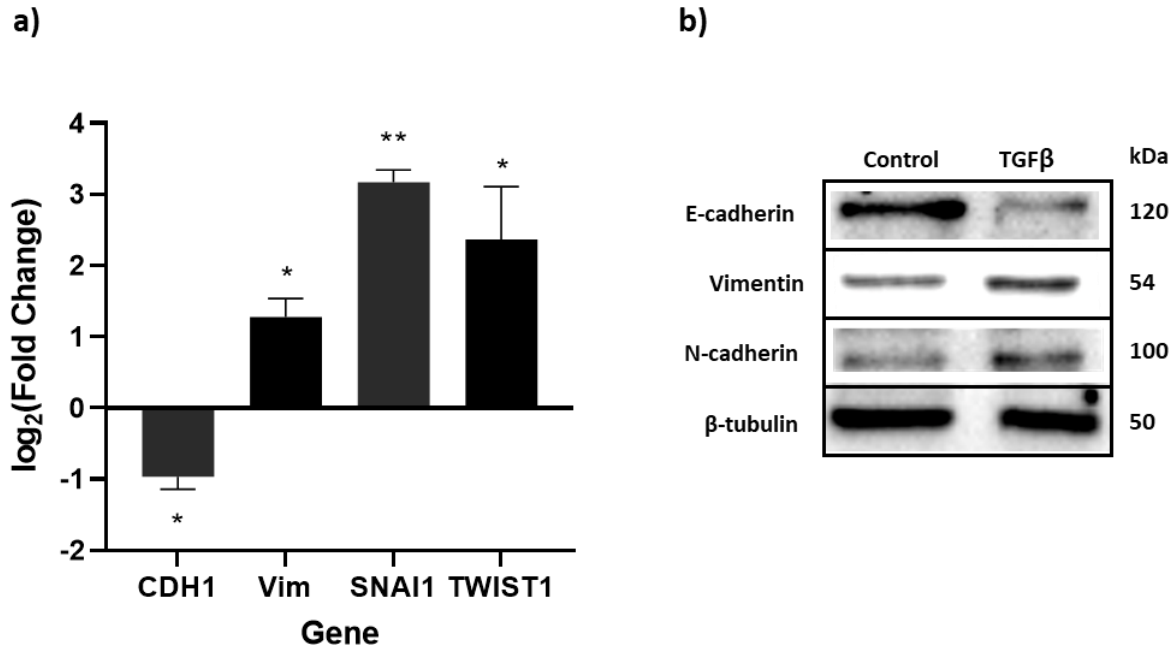

Figure 7: Changes in EMT marker expression in response to TGFβ treatment. (a) RT-qPCR analysis of transcriptional expression of *CDH1, Vimentin, Snail, and Twist* genes in TGFβ-treated cells relative to pre-EMT cells. Relative expression is presented as $\log_2$(fold change) between conditions. Data shown represents mean ± standard deviation. Statistical significance was calculated using a two-tailed unpaired Student's t-test where * $P < 0.05$, ** $P < 0.01$, *** $P < 0.001$, and ns indicates no significant change; n=3. (b) Western blots comparing protein expression of E-cadherin, Vimentin, and N-cadherin pre- and post-EMT with β-tubulin used as a loading control.

3.4 Evaluation of Ki-67 fluorescence in response to EMT induction

Ki-67 is a nuclear protein used as a marker of cell proliferation. It is expressed in proliferating cells. Its absence indicates cell cycle arrest [261]. The expression of Ki-67 was evaluated through immunofluorescence staining in NMuMG cells with and without treatment with 10 ng/mL TGFβ for 48 hours to compare Ki-67 levels pre- and post-EMT. Representative micrograph images are shown in Figure 8a, which show high Ki-67 levels in control, pre-EMT cells and a reduction of Ki-67 levels in post-EMT cells after TGFβ treatment. Fluorescence quantification shown in Figure 8b confirms this reduction, indicating an 85.5% decrease in labelled Ki-67 fluorescence after EMT induction. Values in the graph represent the average corrected total cell fluorescence across 3 technical replicates with 10 micrograph images processed using the ImageJ image processing software for each replicate.

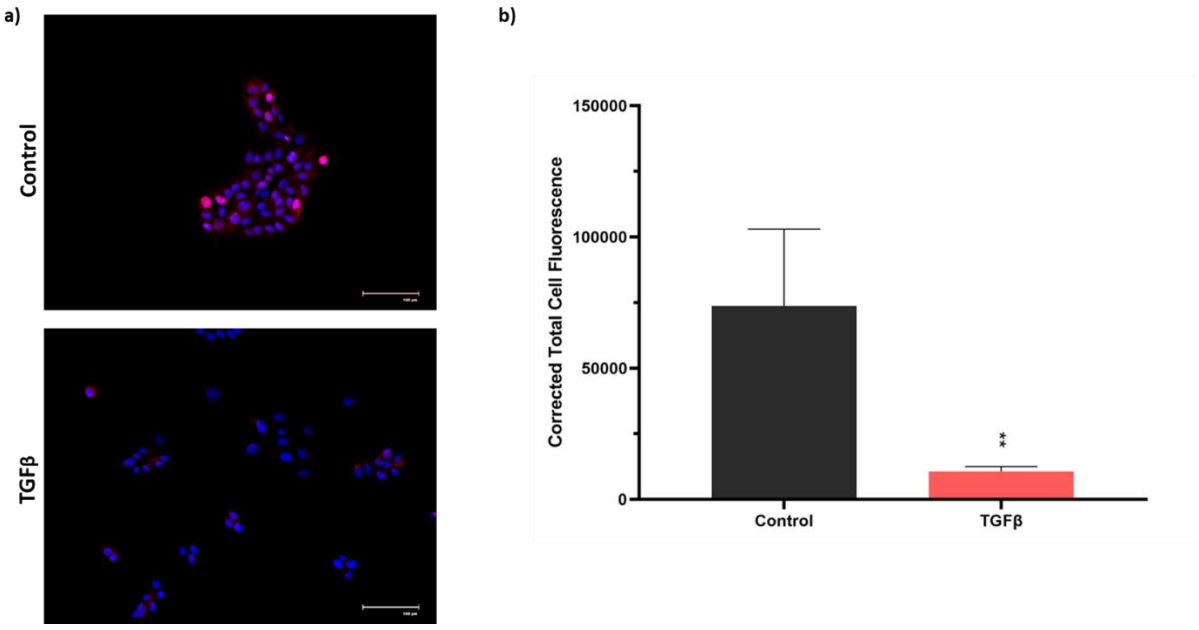

Figure 8: Changes in Ki-67 fluorescence in response to EMT induction. (a) Representative micrograph images showing fluorescent labelling of Ki-67 following 10 ng/mL TGFβ treatment for 48 hours compared to control cells. Ki-67 is stained with a red fluorophore, and nuclei are stained blue with DAPI nuclear stain. Micrographs were generated using the Floid™ Cell Imaging System. (b) Graph representing the corrected total cell fluorescence of labelled Ki-67 in NMuMG cells pre- and post-EMT induction quantified using ImageJ. Data represents the mean ± standard deviation. Statistical significance was calculated using a two-tailed unpaired Student's t-test where * $P < 0.05$, ** $P < 0.01$, *** $P < 0.001$; n=300 cells

3.5 Changes in cholesterol levels in NMuMG cells following TGFβ treatment

Cholesterol levels were measured using different methods to compare the cholesterol content of NMuMG cells before and after EMT induction. Free unesterified membrane and intracellular cholesterol was visualized using Filipin staining. Nuclei were stained red using NucRed™ Dead nuclear stain. CEs were visualized using Bodipy staining, and lipid raft cholesterol was visualized using the Vybrant Alexa Fluor® Lipid Raft Labelling assay, with nuclei stained blue using DAPI in both assays. Figure 9a shows representative micrograph images of the 3 cholesterol stains. The intensity of fluorescent labelling of free cholesterol, CEs, and lipid raft cholesterol each decreased following EMT induction using 10 ng/mL TGFβ treatment for 48 hours, compared to pre-EMT control cells. The corrected total cell fluorescence values were quantified using ImageJ across 3 technical replicates with 10 micrograph images taken per condition, shown in Figure 9b. The intensity of fluorescent labelling of free cholesterol decreased by 43.14% following EMT induction. CE fluorescence

decreased by 71.69% and lipid raft cholesterol fluorescence decreased by 37.04%, showing a general reduction in cellular cholesterol content in NMuMG cells following EMT induction. Lastly, as a quantitative measure of cellular cholesterol content, cholesterol was quantified using a cholesterol quantification assay. Figure 9c shows the average total cholesterol mass (µg) per sample of NMuMG cells pre- and post-EMT induction. Total cholesterol mass per mL was calculated by comparing the sample absorbance at 570 nm to a standard curve (Figure S1) and correcting for sample dilution. The equation of the standard curve was y=0.2879x+0.02924 and the R¬2 value was 0.9813. Cholesterol mass per sample was reduced from an average of 3.59 µg/mL without TGFβ to 0.70 µg/mL after TGFβ addition, which is an 80.5% decrease in total cholesterol.

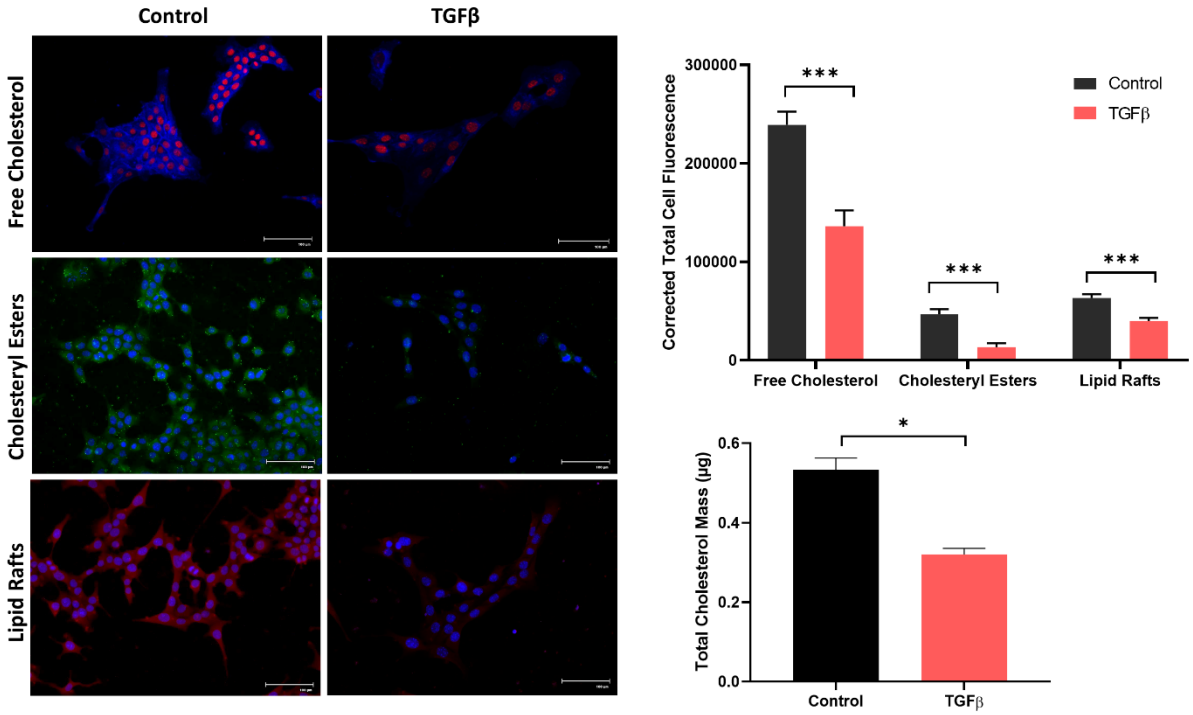

Figure 9: Changes in cellular cholesterol levels in response to EMT induction. (a) Representative micrograph images showing fluorescent labelling of free cholesterol (stained blue with nuclei stained red), CEs (stained green with nuclei stained blue), and lipid raft cholesterol (stained red with nuclei stained blue). Micrographs were generated using the Floid™ Cell Imaging System. (b) Graph representing the corrected total cell fluorescence of free cholesterol, CEs, and lipid raft cholesterol in NMuMG cells pre-EMT (black) and post-EMT (pink) induction quantified using ImageJ. (c) Graph representing the concentration of total cellular cholesterol per mL of sample (µg/mL) in NMuMG cells pre- and post-EMT induction. Data represents the mean ± standard

deviation. Statistical significance was calculated using a two-tailed unpaired Student's t-test where * $P < 0.05$, ** $P < 0.01$, *** $P < 0.001$; n=300 cells

3.6 Changes in cell viability in response to treatment with cholesterol-lowering compounds

The cell viability of NMuMG cells pre- and post-EMT induction and following treatment with 1 mM MβCD, 10 mM HPβCD, and 10 μM simvastatin was assessed using an MTT assay. Figure 10 is a graphical representation of the change**s** in cell viability after treatment with cholesterol-lowering compounds for either 2 hours or 24 hours. Cell viabilities were calculated relative to an untreated control for each treatment group, **i.e.,** treated pre-EMT cells were compared to a vehicle-treated pre-EMT sample and treated post-EMT cells were compared to a vehicle-treated post-EMT sample. The cell viability values of untreated controls were set to 100%. As a positive control, cells were treated with 40 μM of plumbagin, which is known to cause apoptotic cell death [248]. In Figure 10, it is observed that no significant reduction in cell viability occurs when cells were treated with HPβCD and simvastatin pre- and post-EMT for 2 hours. An increase in the number of viable cells was observed when pre-EMT cells were treated with MβCD for 2 hours. Similarly, cell viability increased with 24-hour MβCD treatment pre-EMT and no changes in cell viability were observed with HPβCD and simvastatin treatment of pre-EMT cells for 24 hours. HPβCD and simvastatin reduced cell viability in cells post-EMT after 24 hours to 60.69% and 44.83%, respectively, corresponding to a 39.31% and a 55.17% reduction in cell viability, respectively, relative to the controls.

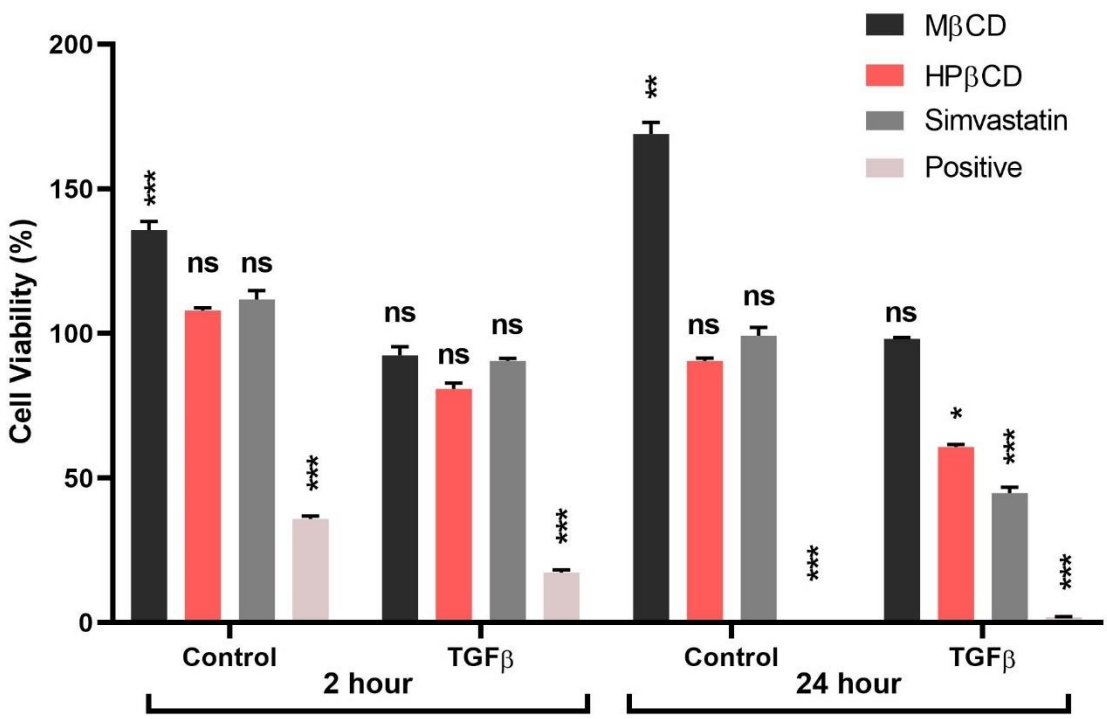

Figure 10: Changes in cell viability after cholesterol-lowering treatment. Representative graph of changes in cell viability of NMuMG cells following treatment with cholesterol-lowering compounds. Control cells are pre-EMT induction and TGFβ-treated cells are post-EMT induction. Both pre- and post-EMT samples were treated with 1 mM MβCD, 10 mM HPβCD, or 10 μM simvastatin, and a positive control for cell death, 40 μM plumbagin. Treatments were either 2 hours or 24 hours long and cell viability was calculated as a percentage, relative to the corresponding pre- or post-EMT untreated samples. Control samples were set to 100% cell viability. Data shown represents mean ± standard deviation. Statistical significance was calculated using a two-tailed unpaired Student's t-test where * $P < 0.05$, ** $P < 0.01$, *** $P < 0.001$, and ns indicates no significant change; n=3. Z' factor was greater than 0.6 for each plate tested.

3.7 Changes in free cholesterol following treatment with cholesterol-lowering compounds

Filipin staining was used to visualise free intracellular and membrane cholesterol in pre- and post-EMT NMuMG cells after treatment with 1 mM MβCD, 10 mM HPβCD, and 10 μM simvastatin. Free cholesterol was stained blue, and nuclei were stained red using NucRed™ Dead nuclear stain. Figure 11a shows representative micrograph images, which were quantified using the ImageJ image processing software in Figure 11b. In pre-EMT cells, treatment with MβCD decreased free cholesterol fluorescence intensity by 31.74%, HPβCD decreased fluorescence by 66.38%, and simvastatin decreased fluorescence by 30.02%,

indicating a reduction in free cholesterol after treatment with cholesterol-lowering compounds. Post-EMT, MβCD treatment reduced free cholesterol fluorescence intensity by 29.88% and HPβCD treatment reduced fluorescence by 50.28% compared to the post-EMT untreated control. Simvastatin had no significant effect on free cholesterol levels post-EMT. The graph depicted in Figure 11b represents the average corrected total cell fluorescence of 10 cells per microscope field, 10 microscope fields per experimental repeat and 3 experimental repeats (n=300 cells per condition).

3.8 Changes in CEs following treatment with cholesterol-lowering compounds

CEs stored in lipid droplets were stained green using the BODIPY fluorescent probe with nuclei stained blue with DAPI. This was performed to visualise changes in cholesteryl ester content in NMuMG cells pre- and post-EMT after treatment with 1 mM MβCD, 10 mM HPβCD, and 10 μM simvastatin for 2 hours. Figure 12a shows representative micrograph images of cholesteryl ester staining, which were quantified using the ImageJ image processing software, represented as a graph in Figure 12b. In pre-EMT cells, treatment with MβCD reduced cholesteryl ester fluorescent staining intensity by 45.39%, HPβCD reduced fluorescence by 62.24%, and simvastatin reduced fluorescence by 56.14%, compared to untreated pre-EMT cells. Post-EMT, HPβCD treatment reduced cholesteryl ester staining by 50.18% and simvastatin treatment caused a 62.39% reduction compared to untreated post-EMT cells. MβCD treatment caused a 48.23% increase in cholesteryl ester staining intensity. The graph depicted in Figure 12b represents the average corrected total cell fluorescence of 10 cells per microscope field, 10 microscope fields per experimental repeat and 3 experimental repeats (n=300 cells per condition).

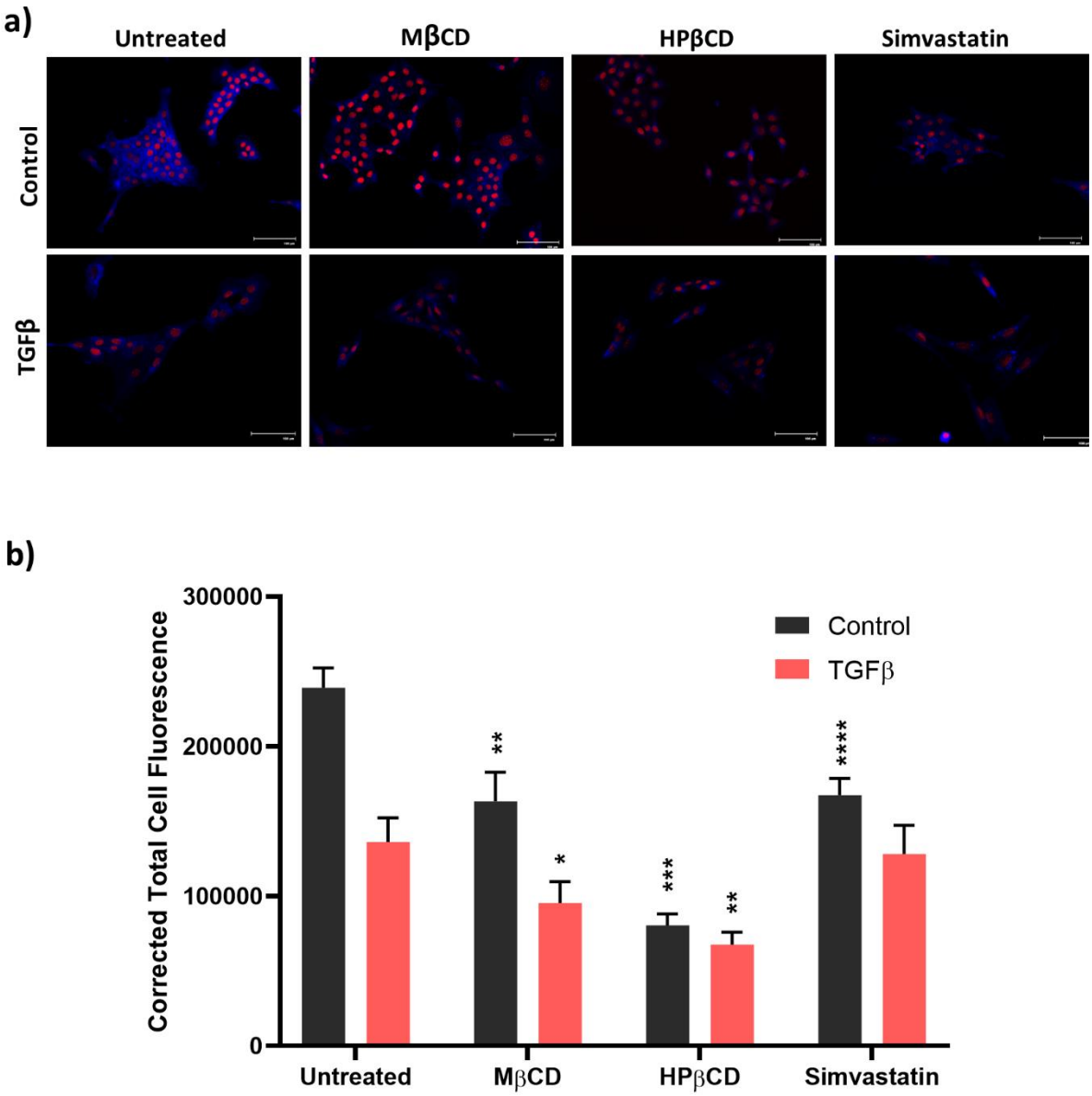

Figure 11: Filipin staining of free cholesterol after cholesterol depletion. (a) Representative micrograph images showing blue fluorescent labelling of free cholesterol using Filipin with nuclei stained red using NucRed™ Dead nuclear stain. Control cells are NMuMG cells pre-EMT and TGFβ-treated cells are post-EMT. Both pre- and post-EMT cells were treated with 1 mM MβCD, 10 mM HPβCD, and 10 μM simvastatin for 2 hours prior to staining. Micrographs were generated using the Floid™ Cell Imaging System. (b) Graph representing the corrected total cell fluorescence of stained free cholesterol in NMuMG cells pre- and post-EMT induction with treatment using cholesterol-lowering compounds, quantified using ImageJ. Data represents the mean ± standard deviation. Statistical significance was calculated using a one-way ANOVA with Bonferroni's multiple comparisons test used for pairwise analyses, where * $P < 0.05$, ** $P < 0.01$, *** $P < 0.001$; n=300 cells.

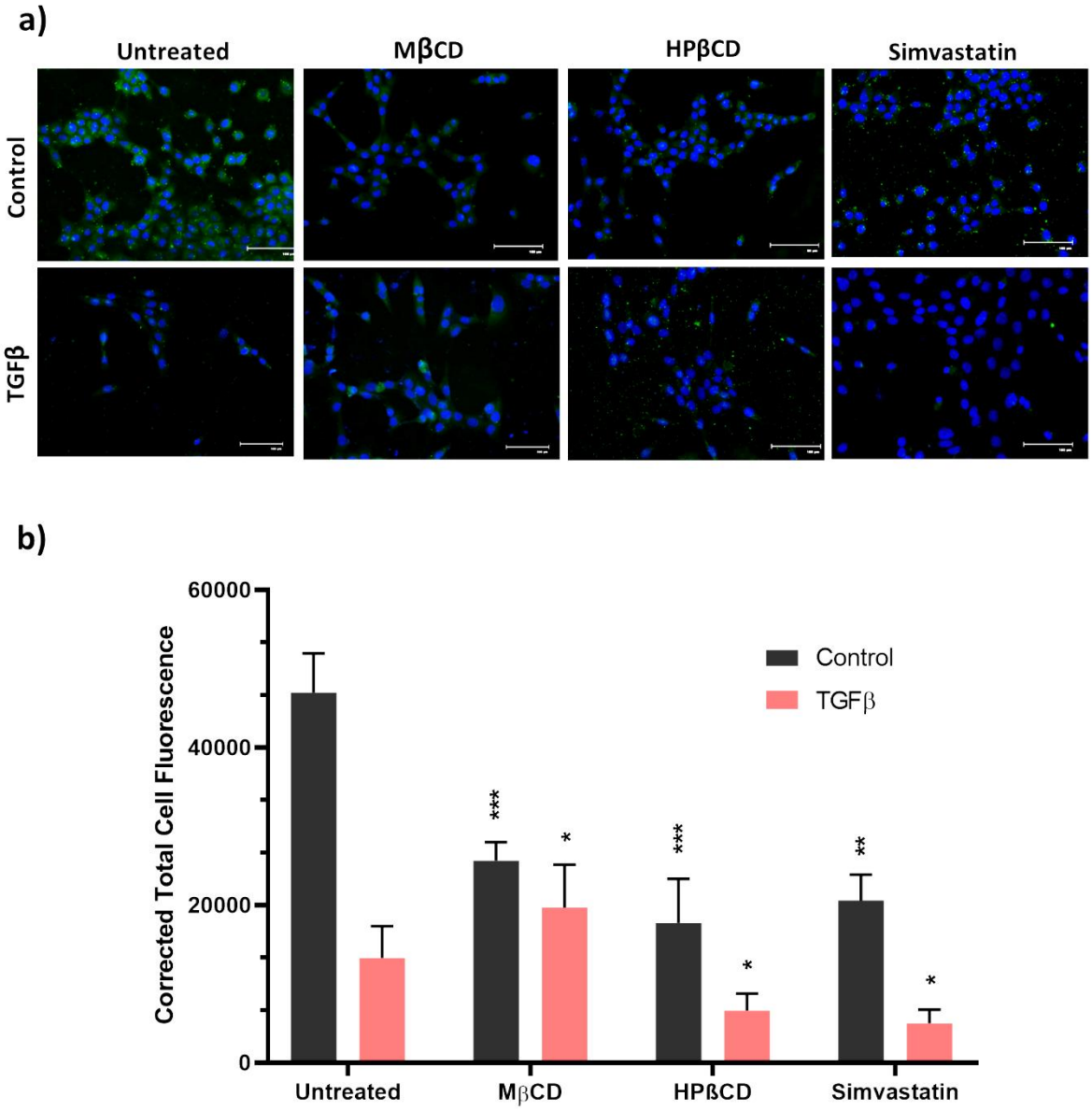

Figure 12: BODIPY staining of CEs after cholesterol depletion. (a) Representative micrograph images showing green fluorescent labelling of CEs using BODIPY with nuclei stained blue using DAPI nuclear stain. Control cells are NMuMG cells pre-EMT and TGFβ-treated cells are post-EMT. Both pre- and post-EMT cells were treated with 1 mM MβCD, 10 mM HPβCD, and 10 μM simvastatin for 2 hours prior to staining. Micrographs were generated using the Floid™ Cell Imaging System. (b) Graph representing the corrected total cell fluorescence of stained CEs in NMuMG cells pre- and post-EMT induction with treatment using cholesterol-lowering compounds, quantified using ImageJ. Data represents the mean ± standard deviation. Statistical significance was calculated using a one-way ANOVA with Bonferroni's multiple comparisons test used for pairwise analyses, where * $P < 0.05$, ** $P < 0.01$, *** $P < 0.001$; n=300 cells.

3.9 Changes in lipid raft cholesterol following treatment with cholesterol-lowering compounds

Lipid raft cholesterol was stained red using the Vybrant Alexa Fluor® Lipid Raft Labelling, with nuclei stained blue using the DAPI nuclear stain. Staining was performed on NMuMG cells pre- and post-EMT, following treatment with 1 mM MβCD, 10 mM HPβCD, and 10 μM simvastatin for 2 hours. Figure 13a shows representative micrograph images of lipid raft staining, which were quantified using the ImageJ image processing software, represented as a graph in Figure 13b. In pre-EMT cells, treatment with MβCD reduced lipid raft cholesterol fluorescent staining intensity significantly by 22.05%. Treatment with HPβCD and simvastatin decreased lipid raft cholesterol significantly in pre-EMT cells by 33.22% and 58.78%, respectively. Post-EMT, MβCD treatment reduced lipid raft cholesterol fluorescent intensity significantly by 16.08%, HPβCD treatment reduced fluorescence by 28.05%, and simvastatin treatment reduced lipid raft cholesterol by 28.37% compared to the post-EMT untreated control. The graph depicted in Figure 13b represents the average corrected total cell fluorescence of 10 cells per microscope field, 10 microscope fields per experimental repeat and 3 experimental repeats (n=300 cells per condition).

3.10 Cholesterol-lowering compounds reduce invasive potential of TGFβ-treated cells

The effect of EMT induction through TGFβ treatment and the effect of treatments with cholesterol-lowering compounds on EMT-induced cells on invasive potential was assessed using the Transwell invasion assay. DAPI-labelled cells that invaded through the membrane were visualised and counted. Representative images for each treatment condition are presented in Figure 14a. Percentage invasion was calculated relative to the untreated pre-EMT control, which was set to 100% to represent the population of invasive cells in a sample of cells not undergoing EMT. The invasive potential of TGFβ-treated cells was compared to control cells to determine whether EMT induction increased the ability of cells to invade. TGFβ-induced cells were treated with 1 mM MβCD, 10 mM HPβCD, and 10 μM simvastatin for 2 hours, which were compared to untreated TGFβ-induced cells. This is represented as a graph in Figure 14b. EMT induction using TGFβ resulted in a 400% increase in the number of invasive cells counted. Treatment of cells post-EMT with MβCD, HPβCD, and simvastatin each resulted in a reduction of invasive potential to 53.84%, 103.08%, and 92.31%, respectively, relative to the control cells. The experiment was repeated 3 times, and all cells on 10 microscope fields were counted for each treatment condition and each experimental repeat.

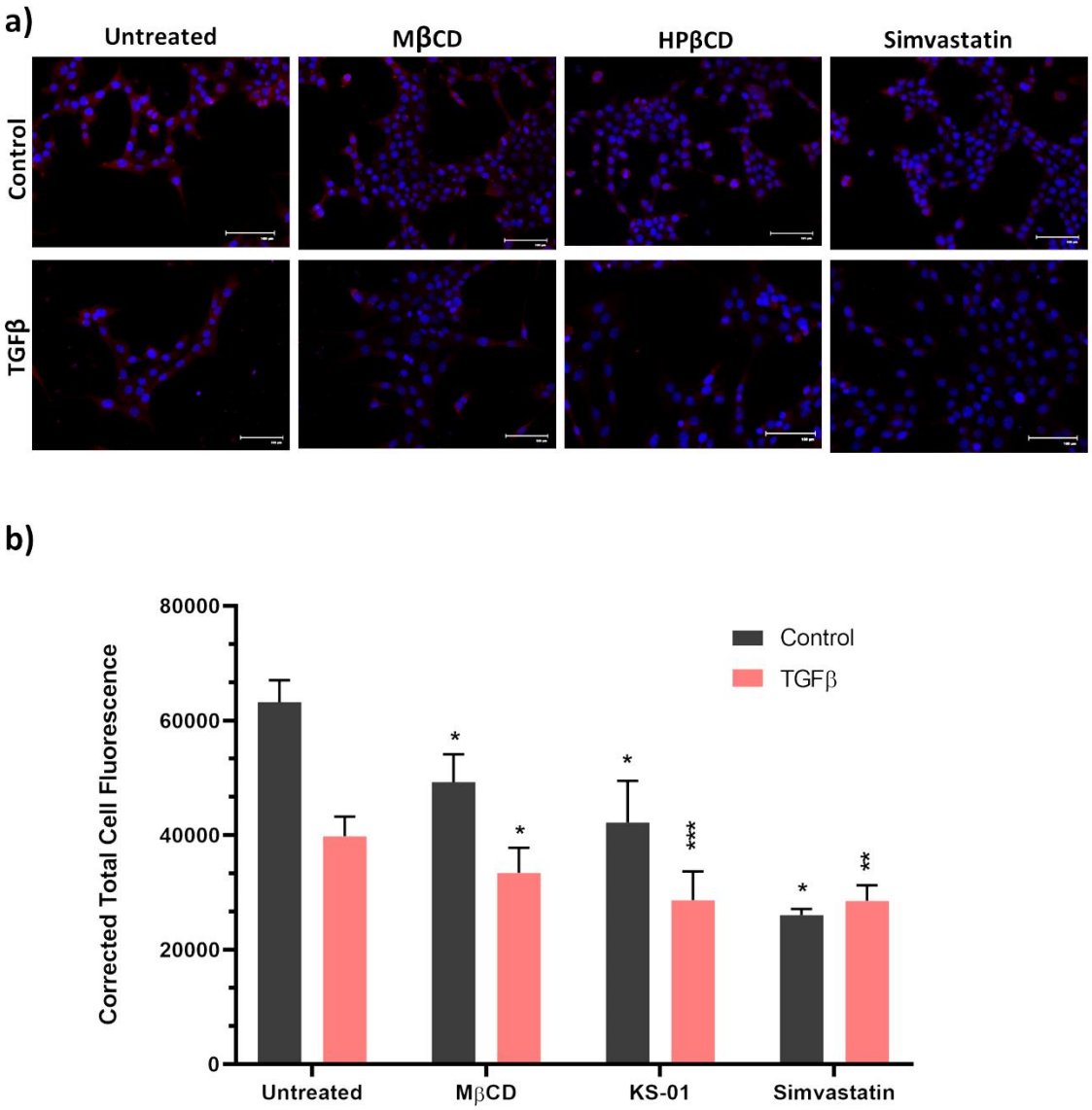

Figure 13: Vybrant Alexa Fluor® Lipid Raft staining after cholesterol depletion. (a) Representative micrograph images showing red fluorescent labelling of lipid raft cholesterol using Vybrant Alexa Fluor® Lipid Raft Labelling Kit with nuclei stained blue using DAPI nuclear stain. Control cells are NMuMG cells pre-EMT and TGFβ-treated cells are post-EMT. Both pre- and post-EMT cells were treated with 1 mM MβCD, 10 mM HPβCD, and 10 μM simvastatin for 2 hours prior to staining. Micrographs were generated using the Floid™ Cell Imaging System. (b) Graph representing the corrected total cell fluorescence of labelled lipid raft cholesterol in NMuMG cells pre- and post-EMT induction with treatment using cholesterol-lowering compounds, quantified using ImageJ. Data represents the mean ± standard deviation. Statistical significance was calculated using a one-way ANOVA with Bonferroni's multiple comparisons test used for pairwise analyses, where * $P < 0.05$, ** $P < 0.01$, *** $P < 0.001$; n=300 cells.

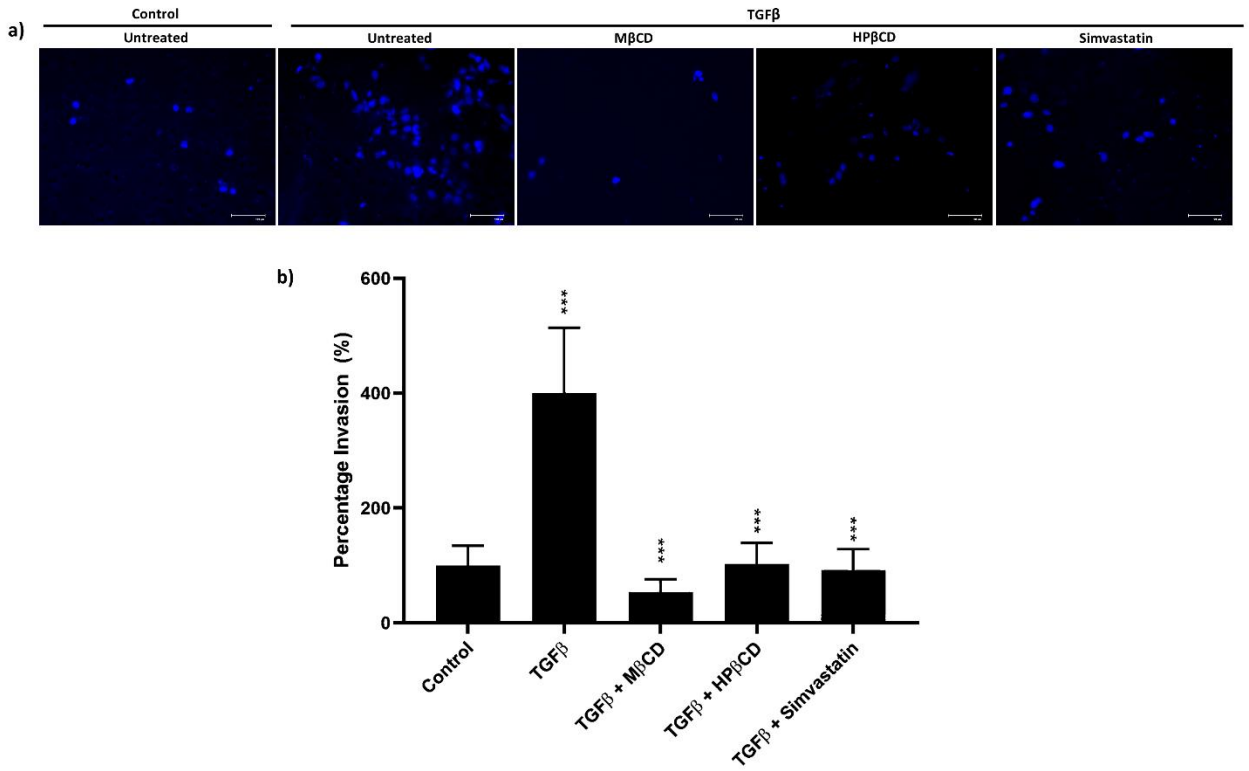

Figure 14: Invasive potential of NMuMG cells following EMT induction and cholesterol depletion. (a) Representative micrograph images showing blue fluorescent labelling of cell nuclei using DAPI. Control represents untreated cells pre-EMT and TGFβ represents EMT-induced cells. Cells were treated with 1 mM MβCD, 10 mM HPβCD, and 10 μM simvastatin for 2 hours. The scale bar represents 100 μm (b) Graphical representation of the percentage of invasive cells relative to the control sample. Data represents the mean ± standard deviation. Statistical significance was calculated using a one-way ANOVA with Bonferroni's multiple comparisons test used for pairwise analyses, where * $P < 0.05$, ** $P < 0.01$, *** $P < 0.001$; n=3.

3.11 Cholesterol-lowering compounds increase E-cadherin and reduce Vimentin post-EMT

The effect of treatment with cholesterol lowering compounds on the expression of E-cadherin and vimentin post-EMT induction was assessed through immunocytochemistry. NMuMG cells induced to undergo EMT using TGFβ were treated with 1 mM MβCD, 10 mM HPβCD, and 10 μM simvastatin for 2 hours and E-cadherin and Vimentin expression was assessed through staining with fluorophore-conjugated antibodies.

Figure 15a shows representative micrograph images of E-cadherin and Vimentin staining. As shown previously in Figure 6, EMT induction reduced the E-cadherin fluorescent labelling intensity and increased vimentin labelling fluorescence. Lowering cholesterol using MβCD,

HPβCD, and simvastatin each caused an increase in E-cadherin fluorescence and a decrease in vimentin fluorescence. Processing 10 microscope fields per coverslip per condition with 3 experimental replicates using ImageJ software yielded corrected total cell fluorescence values, which are represented in Figures 15b and 15c.

Figure 15b shows a 70.02% reduction in E-cadherin fluorescence intensity from pre-EMT cells to post-EMT cells, indicating a lowered E-cadherin expression. MβCD treatment resulted in a 180.51% increase in labelled E-cadherin fluorescence, compared to untreated post-EMT cells. HPβCD treatment resulted in a 232.79% increase and simvastatin treatment resulted in a 140.6% increase in E-cadherin fluorescence intensity compared to untreated post-EMT cells. Overall, cholesterol-lowering treatment significantly increased E-cadherin fluorescence post-EMT, which was initially reduced compared to pre-EMT E-cadherin fluorescence.

Figure 15c shows a 449.86% increase in Vimentin fluorescence intensity from pre-EMT cells to post-EMT cells, indicating an increase in Vimentin expression. Treatment of cells post-EMT with MβCD resulted in a 65.26% reduction in Vimentin fluorescence, HPβCD treatment resulted in a 62.22% decrease, and simvastatin treatment resulted in a 59.99% reduction, compared to untreated post-EMT cells. Cholesterol-lowering treatment significantly lowered Vimentin fluorescence post-EMT, which was increased upon EMT induction.

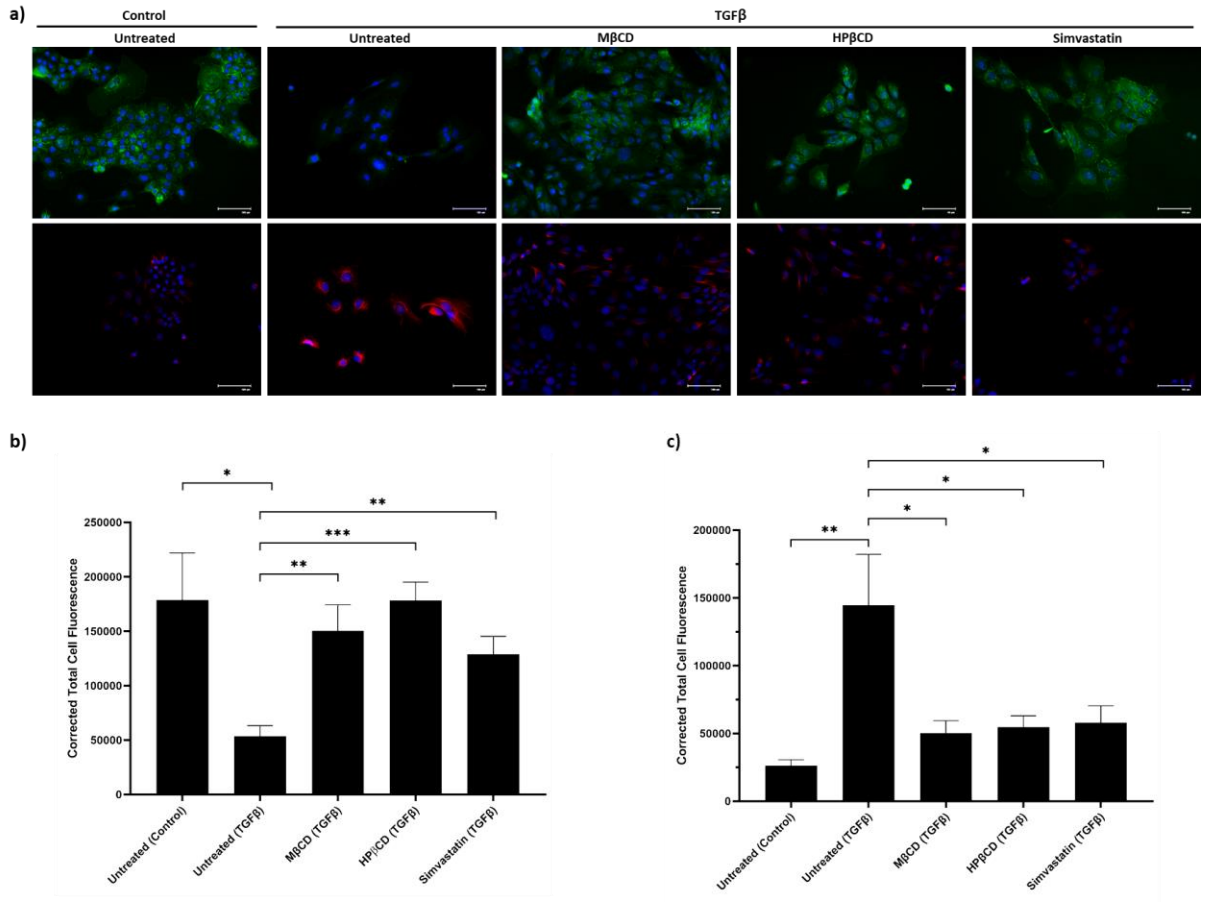

Figure 15: Changes in E-cadherin and Vimentin fluorescence in response to cholesterol depletion. (a) Representative micrograph images showing fluorescent labelling of E-cadherin and Vimentin following 10 ng/mL TGFβ treatment for 48 hours compared to control cells and following treatment with 1 mM MβCD, 10 mM HPβCD, and 10 μM simvastatin for 2 hours compared to untreated TGFβ-induced cells. E-cadherin staining which is depicted in green with nuclei stained blue with DAPI. Vimentin staining which is depicted in red with nuclei stained blue with DAPI. The scale bar represents 100 μm. Micrographs were generated using the Floid™ Cell Imaging System. (b) Graph representing the corrected total cell fluorescence of E-cadherin in NMuMG cells pre- and post-EMT induction and after cholesterol-lowering treatment, quantified using ImageJ. (c) Graph representing the corrected total cell fluorescence of Vimentin in NMuMG cells pre- and post-EMT induction and after cholesterol-lowering treatment, quantified using ImageJ. Data represents the mean ± standard deviation. Statistical significance was calculated using a one-way ANOVA with Bonferroni's multiple comparisons test used for pairwise analyses, where * $P < 0.05$, ** $P < 0.01$, *** $P < 0.001$; n=300 cells

3.12 Cholesterol-lowering compounds reduce N-cadherin fluorescence post-EMT

The effect of treatment with cholesterol lowering compounds on the expression of N-cadherin post-EMT induction was assessed through immunocytochemistry NMuMG cells induced to undergo EMT using TGFβ were treated with 1 mM MβCD, 10 mM HPβCD, and 10 μM simvastatin for 2 hours and N-cadherin expression was assessed by staining with fluorophore-conjugated antibodies.

Figure 16a shows representative micrograph images of N-cadherin staining. The fluorescence of labelled N-cadherin increased upon EMT induction. Post-EMT treatment with MβCD, HPβCD and simvastatin each decreased N-cadherin fluorescence from levels observed in untreated cells post-EMT. Images were processed in ImageJ and corrected total cell fluorescence values are presented in Figure 16b. Upon EMT induction, labelled N-cadherin fluorescence increased significantly by 717.96%. Post-EMT treatment with cholesterol-lowering compounds reversed this increase with MβCD treatment reducing N-cadherin fluorescence by 71.9%, HPβCD reducing N-cadherin fluorescence by 66.32%, and simvastatin by 72.45%, compared to untreated cells post-EMT. The experiment was repeated 3 times, and all cells on 10 microscope fields were counted for each treatment condition and each experimental repeat.

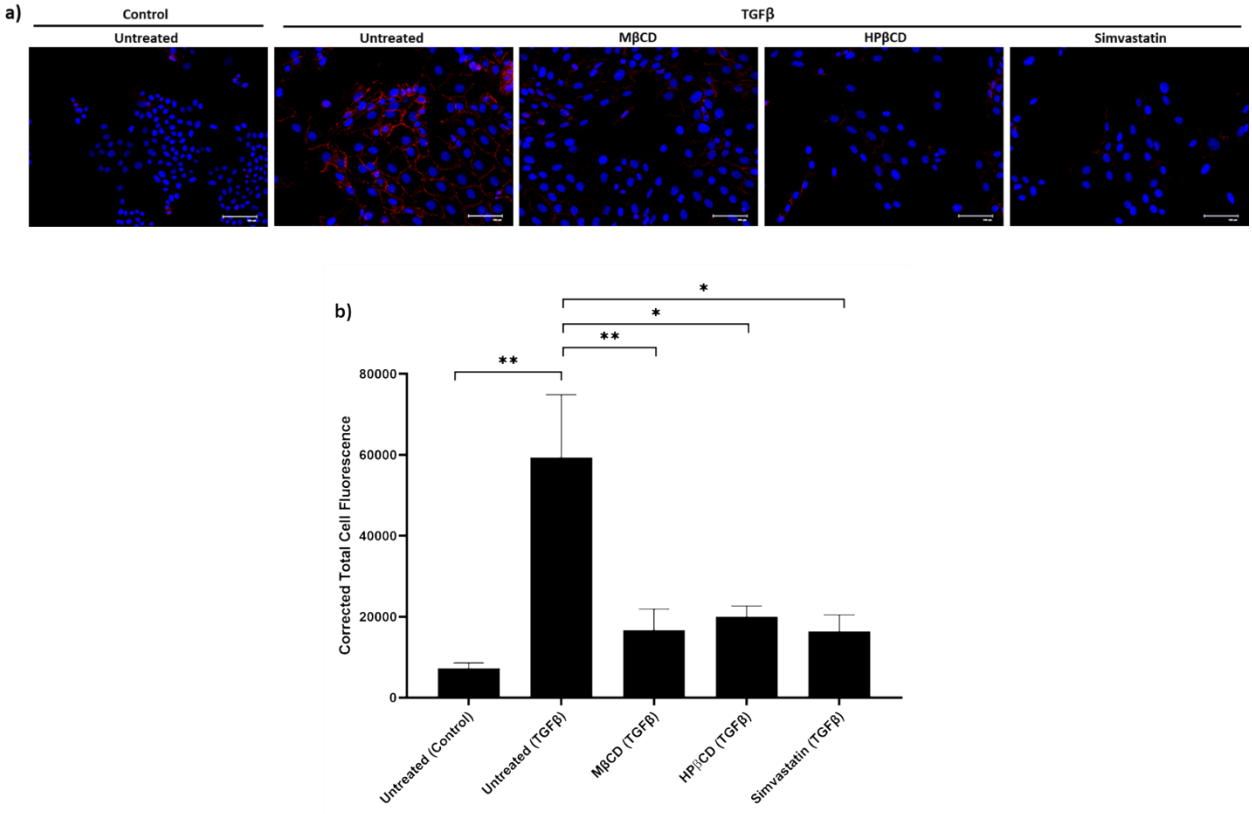

Figure 16: Changes in N-cadherin fluorescence in response to EMT induction and cholesterol depletion. (a) Representative micrograph images showing fluorescent labelling of N-cadherin following 10 ng/mL TGFβ treatment for 48 hours compared to control cells and following treatment with 1 mM MβCD, 10 mM HPβCD, and 10 µM simvastatin for 2 hours compared to untreated TGFβ-induced cells. N-cadherin was stained with a red fluorophore with nuclei stained blue with DAPI. The scale bar represents 100 µm. Micrographs were generated using the Floid™ Cell Imaging System. (b) Graph representing the corrected total cell fluorescence of N-cadherin in NMuMG cells pre- and post-EMT induction and after cholesterol-lowering treatment, quantified using ImageJ. Data represents the mean ± standard deviation. Statistical significance was calculated using a one-way ANOVA with Bonferroni's multiple comparisons test used for pairwise analyses, where * $P < 0.05$, ** $P < 0.01$, *** $P < 0.001$; n=300 cells.

3.13 Changes in EMT pathway gene expression in response to cholesterol depletion

Gene expression levels in EMT signalling pathways was measured using RT-qPCR and Western blotting. Changes in gene expression were measured between cells pre- and post-EMT, and post-EMT after treatment with cholesterol-lowering compounds. RT-qPCR was used to assess transcriptional expression changes of *CDH1, Vim, SNAI1, TWIST1, ZEB1, CTBP1,* and *SNAD4* genes between pre- and post-EMT cells (Figure 17a) and post-EMT in response to treatment with 1 mM MβCD, 10 mM HPβCD, and 10 µM simvastatin for 2 hours

(Figure 17b). Figure 17a represents transcriptional expression changes in response to EMT induction. Upon EMT induction with TGFβ, expression of *CDH1*, which codes for the epithelial marker E-cadherin, decreased significantly with a $\log_2$ fold change of -0.97. Expression of *Vim*, encoding the mesenchymal marker Vimentin, increased with a $\log_2$ fold change of 1.28. Expression of EMT-TFs, *SNAI1*, *TWIST1*, *ZEB1*, and *SMAD4* increased significantly with $\log_2$ fold changes of 3.17, 2.42, 2.28, and 2.955, respectively, indicating an increase in expression of EMT-TFs upon EMT induction. Finally, expression of the EMT-associated transcriptional corepressor *CTBP1* increased upon EMT induction with a $\log_2$ fold change of 1.76.

To measure expression changes caused by cholesterol depletion, RT-qPCR was used to compare transcriptional expression levels between untreated cells post-EMT induction with cells treated with cholesterol-lowering compounds, MβCD, HPβCD, and simvastatin, post-EMT. The changes in expression are represented in Figure 17b. All three cholesterol-lowering compounds increased the expression of *CDH1*, with $\log_2$ fold changes of 1.41 after MβCD treatment, 2.03 after HPβCD treatment, and 1.36 after simvastatin treatment. Similarly, each treatment significantly reduced the expression of *Vim* with $\log_2$ fold changes of -1.69 after MβCD treatment, -1.01 after HPβCD treatment, and -1.44 after simvastatin treatment. These changes oppose the changes to *CDH1*, and *Vim* expression observed after EMT induction. Treatment with the three cholesterol-lowering compounds did not significantly change the expression of *SNAI1 but* decreased the expression of *TWIST1* significantly with $\log_2$ fold changes of -1.13 after MβCD treatment, -3.02 after HPβCD treatment, and -4.07 after simvastatin treatment. Expression of *ZEB1* was decreased following treatment with $\log_2$ fold changes of -2.28 after MβCD treatment, -1.8 after HPβCD treatment, and -1.28 after simvastatin treatment. The expression of *SMAD4* decreased significantly with $\log_2$ fold changes of -4.01 after MβCD treatment, -2.76 after HPβCD treatment, and -0.41 after simvastatin treatment. Finally, the expression of *CTBP1* was decreased following treatment with $\log_2$ fold changes of -3.27 after MβCD treatment, -0.64 after HPβCD treatment, and -1.01 after simvastatin treatment, compared to untreated post-EMT cells.

Western blotting was used to assess protein expression changes of E-cadherin, Vimentin, and N-cadherin between pre- and post-EMT cells and post-EMT cells in response to treatment with 1 mM MβCD, 10 mM HPβCD, and 10 μM simvastatin for 2 hours (Figure 17c). The control lane represents NMuMG cells pre-EMT, the TGFβ lane represents cells post-EMT,

and the MβCD, HPβCD, and simvastatin lanes represent cells post-EMT treated with the respective cholesterol-lowering compound. Protein levels are assessed using band size on the blot. Upon EMT induction, E-cadherin protein levels decreased. Treatment with MβCD and simvastatin increased E-cadherin protein levels. HPβCD treatment did not change the protein expression level of E-cadherin compared to untreated cells post-EMT. Protein expression of Vimentin increased upon EMT induction and decreased slightly when cells were treated with MβCD, HPβCD and simvastatin. Similarly, N-cadherin expression increased upon EMT induction and decreased following treatment with MβCD, HPβCD and simvastatin. Blots shown in Figure 4.13c are representative blots from 3 independent experimental repeats.

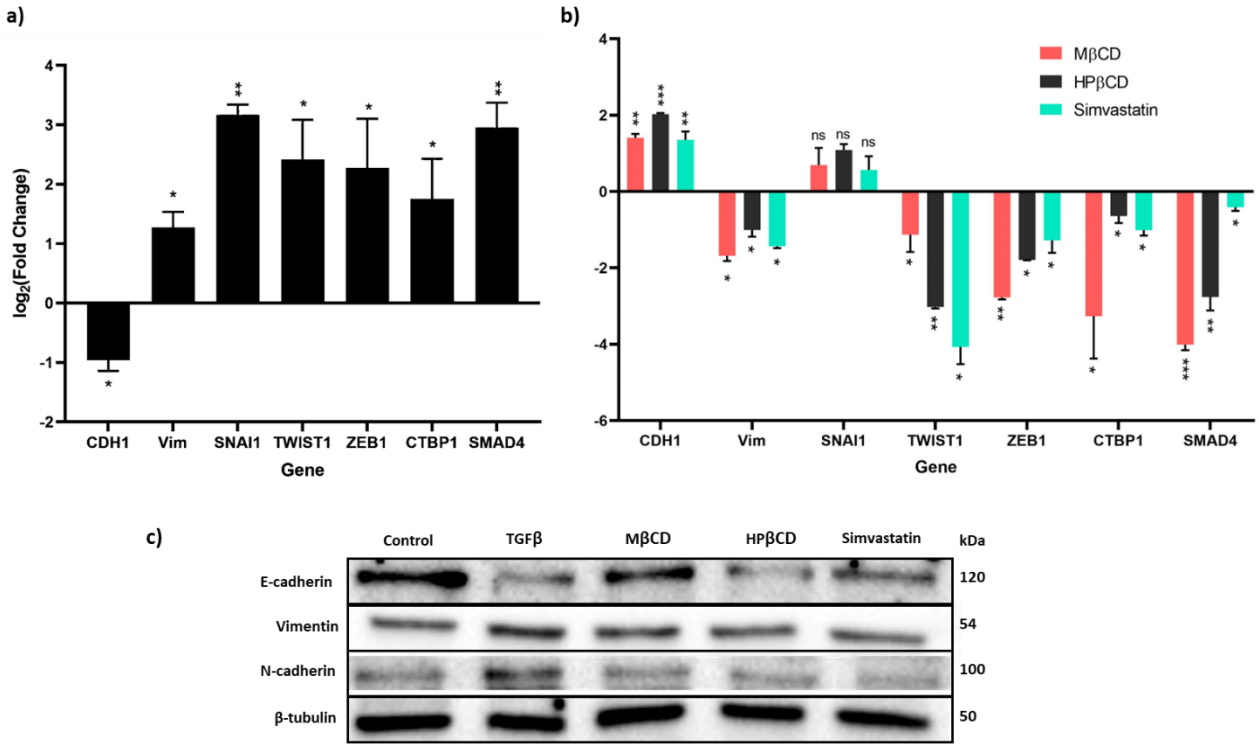

Figure 17: Changes in EMT-related gene expression in response to cholesterol depletion. (a) RT-qPCR analysis of transcriptional expression of *CDH1, Vim, SNAI1, TWIST1, ZEB1, CTBP1,* and *SMAD4* genes in TGFβ-treated cells relative to pre-EMT cells. (b) RT-qPCR analysis of transcriptional expression of *CDH1, Vim, SNAI1, TWIST1, ZEB1, CTBP1,* and *SMAD4* genes between untreated cells post-EMT and post-EMT cells treated with 1 mM MβCD, 10 mM HPβCD, and 10 μM simvastatin for 2 hours. Relative expression is presented as $\log_2$ fold changes between conditions. Data shown represents mean ± standard deviation. Statistical significance was calculated using a two-tailed unpaired Student's t-test where * $P < 0.05$, ** $P < 0.01$, *** $P < 0.001$, and ns indicates no significant change; n=3. (c) Western blots comparing protein expression of E-

cadherin, Vimentin, and N-cadherin pre- and post-EMT and post-EMT treated with 1 mM MβCD, 10 mM HPβCD, and 10 μM simvastatin for 2 hours with β-tubulin used as a loading control.

3.14 Changes in cholesterol pathway gene expression in response to cholesterol depletion

The expression levels of genes in cholesterol signalling pathways were measured using RT-qPCR and Western blotting. Changes in gene expression were measured between cells pre- and post-EMT, and post-EMT after treatment with cholesterol-lowering compounds. RT-qPCR was used to assess transcriptional expression changes of *ABCA1, ABCG1, SREBF2, LXR, LDLR, HMGCR, PCSK9,* and *LCAT* genes between pre- and post-EMT cells (Figure 18a) and post-EMT in response to treatment with 1 mM MβCD, 10 mM HPβCD, and 10 μM simvastatin for 2 hours (Figure 18b). Figure 18a represents transcriptional expression changes in response to EMT induction. Upon EMT induction with TGFβ, expression of *ABCA1* increased with a $\log_2$ fold change of 0.92. *ABCG1* expression increased significantly with a $\log_2$ fold change of 4.54. Expression of *SREBF2, LXR, LDLR,* and *HMGCR* increased upon EMT induction with $\log_2$ fold changes of 1.09, 0.885, 1.08, and 1.43, respectively. There was no significant difference between the transcriptional expression of *PCSK9* pre- and post-EMT. Finally, the expression of *LCAT* decreased upon EMT induction with a $\log_2$ fold change of -0.79, compared to untreated pre-EMT cells.

To measure expression changes caused by cholesterol depletion, RT-qPCR was used to compare transcriptional expression levels between untreated cells post-EMT induction with cells treated with cholesterol-lowering compounds, MβCD, HPβCD, and simvastatin, post-EMT. The changes in expression are represented in Figure 18b. All three cholesterol-lowering compounds decreased the expression of *ABCA1* post-EMT, with $\log_2$ fold changes of -0.98 after MβCD treatment, -1.74 after HPβCD treatment, and -1.51 after simvastatin treatment. Similarly, *ABCG1* expression was reduced after cholesterol-lowering treatment with $\log_2$ fold changes of -2.62 after MβCD treatment, -4.81 after HPβCD treatment, and -5.81 after simvastatin treatment. Treatment with cholesterol-lowering compounds did not significantly change the expression of *SREBF2* or *PCSK9* post-EMT. *LXR* expression was decreased following treatment with MβCD, with a $\log_2$ fold change of -2.42, and HPβCD treatment, with a $\log_2$ fold change of -3.08, but no significant change was observed following simvastatin treatment. Expression of *HMGCR* was reduced after cholesterol-lowering treatment with $\log_2$ fold changes of -1.86 after MβCD treatment, -1.72 after HPβCD treatment, and -0.94 after simvastatin treatment. Finally, the expression levels of both *LDLR*

and *LCAT* were reduced by MβCD treatment, with $\log_2$ fold changes of -1.38 and -1.1, respectively, and increased by simvastatin treatment, with $\log_2$ fold changes of 1.19 and 1.79, respectively. HPβCD treatment had no significant effect on the expression of *LDLR* or *LCAT*.

Western blotting was used to assess protein expression changes of ABCG1, HMGCR, LXR, SREBP1, and SREBP2 between pre- and post-EMT cells and post-EMT cells in response to treatment with 1 mM MβCD, 10 mM HPβCD, and 10 μM simvastatin for 2 hours (Figure 18c). The control lane represents NMuMG cells pre-EMT, the TGFβ lane represents cells post-EMT, and the MβCD, HPβCD, and simvastatin lanes represent cells post-EMT treated with the respective cholesterol-lowering compound. Protein levels are assessed using band size on the blot. Upon EMT induction, ABCG1 protein levels increased. After treatment with MβCD, there is a slight reduction in protein levels and treatment with HPβCD and simvastatin reduced ABCG1 expression further compared to untreated cells post-EMT. HMGCR levels increased upon EMT induction and were reduced by MβCD, HPβCD and simvastatin treatment. LXR protein levels were low pre-EMT and were increased upon EMT induction. Treatment with MβCD led to a slight reduction in LXR protein levels, while HPβCD and simvastatin further reduced LXR protein expression. SREBP1 and SREBP2 antibodies bind to both cytoplasmic (C-SREBP1 and C-SREBP2) and nuclear (N-SREBP1 and N-SREBP2) variants of the SREBP proteins. Protein levels of C-SREBP1 did not differ pre- and post-EMT and following treatment with MβCD, while there was a minor reduction of C-SREBP1 following HPβCD and simvastatin treatment. N-SREBP2 levels increased post-EMT compared to pre-EMT cells. Treatment with cholesterol-lowering compounds did not affect N-SREBP1 levels post-EMT. C-SREBP2 showed expression pre-EMT, which was reduced upon EMT induction. Treatment with cholesterol-lowering compounds did not affect C-SREBP2 levels post-EMT. N-SREBP2 levels pre-EMT were low and increased upon EMT induction. MβCD treatment did not change levels of N-SREBP2, while HPβCD and simvastatin treatment post-EMT show a reduction in N-SREBP2 levels. Blots shown in Figure 18c are representative blots from 3 independent experimental repeats.

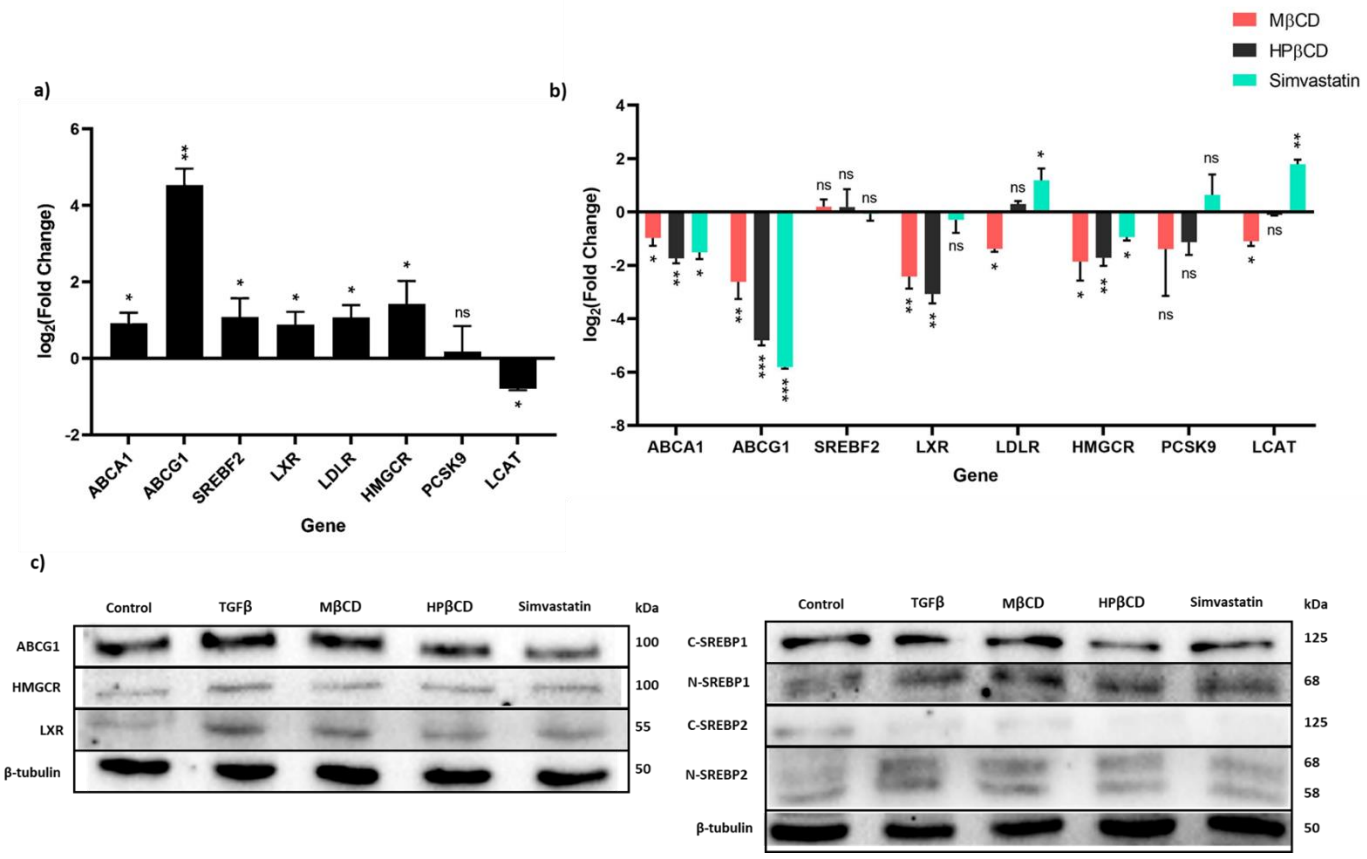

Figure 18: Changes in cholesterol-related gene expression in response to cholesterol depletion. (a) RT-qPCR analysis of transcriptional expression of *ABCA1*, *ABCG1*, *SREBF2*, *LXR*, *LDLR*, *HMGCR*, *PCSK9*, and *LCAT* genes in TGFβ-treated cells relative to pre-EMT cells. (b) RT-qPCR analysis of transcriptional expression of *ABCA1*, *ABCG1*, *SREBF2*, *LXR*, *LDLR*, *HMGCR*, *PCSK9*, and *LCAT* genes between untreated cells post-EMT and post-EMT cells treated with 1 mM MβCD, 10 mM HPβCD, and 10 μM simvastatin for 2 hours. Relative expression is presented as $\log_2$ fold changes between conditions. Data shown represents mean ± standard deviation. Statistical significance was calculated using a two-tailed unpaired Student's t-test where * $P < 0.05$, ** $P < 0.01$, *** $P < 0.001$, and ns indicates no significant change; n=3. (c) Western blots comparing protein expression of ABCG1, HMGCR, LXR, SREBP1, and SREBP2 pre- and post-EMT and post-EMT treated with 1 mM MβCD, 10 mM HPβCD, and 10 μM simvastatin for 2 hours with β-tubulin used as a loading control.

Chapter 4: DISCUSSION

Cholesterol plays an important role in cell signalling and structure and its dysregulation has been associated with numerous diseases including cancer. High cholesterol levels have been

reported in various cancer types, but the meaning of this increase has yet to be determined. An example of this is the accumulation of cholesterol in prostate cancer cells, which is associated with increased cancer cell growth [262]. In breast cancer, LDL cholesterol promotes cell proliferation and in mouse models of breast cancer, hypercholesterolemia was associated with larger and more proliferative tumours [263]. These findings led to studies assessing the efficacy of cholesterol-lowering treatment in reducing cancer risk, severity, and mortality. The use of statins was associated with lower breast cancer mortality [264], and a lower recurrence rate in patients diagnosed with invasive breast carcinoma [265].

There are, however, studies that show no association between cholesterol and cancer or a negative effect of cholesterol lowering on patient prognosis. A meta-analysis of 26 randomised clinical trials found no beneficial effect of statin use on cancer incidence or mortality [266]. Surprisingly, a longitudinal study from the UK Algorithm for Comorbidities Associations, Length of stay and Mortality (ACALM) registry found that women over the age of 40 with higher cholesterol levels had lower incidence of breast cancer than non-hyperlipidaemia patients [267]. Conflicting evidence about the role of cholesterol in cancer progression has led to uncertainty regarding the use of cholesterol-lowering drugs as a potential treatment for cancer. In addition, the lack of research delineating the molecular pathways in which cholesterol contributes to cancer progression has compounded this uncertainty. This study aimed to elucidate the role that cholesterol plays in EMT in cancer, a critical step in the development of advanced metastatic cancer, to contribute to the understanding of the potential effects of lowering cholesterol in cancer patients.

4.1 TGFβ-mediated induction of EMT in NMuMG cells

TGFβ is a secreted cytokine responsible for regulating proliferation, differentiation, and migration of different cell types. It plays a key role in mediating embryonic development, tissue repair, and inflammation [268]. TGFβ promotes EMT by inducing the expression of several EMT-TFs, including SNAIL1, a strong repressor of E-cadherin [269]. E-cadherin, through its interaction with the PDZ (postsynaptic density protein 95 (PSD-95), Drosophila disc large (Dlg1), and Zonula occludens 1 (ZO-1)) domain of the Scribble (SCRIB) protein, maintains cell polarity and orientation and the integrity of the epithelial layer [270]. The loss of E-cadherin following exposure of NMuMG cells to recombinant TGFβ can be visualised in Figure 4.2, where fluorescently marked E-cadherin decreased in response to activation TGFβ pathways. This is confirmed in Figure 7 with a decrease in both the RNA and protein

level expression of E-cadherin after TGFβ exposure. E-cadherin is responsible for maintaining the rectangular morphology, polarity, and cell-cell adhesion observed in epithelial cells [271]. The loss of E-cadherin causes cells to adopt an irregular and elongated shape, lacking apical-basal polarity, as well as fewer cell-cell contacts. This is apparent in Figure 4.1, which compares morphology of cells before and after TGFβ exposure. Control cells maintain a regular epithelial shape with intact cell-cell adhesion junctions and are tightly packed in a single layer, whereas TGFβ-treated cells are irregularly shaped and more spread apart with fewer cell-cell contacts, enabling increased motility. As E-cadherin suppresses cell invasion, its loss may promote an invasive phenotype [271].

A prominent feature of EMT is the cadherin switch, whereby E-cadherin expression is lost in favour of N-cadherin expression [272]. Along with the loss of E-cadherin protein expression observed in Figure 7b, a gain of N-cadherin expression was observed after TGFβ exposure. This change in expression can be visualised in Figure 16, which shows an increase in fluorescently labelled N-cadherin after TGFβ exposure compared to control cells. In adults, N-cadherin is expressed in endothelial and neural cells, playing a role in vascular stability and synapse function [273, 274]. In cancer, N-cadherin mediates both pro-metastatic signalling and the cell-cell adhesion required for cell invasion. N-cadherin is critical for trans-endothelial migration through its interaction with vascular endothelial (VE)-cadherin [275]. It mediates interaction between cancer cells and stromal cells, promoting cancer cell invasion [276]. N-cadherin also associates with β-catenin, forming a complex that mediates N-cadherin-associated cell-cell adhesion. This interaction enhances the nuclear translocation and transcriptional activity of β-catenin, suggesting a role for N-cadherin in Wnt signalling [277].

Further indication of the induction of EMT is the gain of Vimentin expression. Vimentin, an intermediate filament protein expressed in mesenchymal cells, is a commonly used marker of EMT, as its expression indicates a transition toward a mesenchymal state [278]. Along with a switch in cadherin expression, advanced malignant cells undergoing EMT experience a switch in intermediate filament type. Specifically, the epithelial-associated cytokeratin is downregulated in favour of the mesenchymal-associated Vimentin in aggressive subtypes of breast cancer [279]. This expression of Vimentin is associated with a poor clinical outcome [126]. A gain of Vimentin expression is observed after TGFβ exposure in Figure 6, which shows a significant increase in fluorescently labelled Vimentin in cells before and after TGFβ exposure. This is confirmed through expression studies represented by Figure 7, which show

an increase in transcriptional expression of *Vim*, and increase in the protein expression of Vimentin after TGFβ exposure.

Vimentin is involved in reorganising the cytoskeleton, altering the orientation and polarity of the cell from apical-basal polarity to a front-back polarity observed in mesenchymal cells [280]. The reorganization of the cytoskeleton may be responsible for the change in cellular morphology observed in Figure 5, where TGFβ exposure, which increased Vimentin expression, resulted in a change from rectangular shape to an elongated shape. Vimentin expression is also associated with increased cell stiffness, focal adhesion formation, and loss of junctional E-cadherin, each contributing to the invasive and migratory potential of cancer cells [280]. In addition, Vimentin contributes to the mechanical integrity of the cell, supporting directional force transmission required for single cells to invade and migrate during metastasis [281]. In this way, Vimentin enables metastasis, explaining why EMT is critical for successful metastasis in advanced cancer.

In addition to its structural role in cells undergoing EMT, Vimentin has an important role in EMT-related signalling. The *Vim* promoter contains binding motifs for Smad proteins, which are key regulators of EMT [282]. Translocation of the Smad2/3/4 complex modulates transcription of *Vim.* Vimentin expression is also activated by β-catenin/TCF binding to the *Vim* promoter, which promotes invasion and migration [283]. The EMT-TF Twist1 is shown to promote EMT by increasing Vimentin expression [284]. Vimentin regulates the expression of Snail and knock-down of Vimentin decreased *Snai1* transcription [285]. Vimentin also regulates the expression and function of Slug by enhancing its expression, interacting with ERK, and promoting ERK-mediated phosphorylation of Slug [286]. Following exposure to TGFβ, *TWIST1* and *SNAI1* expression increased significantly (Figure 7). Figure 17 also shows an increase in *SMAD4* expression after TGFβ treatment. This shows that an increase in Smad4 and Twist1 expression may induce the transcription of *Vim*, causing Vimentin expression to increase. The increased Vimentin expression then induces the transcription of *SNAI1*, increasing Snail activity in the cell, which represses E-cadherin expression as shown above.

Further pathway changes in response to TGFβ exposure include the significant increase in *ZEB1* and *CTBP1* expression compared to untreated control cells, shown in Figure 17. ZEB1 is a downstream target of TGFβ and is therefore expected to increase with TGFβ treatment [287]. ZEB1 promotes EMT by directly repressing E-cadherin expression [67]. CtBP proteins

are transcriptional corepressors overexpressed in aggressive cancers with poor clinical outcomes [288-290]. CtBP plays a role in EMT by repressing the expression of the E-cadherin gene, *CDH1*. It is recruited to the *CDH1* promoter region, where it interacts with ZEB1 and recruits chromatin remodelling enzymes such as histone deacetylases (HDACs), and histone methyltransferases (HMTs), forming a complex that represses *CDH1* chromatin, leading to a decrease in gene expression [291]. Together, the expression changes observed in this study confirm that TGFβ induces EMT, which results in a shift in transcriptional regulation of the cell, resulting in altered cadherin and intermediate filament expression and a change in cellular morphology.

While TGFβ displays pro-oncogenic effects in the induction of EMT, it also exhibits characteristics of a tumour suppressor. TGFβ triggers G1 cell cycle arrest, inhibiting cell proliferation [292]. One mechanism of this growth inhibition is through the activation of Smad4, which promotes the expression of eukaryotic translation initiation factor 4E (eIF4E)-binding protein 1 (4E-BP1), which plays a role in cell proliferation and translation through mTORC1 signalling [293]. TGFβ also induces expression of cyclin-dependent kinase (CDK) inhibitors, p27KIP1, p15INK4b, and p21WAF1, which inhibit the formation of CDK-cyclin complexes and induce G1 cell cycle arrest [294]. A decrease in fluorescent labelling of the marker of proliferation Ki-67 observed in Figure 8 following TGFβ exposure confirms the inhibitory effect TGFβ has on cell proliferation. Ki-67 accumulates during S, G2, and M phases of the cell cycle and its expression is used as a marker of cell cycle progression and proliferation [295]. It is degraded during G1 and G0 phases of the cell cycle, and therefore the G1 cell cycle arrest triggered by TGFβ exposure should decrease cellular Ki-67 levels compared to proliferating cells, which is observed and quantified in Figure 8. A decrease in cell proliferation is commonly observed in invasive cells undergoing EMT [296]. Following invasion, tumour cells undergo the reverse of EMT, MET, in which cells regain their epithelial-associated proliferative capacity, allowing for the growth of secondary metastases [297]. In these cases, cells may retain mesenchymal properties in addition to the proliferative properties associated with the epithelial phenotype due to epithelial/mesenchymal plasticity.

Epithelial/mesenchymal plasticity refers to the ability of cells undergoing EMT or MET to assume hybrid states exhibiting characteristics of epithelial and mesenchymal phenotypes. EMT and MET are reversable transitional processes with stable and metastable intermediary states on a spectrum between epithelial and mesenchymal states [296]. It is therefore rare to observe a complete EMT in which cells completely lose epithelial characteristics and assume

a fully mesenchymal state. The various intermediary states of EMT are termed partial EMT to describe the incomplete transition from epithelial to mesenchymal phenotypes. In figure 7b, Western blotting shows that although reduced E-cadherin is observed in TGFβ-treated cells compared to control, E-cadherin expression is not totally lost. It should also be noted that Vimentin and N-cadherin expression were not completely absent pre-EMT in control cells, suggesting that EMT stimuli such as TGFβ induce progression from one transitionary state of partial EMT towards a more mesenchymal state without the complete loss of epithelial characteristics or complete gain of all mesenchymal characteristics.

4.2 Changes in cholesterol levels in NMuMG cells following EMT induction

The role of cholesterol in cancer progression is complex, with cholesterol being an important part of cell membrane structure, as well as participating in signalling pathways. As cholesterol is an important structural component of the cell, increased cholesterol levels are required to facilitate the increase in proliferation observed in cancer cells. Cholesterol accumulation is associated with increased growth and proliferation in prostate cancer [262]. A study of breast cancer using a mouse model suggested that cholesterol enhances tumour formation and proliferation [182]. Interestingly, this study showed a decrease in plasma cholesterol during tumour development, which suggests an increase in cholesterol uptake and utilization by cancer cells. These studies establish a link between cholesterol and cancer cell proliferation, but do not highlight the role of cholesterol in EMT, in which cells may have decreased proliferative capacity. In more aggressive subtypes of cancer in which EMT pathways are active, cholesterol pathways may be downregulated. In a study of colorectal cancer, the activation of EMT lowered cholesterol-related pathways and promoted an aggressive, metastatic phenotype [298]. In addition, inhibition of the cholesterol pathway was shown to induce TGFβ-mediated EMT, leading to poor patient outcome in pancreatic ductal adenocarcinoma [213]. On the contrary, cholesterol is shown to induce EMT in prostate cancer [299]. To address the conflicting evidence on the role of cholesterol in EMT, we aimed to characterize cellular cholesterol content and changes in cholesterol-related signalling pathways following TGFβ-mediated EMT induction.

As TGFβ induces cell cycle arrest, it is expected that cells require lower cholesterol levels for proliferative requirements. Free cholesterol, CEs, and lipid raft cholesterol all decreased significantly after TGFβ-mediated EMT induction (Figure 9). Quantitatively measuring total cellular cholesterol, presented in Figure 9c, also revealed a decrease in cellular cholesterol content after TGFβ exposure. This highlights a decrease in membrane biosynthesis caused by

a decrease in proliferative capacity. In addition, EMT induction may repress cholesterol synthesis and pathways through CtBP-associated co-repression [214]. CtBP is shown to regulate cholesterol homeostasis by forming a complex with ZEB1 and repressing the transcription on *SREBF2*, decreasing cholesterol biosynthesis [214]. An increase in EMT-TFs Twist and Slug were also associated with a decrease in cellular cholesterol, suggesting that decreased cholesterol levels are associated with EMT. [214]. The decrease in cholesterol may promote TGFβ signalling, as TGFβ receptors are shown to undergo cholesterol-mediated endocytosis and degradation, which inhibits TGFβ signalling [300].

It should be noted that despite the repressive effect of CtBP on *SREBF2* expression, a low cellular cholesterol level induces the expression of SREBP1 and SREBP2 [213]. SREBP1 is shown to induce TGFβ expression and signalling, and promote EMT [213]. This suggests that cholesterol biosynthesis pathways play different roles in EMT, depending on the current state of EMT the cell is in. A reduction in cholesterol seems to be important upon initial induction of EMT and an increase in cholesterol biosynthesis may be important to maintain EMT signalling after induction. Figure 18 shows changes in cholesterol signalling after TGFβ-mediated EMT induction. An increase in *SREBF2* and *HMGCR* expression is observed in Figure 18a, which is confirmed by an increase in HMGCR, N-SREBP1 and N-SREBP2 protein expression observed in Figure 18c in TGFβ treated cells compared to pre-EMT control. C-SREBP2 is reduced post-EMT compared to pre-EMT, suggesting nuclear translocation of SREBP2 following EMT induction, allowing it to induce transcription of its target genes. This indicates an increase in cholesterol biosynthesis pathways caused by EMT induction, despite the decreased cellular cholesterol levels.

An increase in cholesterol biosynthesis has many implications in cancer cells. HMGCR expression is associated with EMT and metastasis and its targeted inhibition is shown to attenuate TGFβ-mediated tumour progression [301]. Squalene epoxidase, which is an enzyme involved in cholesterol synthesis downstream of HMGCR, is negatively correlated with E-cadherin expression and is associated with metastasis and poor overall survival in patients [302]. The increase in cholesterol biosynthesis also increases cellular 27HC content, which is shown to induce EMT in breast cancer [303]. This EMT induction may be mediated by the ability of 27HC to act as a ligand for LXR, which promotes EMT induction in breast cancer cells [192]. An increase in *LXR* expression after TGFβ exposure is observed in Figure 18a, which translates to an increase in LXR protein expression shown in Figure 18c. This increase

in LXR coupled with the observed increase in cholesterol biosynthesis pathway expression may promote an invasive EMT phenotype.

Even though cholesterol biosynthesis pathways were upregulated, cellular cholesterol content in the cell was significantly lower after EMT induction. This may be caused by an increase in cholesterol efflux protein expression, which decreases cellular cholesterol levels. Expression analyses shown in Figure 18a show a significant increase in *ABCA1* and *ABCG1* expression in TGFβ-treated cells compared to the pre-EMT control. ABCG1 protein expression is also increased upon EMT induction, shown in Figure 18c, when comparing control cell expression of ABCG1 to TGFβ-treated expression levels. ABCA1 and ABCG1 mediate the efflux of cholesterol from the cell, and are responsible for reduced cellular cholesterol content [304]. The increase in ABCA1 and ABCG1 expression may be due to the increased LXR expression observed in Figure 18. LXR binds to the promoters of both ABCA1 and ABCG1, increasing their expression [164]. The upregulation of ABCA1 observed after TGFβ exposure is consistent with literature showing that ABCA1 is upregulated in breast cancer EMT [305]. It may also play a role in cancer drug resistance, a characteristic of EMT, as it is associated with acquired chemotherapy resistance in ovarian cancer [197]. ABCG1 is associated with a metastatic cancer phenotype and its inhibition triggers tumour regression in three-dimensional colon cancer models [199]. Its upregulation, together with upregulated Wnt signalling, is associated with oxaliplatin resistance in hepatocellular carcinoma [198]. Thus, the upregulation of ABCA1 and ABCG1 following TGFβ exposure explains the decrease in cellular cholesterol content observed after TGFβ exposure and may also play a role in EMT-associated drug resistance observed in advanced cancer cases.

The expression of LDLR was upregulated after TGFβ exposure (Figure 18a). LDLR facilitates cholesterol uptake and is upregulated in TNBC cell lines [186]. In a study of thyroid carcinoma, increased LDLR expression was associated with an increased intratumoral accumulation of 27HC, and an increase in tumour cell migration [306]. Figure 18a also shows a downregulation of LCAT following EMT induction. The role of LCAT in cancer and EMT is not fully understood. LCAT enables the conversion of free cholesterol to CEs and transport of cholesterol to the liver for excretion. LCAT levels were found to be decreased in breast cancer patients compared to a control group [307]. Since LCAT leads to the esterification and eventual excretion of cholesterol, it functions to decrease serum cholesterol levels and prevent cellular cholesterol intake. In the absence of LCAT, rates of cholesterol influx and efflux were equal, resulting in no net transfer of cholesterol out of the cell, due to the

availability of serum cholesterol for cellular intake after efflux [308]. The presence of LCAT led to a net cholesterol efflux, due to the esterification of cholesterol enabling cholesterol excretion.

Together, the cholesterol pathway expression changes indicate a complex role of cholesterol in EMT with an increase in both cholesterol biosynthesis and efflux, ultimately resulting in a lower cellular cholesterol level post-EMT compared to pre-EMT. The decrease of LCAT and increase in both influx (LDLR) and efflux (ABCA1 and ABCG1) proteins, as well as cholesterol biosynthesis proteins (SREBP1/2 and HMGCR), observed in Figure 18a and 18c suggests a continuous flow of cholesterol out of the cell, fuelled by serum cholesterol intake back to the cell and increased cholesterol biosynthesis. This mechanism may indicate an importance of cholesterol in the maintenance of the EMT phenotype, as well as an importance of cholesterol efflux pathways which contribute to drug resistance. Cholesterol may have pro- and anti-EMT properties, depending on the current cellular state, which explains the continuous synthesis, intake, and efflux of cholesterol, instead of a complete inhibition of cholesterol synthesis and intake in favour of cholesterol efflux pathways.

4.3 The effects of cholesterol depletion on the EMT phenotype

While cellular cholesterol levels are decreased following EMT induction using TGFβ, expression analysis suggest that a continuous source of cholesterol seems to be an important driving force in the maintenance of the EMT phenotype. Thus, removing this cholesterol source and interrupting the cycle of cholesterol biosynthesis, intake, and efflux may inhibit the EMT phenotype. The cholesterol-lowering compounds MβCD, HPβCD, and simvastatin were selected to lower cellular cholesterol levels through different mechanisms.

The effect of treatment with cholesterol-lowering compounds on cell viability was assessed after treatment with MβCD, HPβCD, and simvastatin for 2 hours and 24 hours. In order to study the molecular mechanisms of cholesterol-lowering in EMT, it was important to maintain cell viability, as inducing cell death would interfere with expression analysis and cellular behaviour. Figure 10 represents the percentage viability of cells treated with cholesterol-lowering compounds pre- and post-EMT, compared to pre- and post-EMT untreated controls. After 2 hours, no significant reduction in cell viability was observed pre- or post-EMT. Treatment with HPβCD and simvastatin reduced cell viability after 24 hours. Therefore, the 2-hour treatment period was selected to elucidate the underlying mechanisms of cholesterol in EMT. Notably, following MβCD treatment of cells pre-EMT for 2 and 24-

hour periods, cell viability increased significantly compared with the untreated control. This may be due to an increase in glucose uptake caused by an increase in the activity of the glucose transported GLUT1, shown to follow MβCD-mediated cholesterol depletion [309]. High glucose is associated with increased cell growth and proliferation [310] and GLUT1 expression is shown to promote cell proliferation [311].

As expected, the use of MβCD, HPβCD, and simvastatin reduced cellular cholesterol levels both pre- and post-EMT. Figures 11, 12, and 13 show the decrease in free cholesterol, CEs, and lipid raft cholesterol, respectively, pre- and post-EMT after treatment with cholesterol-lowering compounds. There were exceptions to the general trend of cholesterol reduction. In Figure 11, simvastatin did not significantly change the levels of free cholesterol post-EMT, compared to untreated cells post-EMT. In Figure 12, MβCD treatment of cells post-EMT led to a statistically significant increase in cholesteryl ester content. In general, cholesterol-lowering compounds lowered cellular cholesterol levels.

Treatment with cholesterol-lowering compounds ameliorates the increase in invasive potential observed after TGFβ exposure. Figure 14 shows a comparison of invasive potential of pre- and post-EMT cells and of post-EMT cells after treatment with cholesterol-lowering compounds. Compared to pre-EMT control cells, TGFβ-treated cells have a significantly higher invasive potential. This is explained by the increased EMT-TF expression, as well as the loss of E-cadherin expression and gain of N-cadherin and Vimentin expression discussed above. Treatment with MβCD, HPβCD, and simvastatin each reduced invasive potential significantly compared to untreated cells post-EMT. The expression changes contributing to the loss of invasive potential will be discussed below. In addition, cholesterol lowering using both MβCD and simvastatin causes membrane lipid raft disruption and suppresses tumour cell migration [312]. Cholesterol lowering using statins has been shown to decrease migration and invasion in various cancer types, including melanoma [313], prostate cancer [314], and breast cancer [220]. Interestingly, it was found that lovastatin treatment disrupted microtubule and actin organisation and inhibited the formation of integrin-mediated focal adhesions, reducing lung metastases in a mouse model of breast cancer [315]. This counteracts the changes in cytoskeleton organisation and focal adhesion formation associated with increased Vimentin expression, suggesting a decreased expression of Vimentin after cholesterol-lowering treatment.

Analysis of EMT-associated gene expression following cholesterol-lowering treatment enabled the elucidation of mechanisms altered by decrease in cellular cholesterol. Figure 15 shows an increase in E-cadherin and a decrease in Vimentin fluorescent staining following treatment with MβCD, HPβCD, and simvastatin post-EMT. This is confirmed in Figure 17b, which shows an increase in the transcription of *CDH1* and a decrease in *Vim* transcription following cholesterol-lowering treatment. Figure 17c shows an increase in E-cadherin protein abundance after treatment with MβCD and simvastatin but HPβCD did not exhibit the same increase in E-cadherin as previous experiments, including RT-qPCR and immunofluorescent staining. Further investigation is required to determine the lack of response to HPβCD treatment in Western blotting, compared with the presence of a response in other assays. Similarly, Figure 17c shows a decrease in Vimentin and N-cadherin expression after cholesterol-lowering treatment. The decrease in N-cadherin is confirmed through immunofluorescent staining, shown in Figure 16.

The above results demonstrate a reversal of EMT-associated marker expression and a shift toward a more epithelial state. The increase in E-cadherin expression and decrease in N-cadherin expression shows a reversal of the cadherin switch observed during EMT. As E-cadherin is a suppressor of tumour invasion and metastasis, its re-expression could explain the decreased invasive potential observed following cholesterol-lowering treatment [316]. The concomitant loss of N-cadherin expression may inhibit trans-endothelial migration and invasion associated with EMT [275]. Downregulation of Vimentin is associated with a loss of migration and invasion in both colon and breast cancer [317]. As Vimentin plays a predominant role in EMT-associated changes in cell morphology, polarity, and motility, loss of Vimentin expression may cause a reorganisation of the cytoskeleton and gain of apical-basal polarity, leading to a more epithelial phenotype with a lower invasive potential [318].

Additional transcriptional changes post-EMT in response to cholesterol-lowering are presented in Figure 17b. With the reversal of post-EMT E-cadherin, Vimentin, and N-cadherin expression following cholesterol-lowering treatment, it was expected that *SNAI1* expression would be reduced. However, no significant change in *SNAI1* expression was observed after cholesterol was lowered. There was, however, a significant reduction in *TWIST1, ZEB1, CTBP1,* and *SMAD4* expression following treatment. As TWIST1 and Smad4 both increase Vimentin expression, their downregulation is likely responsible for the observed decrease in Vimentin [282, 284]. Since Snail1 expression was unchanged by cholesterol-lowering treatment, the increase in E-cadherin expression is likely due to the

reduced *ZEB1* and *CTBP1* expression. Both Zeb1 and CtBP act as repressors of E-cadherin expression [291]. It should be noted that the TGFβ-treated NMuMG model of EMT used in this study involves constant exposure to recombinant TGFβ, even upon treatment with cholesterol-lowering compounds. Lowering cholesterol may affect downstream TGFβ signalling, while constant exposure to TGFβ may allow for the continued expression of *SNAI1*, since Snail is an immediate target of TGFβ signalling [319]. This may explain the lack of significant reduction in *SNAI1* expression post-EMT after cholesterol-lowering treatment, but the reversal of downstream EMT signalling and the ability of cholesterol-lowering compounds to promote a more epithelial phenotype.

Cholesterol-lowering treatment also altered the expression of cholesterol pathway genes post-EMT, presented in Figure 18. Cholesterol biosynthesis genes *SREBF2* and *HMGCR* were upregulated by EMT induction, but cholesterol depletion only reduced *HMGCR* expression and had no significant effect on *SREBF2* expression. Protein abundance measured by Western blotting in Figure 18c confirms HMGCR reduction after cholesterol-lowering treatment, but also shows a slight reduction in N-SREBP2 levels. Despite no significant change in transcription of *SREBF2*, a decrease in N-SREBP2 suggests a reduction in nuclear translocation and transcription regulatory activity. *LCAT* expression was not affected by HPβCD treatment but was decreased by MβCD treatment and increased by simvastatin treatment. Similarly, *LDLR* expression was not affected by HPβCD treatment, but was decreased by MβCD treatment and increased by simvastatin treatment. Genes in the cholesterol efflux pathway, *ABCA1*, *ABCG1*, and *LXR* were decreased significantly by cholesterol-lowering treatment post-EMT, except for simvastatin, which did not affect *LXR* expression post-EMT. Protein abundance of LXR also decreased in response to cholesterol-lowering treatment (Figure 18c). In general, the changes in cholesterol pathway expression after treatment with cholesterol-lowering compounds post-EMT reversed the changes observed following EMT induction. Together with the reversal of EMT pathway genes, these expression changes suggest that treatment with cholesterol-lowering compounds is capable of reversing cellular changes caused by EMT induction and promoting a more epithelial phenotype.

Reducing intracellular cholesterol levels led to a reversal of TGFβ-mediated EMT expression changes, in addition to a reduction in invasive potential post-EMT. Although cholesterol levels were decreased overall after TGFβ-mediated EMT induction, the increase in cholesterol intake, biosynthesis, and efflux pathways suggest that a continuous cycle of

increasing and decreasing intracellular cholesterol levels is required to maintain a post-EMT phenotype. The initial increase in cholesterol levels caused by biosynthesis and intake can cause an increase in cholesterol levels in the mitochondria or the endoplasmic reticulum [320]. Mitochondrial cholesterol stimulates the biosynthesis of 27HC, which is shown to promote EMT induction by activating signal transducer and activator of transcription 3 (STAT3), and promote metastasis by increasing MMP9 expression [321]. 27HC also acts as a ligand for LXR, promoting LXR-dependent metastasis in breast cancer models [192]. Activated LXR acts as a TF, promoting the expression of ABCA1 and ABCG1, which efflux cholesterol from the cell, decreasing cellular cholesterol content [320]. ABCA1 expression is found to be higher in metastatic, mesenchymal breast cancer cells and lower in non-metastatic, epithelial cells [305]. Additionally, elevated expression of ABCG1 is associated with metastatic cancer cases [199]. This indicates the importance of cholesterol efflux pathways in EMT, and downregulating cholesterol efflux may inhibit EMT progression and maintenance. It should be noted that reducing cellular cholesterol levels using MβCD, HPβCD, and simvastatin had no effect on E-cadherin and Vimentin expression pre-EMT (Fig S2).

Increased cholesterol usually induces the proteolysis of LDLR and the sequestration of SREBPs, causing a decrease in cholesterol intake and biosynthesis [320]. However, following TGFβ-mediated EMT induction, SREBP2, HMGCR, and LDLR expression levels were upregulated, due to the overall decrease in cellular cholesterol observed after EMT induction. This enables continued 27HC production, LXR activation, and ABC protein efflux activity, leading to a feedback loop that maintains EMT stimulatory signals. This is exacerbated by the decrease in LCAT expression post-EMT, which prevents the esterification and subsequent excretion of cholesterol, maintaining a high serum cholesterol level, which facilitates cellular cholesterol uptake. Treating cells with cholesterol-lowering compounds may break this feedback loop by decreasing cellular cholesterol levels before 27HC is synthesised, preventing LXR activation and the overexpression of ABC efflux proteins.

The mechanisms of EMT reversal in response to cholesterol-lowering treatment are not fully apparent. Changes in EMT- and cholesterol-associated gene expression after EMT induction and after cholesterol-lowering treatment, it is likely that cholesterol biosynthesis, intake, and efflux pathways are important in the induction and maintenance of EMT. Removing cholesterol with cyclodextrins or statins attenuates the activation of cholesterol efflux pathways, which may prevent ABC-associated drug efflux. In addition, the expression of

cholesterol efflux proteins and EMT-TFs may be closely linked. A study showed the regulation of *ABCG1* and *SNAI2* expression by a common TF, HOXB13 [322]. The stability and function of EMT-associated N-cadherin depends on its association with cholesterol-rich lipid rafts [323]. Conversely, the stability of TGFβ receptors is inhibited by membrane cholesterol and lowering cholesterol levels increased the expression and stability of these receptors, promoting TGFβ-mediated EMT [324]. This conflicting role of cholesterol in promoting and inhibiting EMT progression suggests a more complex, context-dependent role of cholesterol in EMT, whereby cholesterol reduction is important for the initiation of EMT through TGFβ signalling, but cholesterol accumulation may be important for the maintenance of an invasive and treatment-resistant phenotype. This is summarised in Figure 19. Depleting cholesterol with cholesterol-lowering treatment reverses pathway changes observed following EMT induction and may prevent the cell from altering cholesterol content to suit the requirements of active EMT signalling pathways.

While the results achieved using simvastatin and the cyclodextrins were similar, their mechanisms of action differ. This suggests that lowering cholesterol reverses the EMT phenotype, regardless of the method used. As mentioned in the introduction, statins competitively inhibit HMGCR, thus inhibiting cholesterol biosynthesis through the mevalonate pathway [215]. β-cyclodextrins deplete cholesterol from the cell membrane by forming an inclusion body with cholesterol encapsulated within the hydrophobic cavity [236]. While the use of both types of compounds resulted in attenuated EMT signalling, the use of statins is limited to patients with hypercholesterolemia. In addition, associated side effects of statin use, particularly in African and Asian women, limits their use in cancer therapy [231]. Similarly, MβCD may exhibit cytotoxic effects in non-tumorigenic cells, making it unsuitable for use in a clinical setting [241]. The improved solubility and toxicologically benign nature of HPβCD may be more suitable for clinical use [242]. In addition, with targeted delivery, the cholesterol-lowering effects of HPβCD may be localised to the tumour area, allowing normal cells to function normally. This contrasts statins, which in inhibiting cholesterol biosynthesis, may limit the production of steroid hormones, bile acids, and vitamin D, which are all dependent on cholesterol as a precursor molecule [325]. The results of this study therefore provide justification for the further evaluation of HPβCD as a potential therapeutic agent in cancer treatment.

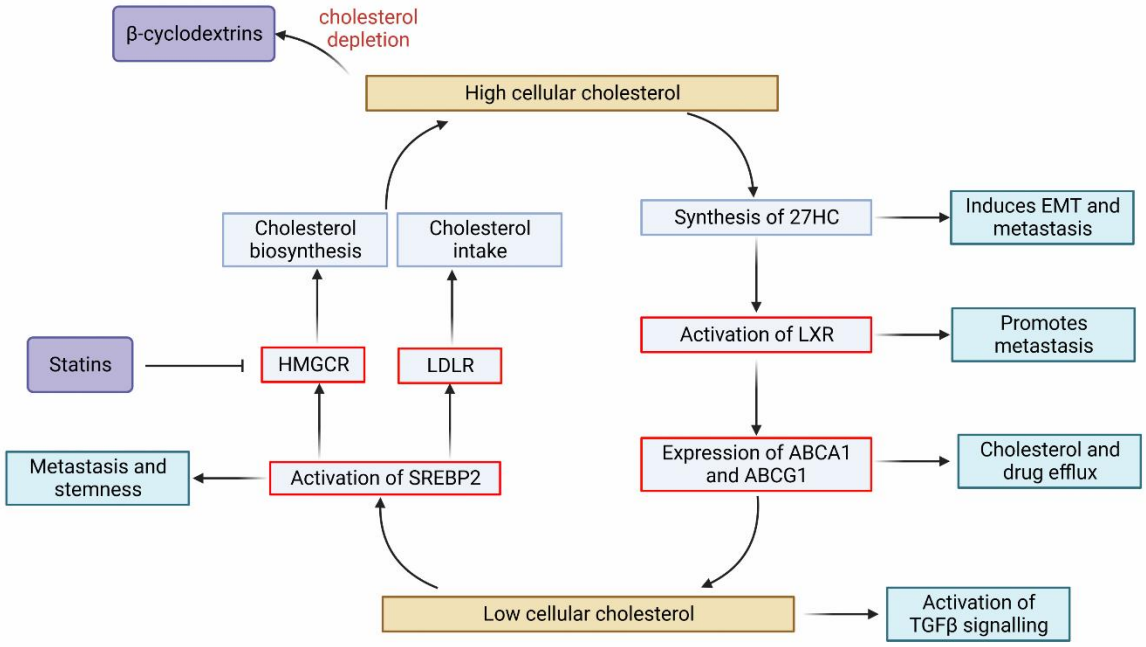

Figure 19: Illustration of the role of cholesterol regulation in EMT and metastasis. TGFβ signalling is shown to reduce cellular cholesterol through the activation of CtBP and Zeb1. Low cellular cholesterol stabilises the TGFβ receptors, promoting the TGFβ signalling pathway and EMT induction. Low cellular cholesterol also activates SREBP2 and promotes its nuclear translocation, where it activates the transcription of genes involved in cholesterol biosynthesis, such as *HMGCR*, and genes involved in cholesterol uptake, such as *LDLR*. Activation of SREBP2 is associated with metastasis and stemness in cancer cells [326]. The activation of cholesterol biosynthesis and cholesterol uptake pathways increases cellular cholesterol. This is inhibited by statins, which inhibit HMGCR. β-cyclodextrins deplete cholesterol from the cell, which also acts to lower cellular cholesterol. High cellular cholesterol leads to the accumulation of 27HC, which induces EMT and promotes metastasis [321]. 27HC also acts as a ligand for LXR activating its expression, which is associated with metastasis [327]. LXR activates the expression of ABCA1 and ABCG1, which are efflux proteins involved in reverse cholesterol transport and associated with drug resistance in cancer. The efflux of cholesterol reduces cellular cholesterol levels back to a state of low cellular cholesterol. This regulatory loop is a normal part of cholesterol homeostasis but seems to play a role in EMT progression with many steps in the pathways contributing to an invasive, EMT-like phenotype. Red boxed indicate genes that were shown to be upregulated in this study. Figure created with BioRender.com.

CONCLUSIONS

In summary, this study aimed to elucidate the role of cholesterol pathways in cancer EMT and assess the effect of cholesterol-lowering treatment on the induction and maintenance of EMT. TGFβ exposure induced an EMT phenotype with the expression of EMT-TFs, mesenchymal markers, and the decrease in expression of epithelial markers. EMT induction increased the invasive potential of the cell, while reducing their proliferative capacity. Cellular cholesterol was found to be reduced after TGFβ-mediated EMT induction; however, cholesterol uptake and biosynthesis pathway expression was still increased. The expression of cholesterol efflux proteins was responsible for the decrease in cholesterol content observed after EMT induction, which relies on an initial increase in cholesterol to activate efflux pathways. This suggests a context-dependent role of cholesterol in EMT induction and maintenance, where increased cholesterol is necessary for the initiation of certain EMT pathways, and decreased cholesterol is a consequence of their activation, as well as a requirement for the initiation of other EMT-inducing pathways.

Depleting cellular cholesterol with MβCD, HPβCD, and simvastatin decreased EMT marker expression, as well as the expression of EMT and cholesterol pathway genes that were upregulated by EMT induction. This significantly reduces the invasive potential of cells post-EMT. As invasion and metastasis are a predominant cause of cancer-related mortality, the reduction of invasive potential by cholesterol-lowering treatment suggests a role of cholesterol-lowering treatment as a novel strategy in cancer therapy but it is also critical to know the tumour make-up and EMT status at which cholesterol-depleting agents may be administered

The role cholesterol plays in cancer EMT is complex and is still not fully understood. Further study in a diverse set of tumour models is required to make concrete conclusions about the exact molecular mechanisms in which cholesterol plays a part in cancer progression and EMT pathways. However, this study has accomplished the first step in evaluating the effect of cholesterol-lowering treatment in reversing the EMT-related changes in cell behaviour. In doing so, this study has revealed a potential role of cholesterol-lowering treatment in inhibiting metastatic characteristics in cancer cells by reducing the expression of EMT-associated markers. With further research, cholesterol-lowering treatment, such as HPβCD and statins, may prove useful in improving currently available cancer treatment strategies.

LIMITATIONS

While *in vitro* cell models provide a homogeneous population of cells with which one can easily elucidate molecular changes in response to a stimulus or treatment, their clinical relevance is limited. Molecular pathways *in vivo* are more complex and may not exactly mimic results obtained *in vitro.* The use of an *in vitro* model of EMT in this study provided information about EMT pathways and the effect of cholesterol depletion on these pathways, but these results may not be consistent in a clinical setting, where interpatient variation may affect the efficacy of treatment. Another limitation of the study of cancer *in vitro* is the lack of a tumour microenvironment, which influences gene expression and cell phenotype. Similarly, cholesterol pathways *in vivo* are influenced by cholesterol synthesis and excretion in the liver, as well as the availability of serum cholesterol for cellular uptake. These factors are not present *in vitro* and therefore speculations have to be made based entirely on end-point results, such as gene expression and measured cholesterol content. Furthermore, *in vitro* models allow for direct treatment of cells with various compounds. In reality, drug treatments are heavily influenced by bioavailability and delivery method and although a specific treatment may be effective, it may not even reach the target cell in a high enough concentration or for a long enough time to exhibit beneficial effects.

Another limitation present in this study is the use of RT-qPCR alone to determine the expression of certain proteins in cholesterol and EMT-related pathways. While transcriptional expression is usually correlated with protein abundance and activity, post-transcriptional and post-translational modifications, as well as protein degradation and sequestration, may alter the activity of pathway proteins, even with an increase in transcriptional expression. Due to cost limitations, antibodies could not be acquired for every important protein studied and therefore transcriptional expression was used as an estimation of expression.

Lastly, the nature of EMT induction *in vitro* relies on constant exposure to an EMT inducer, such as TGFβ. Because of this, any changes in the expression of TGFβ itself could not be measured, since recombinant TGFβ was always present in the cell growth medium. It is possible that cholesterol-lowering treatment caused a change in TGFβ expression, but the effects of that change on downstream signalling and cellular phenotype could not be measured.

FUTURE STUDIES

To assess the validity of EMT reversal by cholesterol-lowering drugs observed in this study, an *in vitro* model should be used. The mouse mammary tumour virus-polyoma middle tumour-antigen (MMTV-PyMT) model is a mouse model of breast cancer in which tumours spontaneously develop and metastasize through EMT induction. Assessing the effect of cholesterol-lowering treatment in the MMTV-PyMT model in reducing tumour formation and metastasis would be the next step in determining the efficacy of cholesterol-lowering treatment in breast cancer therapy.

To fully elucidate the role of cholesterol in EMT, cholesterol replenishment studies should be performed in which cholesterol is loaded into cells, increasing their cholesterol content. Increasing cellular cholesterol levels and observing the effect on EMT induction will further clarify the role that cholesterol plays in the induction or inhibition of EMT progression. Additionally, the effect of cholesterol depletion on cells pre-EMT should be further investigated to determine whether cholesterol depletion affects cells in the absence of EMT signalling, and at different stages of the EMT induction process. Furthermore, while E-cadherin expression was assayed in this study, the splice variants of E-cadherin were not. This would be an opportunity to identify the role of differential splicing in the regulation of EMT.

To fully understand the role of different pathway proteins in EMT induction and in the reversal of EMT induction observed after cholesterol-lowering treatment, overexpression, and knockdown of various proteins in EMT and cholesterol pathways should be performed. This allows for the identification of causal proteins in EMT progression and reversal, which could be targeted directly in future studies.

Finally, the use of cholesterol-lowering compounds in combination with currently used cancer treatments could provide information about their interactions. In a clinical setting, it is common to combine therapeutic agents to formulate a treatment strategy that is appropriate to the type and subtype of cancer presented by individual patients. Using cholesterol-lowering compounds in combination with other therapeutic agents may result in synergistic anticancer effects or may reduce tumour drug resistance. Therefore, it is important to assess the combination of therapeutic agents *in vitro* and *in vivo* before proposing a treatment strategy for clinical use.

REFERENCES

1. Sung H, Ferlay J, Siegel RL, Laversanne M, Soerjomataram I, Jemal A, Bray F: **Global Cancer Statistics 2020: GLOBOCAN Estimates of Incidence and Mortality Worldwide for 36 Cancers in 185 Countries**. *CA: A Cancer Journal for Clinicians* 2021, **71**(3):209-249.
2. Joko-Fru WY, Jedy-Agba E, Korir A, Ogunbiyi O, Dzamalala CP, Chokunonga E, Wabinga H, Manraj S, Finesse A, Somdyala N *et al*: **The evolving epidemic of breast cancer in sub-Saharan Africa: Results from the African Cancer Registry Network**. *International Journal of Cancer* 2020, **147**(8):2131-2141.
3. Hanahan D: **Hallmarks of cancer: new dimensions**. *Cancer discovery* 2022, **12**(1):31-46.
4. Hanahan D, Weinberg RA: **The hallmarks of cancer**. *cell* 2000, **100**(1):57-70.
5. Hanahan D, Weinberg RA: **Hallmarks of cancer: the next generation**. *cell* 2011, **144**(5):646-674.
6. Ramsay D, Kent J, Hartmann R, Hartmann P: **Anatomy of the lactating human breast redefined with ultrasound imaging**. *Journal of anatomy* 2005, **206**(6):525-534.
7. Perou CM, Sørlie T, Eisen MB, Van De Rijn M, Jeffrey SS, Rees CA, Pollack JR, Ross DT, Johnsen H, Akslen LA: **Molecular portraits of human breast tumours**. *nature* 2000, **406**(6797):747-752.
8. O'Brien KM, Cole SR, Tse C-K, Perou CM, Carey LA, Foulkes WD, Dressler LG, Geradts J, Millikan RC: **Intrinsic breast tumor subtypes, race, and long-term survival in the Carolina Breast Cancer Study**. *Clinical Cancer Research* 2010, **16**(24):6100-6110.
9. Brenton JD, Carey LA, Ahmed AA, Caldas C: **Molecular classification and molecular forecasting of breast cancer: ready for clinical application?** *Journal of clinical oncology* 2005, **23**(29):7350-7360.
10. Ahn HJ, Jung SJ, Kim TH, Oh MK, Yoon H-K: **Differences in clinical outcomes between luminal A and B type breast cancers according to the St. Gallen Consensus 2013**. *Journal of breast cancer* 2015, **18**(2):149-159.
11. Nagata Y, Lan K-H, Zhou X, Tan M, Esteva FJ, Sahin AA, Klos KS, Li P, Monia BP, Nguyen NT: **PTEN activation contributes to tumor inhibition by trastuzumab, and loss of PTEN predicts trastuzumab resistance in patients**. *Cancer cell* 2004, **6**(2):117-127.
12. Sotiriou C, Neo S-Y, McShane LM, Korn EL, Long PM, Jazaeri A, Martiat P, Fox SB, Harris AL, Liu ET: **Breast cancer classification and prognosis based on gene expression profiles from a population-based study**. *Proceedings of the National Academy of Sciences* 2003, **100**(18):10393-10398.
13. Rakha E, Putti T, El-Rehim DA, Paish C, Green A, Powe D, Lee A, Robertson J, Ellis I: **Morphological and immunophenotypic analysis of breast carcinomas with basal and myoepithelial differentiation**. *The Journal of pathology* 2006, **208**(4):495-506.
14. Migowski A: **Early detection of breast cancer and the interpretation of results of survival studies/A deteccao precoce do cancer de mama e a interpretacao dos resultados de estudos de sobrevida**. *Ciencia & saude coletiva* 2015, **20**(4):1309-1310.
15. Bednarek AK, Sahin A, Brenner AJ, Johnston DA, Aldaz CM: **Analysis of telomerase activity levels in breast cancer: positive detection at the in situ breast carcinoma stage**. *Clinical cancer research* 1997, **3**(1):11-16.
16. Segal R, Evans W, Johnson D, Smith J, Colletta S, Gayton J, Woodard S, Wells G, Reid R: **Structured exercise improves physical functioning in women with stages I and II breast cancer: results of a randomized controlled trial**. *Journal of clinical oncology* 2001, **19**(3):657-665.
17. Moran MS, Schnitt SJ, Giuliano AE, Harris JR, Khan SA, Horton J, Klimberg S, Chavez-MacGregor M, Freedman G, Houssami N: **Society of Surgical Oncology–American Society for Radiation Oncology consensus guideline on margins for breast-conserving surgery with**

whole-breast irradiation in stages I and II invasive breast cancer. *Annals of surgical oncology* 2014, **21**(3):704-716.
18. Jacquillat C, Weil M, Baillet F, Borel C, Auclerc G, De Maublanc M, Housset M, Forget G, Thill L, Soubrane C: **Results of neoadjuvant chemotherapy and radiation therapy in the breast-conserving treatment of 250 patients with all stages of infiltrative breast cancer**. *Cancer* 1990, **66**(1):119-129.
19. Neuman HB, Morrogh M, Gonen M, Van Zee KJ, Morrow M, King TA: **Stage IV breast cancer in the era of targeted therapy: does surgery of the primary tumor matter?** *Cancer: Interdisciplinary International Journal of the American Cancer Society*

2010, **116**(5):1226-1233.
20. Wang L: **Early diagnosis of breast cancer**. *Sensors* 2017, **17**(7):1572.
21. Pisano ED, Gatsonis C, Hendrick E, Yaffe M, Baum JK, Acharyya S, Conant EF, Fajardo LL, Bassett L, D'Orsi C: **Diagnostic performance of digital versus film mammography for breast-cancer screening**. *New England Journal of Medicine* 2005, **353**(17):1773-1783.
22. Smith S, Taylor CR, Kanevsky E, Povoski SP, Hawley JR: **Long-term safety and efficacy of breast biopsy markers in clinical practice**. *Expert Review of Medical Devices* 2021, **18**(1):121-128.
23. Waks AG, Winer EP: **Breast cancer treatment: a review**. *Jama* 2019, **321**(3):288-300.
24. An KC: **Selective Estrogen Receptor Modulators**. *Asian Spine Journal* 2016, **10**(4):787-791.
25. Fabian C: **The what, why and how of aromatase inhibitors: hormonal agents for treatment and prevention of breast cancer**. *International journal of clinical practice* 2007, **61**(12):2051-2063.
26. Group EBCTC: **Relevance of breast cancer hormone receptors and other factors to the efficacy of adjuvant tamoxifen: patient-level meta-analysis of randomised trials**. *The lancet* 2011, **378**(9793):771-784.
27. Lumachi F, Luisetto G, MM Basso S, Basso U, Brunello A, Camozzi V: **Endocrine therapy of breast cancer**. *Current medicinal chemistry* 2011, **18**(4):513-522.
28. Cakmak H, Rosen MP: **Current clinical approaches to protecting the ovary: GnRH analogues**. In: *Cancer Treatment and the Ovary.* edn.: Elsevier; 2015: 109-132.
29. Bevers TB, Helvie M, Bonaccio E, Calhoun KE, Daly MB, Farrar WB, Garber JE, Gray R, Greenberg CC, Greenup R: **Breast cancer screening and diagnosis, version 3.2018, NCCN clinical practice guidelines in oncology**. *Journal of the National Comprehensive Cancer Network* 2018, **16**(11):1362-1389.
30. Chan A, Moy B, Mansi J, Ejlertsen B, Holmes FA, Chia S, Iwata H, Gnant M, Loibl S, Barrios CH: **Final efficacy results of neratinib in HER2-positive hormone receptor-positive early-stage breast cancer from the phase III ExteNET trial**. *Clinical Breast Cancer* 2021, **21**(1):80-91. e87.
31. Von Minckwitz G, Schneeweiss A, Salat C, Rezai M, Zahm DM, Klare P, Blohmer JU, Tesch H, Khandan F, Jud S: **A randomized phase II trial investigating the addition of carboplatin to neoadjuvant therapy for triple-negative and HER2-positive early breast cancer (GeparSixto)**. In.: American Society of Clinical Oncology; 2013.
32. Bowman KM, Kumthekar P: **Medical management of brain metastases and leptomeningeal disease in patients with breast carcinoma**. *Future Oncology* 2018, **14**(4):391-407.
33. Cardoso F, Bedard PL, Winer EP, Pagani O, Senkus-Konefka E, Fallowfield LJ, Kyriakides S, Costa A, Cufer T, Albain KS: **International guidelines for management of metastatic breast cancer: combination vs sequential single-agent chemotherapy**. *Journal of the National Cancer Institute* 2009, **101**(17):1174-1181.
34. Robson M, Im S-A, Senkus E, Xu B, Domchek SM, Masuda N, Delaloge S, Li W, Tung N, Armstrong A: **Olaparib for metastatic breast cancer in patients with a germline BRCA mutation**. *New England Journal of Medicine* 2017, **377**(6):523-533.
35. Dillekås H, Rogers MS, Straume O: **Are 90% of deaths from cancer caused by metastases?** *Cancer medicine* 2019, **8**(12):5574-5576.

36. Zeeshan R, Mutahir ZJBjobms: **Cancer metastasis-tricks of the trade**. 2017, **17**(3):172.
37. Chambers A, Groom A, MacDonald I: **Dissemination and Growth of Cancer Cells in Metastatic Sites**. *J Rev Cancer* 2002, **2**:563ā.
38. Vogelstein B, Papadopoulos N, Velculescu VE, Zhou S, Diaz LA, Kinzler KWJs: **Cancer genome landscapes**. 2013, **339**(6127):1546-1558.
39. Haslam SZ, Woodward TL: **Host microenvironment in breast cancer development: epithelial-cell–stromal-cell interactions and steroid hormone action in normal and cancerous mammary gland**. *Breast Cancer Research* 2003, **5**(4):208.
40. Price JT, Bonovich MT, Kohn EC, Welch DR, Hershey MS: **The biochemistry of cancer dissemination**. *Critical reviews in biochemistry molecular biology*

1997, **32**(3):175-252.
41. Barinaga M: **Designing therapies that target tumor blood vessels**. *Science* 1997, **275**(5299):482-484.
42. Zetter BR: **Angiogenesis and tumor metastasis**. *Annual review of medicine* 1998, **49**(1):407-424.
43. Wolf K, Wu YI, Liu Y, Geiger J, Tam E, Overall C, Stack MS, Friedl P: **Multi-step pericellular proteolysis controls the transition from individual to collective cancer cell invasion**. *Nature cell biology* 2007, **9**(8):893.
44. Wei SC, Fattet L, Tsai JH, Guo Y, Pai VH, Majeski HE, Chen AC, Sah RL, Taylor SS, Engler AJ: **Matrix stiffness drives epithelial–mesenchymal transition and tumour metastasis through a TWIST1–G3BP2 mechanotransduction pathway**. *Nature cell biology*

2015, **17**(5):678.
45. Spranger S, Gajewski TF: **Mechanisms of tumor cell–intrinsic immune evasion**. *Annual Review of Cancer Biology*

2018, **2**:213-228.
46. Im JH, Fu W, Wang H, Bhatia SK, Hammer DA, Kowalska MA, Muschel RJ: **Coagulation facilitates tumor cell spreading in the pulmonary vasculature during early metastatic colony formation**. *Cancer research* 2004, **64**(23):8613-8619.
47. Hay ED: **An overview of epithelio-mesenchymal transformation**. *Cells Tissues Organs* 1995, **154**(1):8-20.
48. Kalluri R, Neilson EGJTJoci: **Epithelial-mesenchymal transition and its implications for fibrosis**. 2003, **112**(12):1776-1784.
49. Kalluri R, Weinberg RA: **The basics of epithelial-mesenchymal transition**. *J The Journal of clinical investigation* 2009, **119**(6):1420-1428.
50. Zeisberg M, Neilson EGJTJoci: **Biomarkers for epithelial-mesenchymal transitions**. 2009, **119**(6):1429-1437.
51. Okada H, Strutz F, Danoff TM: **Possible mechanisms of renal fibrosis**. In: *Progression of Chronic Renal Diseases: International Symposium, Shizuoka, May 20-23, 1995: 1996*: Karger Medical and Scientific Publishers; 1996: 146.
52. Thiery JP: **Epithelial–mesenchymal transitions in tumour progression**. *J Nature Reviews Cancer* 2002, **2**(6):442.
53. Yang J, Weinberg RA: **Epithelial-mesenchymal transition: at the crossroads of development and tumor metastasis**. *J Developmental cell* 2008, **14**(6):818-829.
54. Singla M, Kumar A, Bal A, Sarkar S, Bhattacharyya S: **Epithelial to mesenchymal transition induces stem cell like phenotype in renal cell carcinoma cells**. *J Cancer cell international* 2018, **18**(1):57.
55. Wang Y, Shi J, Chai K, Ying X, P Zhou B: **The role of snail in EMT and tumorigenesis**. *Current cancer drug targets* 2013, **13**(9):963-972.
56. Nieto MA: **The snail superfamily of zinc-finger transcription factors**. *Nature reviews Molecular cell biology* 2002, **3**(3):155-166.

57. Olmeda D, Moreno-Bueno G, Flores JM, Fabra A, Portillo F, Cano A: **SNAI1 is required for tumor growth and lymph node metastasis of human breast carcinoma MDA-MB-231 cells**. *Cancer research* 2007, **67**(24):11721-11731.
58. Bolós V, Peinado H, Pérez-Moreno MA, Fraga MF, Esteller M, Cano A: **The transcription factor Slug represses E-cadherin expression and induces epithelial to mesenchymal transitions: a comparison with Snail and E47 repressors**. *Journal of cell science* 2003, **116**(3):499-511.
59. Wang Y, Liu J, Ying X, Lin PC, Zhou BP: **Twist-mediated epithelial-mesenchymal transition promotes breast tumor cell invasion via inhibition of hippo pathway**. *Scientific reports* 2016, **6**(1):1-10.
60. Pinho AV, Rooman I, Real FX: **p53-dependent regulation of growth, epithelial-mesenchymal transition and stemness in normal pancreatic epithelial cells**. *Cell cycle* 2011, **10**(8):1312-1321.
61. Tsai JH, Donaher JL, Murphy DA, Chau S, Yang J: **Spatiotemporal regulation of epithelial-mesenchymal transition is essential for squamous cell carcinoma metastasis**. *Cancer cell* 2012, **22**(6):725-736.
62. Eckert MA, Lwin TM, Chang AT, Kim J, Danis E, Ohno-Machado L, Yang J: **Twist1-induced invadopodia formation promotes tumor metastasis**. *Cancer cell* 2011, **19**(3):372-386.
63. Jin-lu M, Su-xia H, Qing Z, Jing Z, Dan Z, Li W, Yi L: **Role of Twist in vasculogenic mimicry formation in hypoxic hepatocellular carcinoma cells in vitro**. *Biochemical and biophysical research communications* 2011, **408**(4):686-691.
64. Zhang P, Sun Y, Ma L: **ZEB1: at the crossroads of epithelial-mesenchymal transition, metastasis and therapy resistance**. *Cell cycle* 2015, **14**(4):481-487.
65. Funahashi J-i, Sekido R, Murai K, Kamachi Y, Kondoh H: **Delta-crystallin enhancer binding protein delta EF1 is a zinc finger-homeodomain protein implicated in postgastrulation embryogenesis**. *Development* 1993, **119**(2):433-446.
66. Hurt EM, Saykally JN, Anose BM, Kalli KR, Sanders MM: **Expression of the ZEB1 (δEF1) transcription factor in human: additional insights**. *Molecular and cellular biochemistry* 2008, **318**(1):89-99.
67. Eger A, Aigner K, Sonderegger S, Dampier B, Oehler S, Schreiber M, Berx G, Cano A, Beug H, Foisner R: **DeltaEF1 is a transcriptional repressor of E-cadherin and regulates epithelial plasticity in breast cancer cells**. *Oncogene* 2005, **24**(14):2375-2385.
68. Zhou Y-M, Cao L, Li B, Zhang R-X, Sui C-J, Yin Z-F, Yang J-M: **Clinicopathological significance of ZEB1 protein in patients with hepatocellular carcinoma**. *Annals of surgical oncology* 2012, **19**(5):1700-1706.
69. Wellner U, Brabletz T, Keck T: **ZEB1 in pancreatic cancer**. *Cancers* 2010, **2**(3):1617-1628.
70. Shen A, Zhang Y, Yang H, Xu R, Huang G: **Overexpression of ZEB1 relates to metastasis and invasion in osteosarcoma**. *Journal of surgical oncology* 2012, **105**(8):830-834.
71. Zhang J, Lu C, Zhang J, Kang J, Cao C, Li M: **Involvement of ZEB1 and E-cadherin in the invasion of lung squamous cell carcinoma**. *Molecular biology reports* 2013, **40**(2):949-956.
72. Zhang G-J, Zhou T, Tian H-P, Liu Z-L, Xia S-S: **High expression of ZEB1 correlates with liver metastasis and poor prognosis in colorectal cancer**. *Oncology letters* 2013, **5**(2):564-568.
73. Aigner K, Dampier B, Descovich L, Mikula M, Sultan A, Schreiber M, Mikulits W, Brabletz T, Strand D, Obrist P: **The transcription factor ZEB1 (δEF1) promotes tumour cell dedifferentiation by repressing master regulators of epithelial polarity**. *Oncogene* 2007, **26**(49):6979-6988.
74. Chaffer CL, Marjanovic ND, Lee T, Bell G, Kleer CG, Reinhardt F, D'Alessio AC, Young RA, Weinberg RA: **Poised chromatin at the ZEB1 promoter enables breast cancer cell plasticity and enhances tumorigenicity**. *cell* 2013, **154**(1):61-74.

75. Zhang P, Wei Y, Wang L, Debeb BG, Yuan Y, Zhang J, Yuan J, Wang M, Chen D, Sun Y: **ATM-mediated stabilization of ZEB1 promotes DNA damage response and radioresistance through CHK1**. *Nature cell biology* 2014, **16**(9):864-875.
76. Arumugam T, Ramachandran V, Fournier KF, Wang H, Marquis L, Abbruzzese JL, Gallick GE, Logsdon CD, McConkey DJ, Choi W: **Epithelial to mesenchymal transition contributes to drug resistance in pancreatic cancer**. *Cancer research* 2009, **69**(14):5820-5828.
77. Yilmaz M, Christofori G: **EMT, the cytoskeleton, and cancer cell invasion**. *Cancer and Metastasis Reviews* 2009, **28**(1):15-33.
78. Schmierer B, Hill CS: **TGFβ–SMAD signal transduction: molecular specificity and functional flexibility**. *Nature reviews Molecular cell biology* 2007, **8**(12):970-982.
79. Heldin C-H, Vanlandewijck M, Moustakas A: **Regulation of EMT by TGFβ in cancer**. *FEBS letters* 2012, **586**(14):1959-1970.
80. Connolly EC, Saunier EF, Quigley D, Luu MT, De Sapio A, Hann B, Yingling JM, Akhurst RJ: **Outgrowth of drug-resistant carcinomas expressing markers of tumor aggression after long-term TβRI/II kinase inhibition with LY2109761**. *Cancer research* 2011, **71**(6):2339-2349.
81. Massagué J: **TGFβ signalling in context**. *Nature reviews Molecular cell biology* 2012, **13**(10):616-630.
82. Shi Y, Massagué J: **Mechanisms of TGF-β signaling from cell membrane to the nucleus**. *cell* 2003, **113**(6):685-700.
83. Wrana JL, Attisano L, Cárcamo J, Zentella A, Doody J, Laiho M, Wang X-F, Massague J: **TGFβ signals through a heteromeric protein kinase receptor complex**. *Cell* 1992, **71**(6):1003-1014.
84. Tsukazaki T, Chiang TA, Davison AF, Attisano L, Wrana JL: **SARA, a FYVE domain protein that recruits Smad2 to the TGFβ receptor**. *Cell* 1998, **95**(6):779-791.
85. Massagué J: **TGFβ in cancer**. *Cell* 2008, **134**(2):215-230.
86. Lu T, Tian L, Han Y, Vogelbaum M, Stark GR: **Dose-dependent cross-talk between the transforming growth factor-β and interleukin-1 signaling pathways**. *Proceedings of the National Academy of Sciences* 2007, **104**(11):4365-4370.
87. Komiya Y, Habas R: **Wnt signal transduction pathways**. *Organogenesis* 2008, **4**(2):68-75.
88. Logan CY, Nusse R: **The Wnt signaling pathway in development and disease**. *Annu Rev Cell Dev Biol* 2004, **20**:781-810.
89. Coelho BP, Fernandes CFdL, Boccacino JM, Souza MCdS, Melo-Escobar MI, Alves RN, Prado MB, Iglesia RP, Cangiano G, Mazzaro GLR: **Multifaceted WNT signaling at the crossroads between epithelial-mesenchymal transition and autophagy in glioblastoma**. *Frontiers in Oncology* 2020, **10**:597743.
90. Ng LF, Kaur P, Bunnag N, Suresh J, Sung ICH, Tan QH, Gruber J, Tolwinski NS: **WNT signaling in disease**. *Cells* 2019, **8**(8):826.
91. Habas R, Dawid IB: **Dishevelled and Wnt signaling: is the nucleus the final frontier?** *Journal of biology* 2005, **4**(1):1-4.
92. He X, Semenov M, Tamai K, Zeng X: **LDL receptor-related proteins 5 and 6 in Wnt/β-catenin signaling: arrows point the way**. 2004.
93. Veeman MT, Axelrod JD, Moon RT: **A second canon: functions and mechanisms of β-catenin-independent Wnt signaling**. *Developmental cell* 2003, **5**(3):367-377.
94. Habas R, Kato Y, He X: **Wnt/Frizzled activation of Rho regulates vertebrate gastrulation and requires a novel Formin homology protein Daam1**. *Cell* 2001, **107**(7):843-854.
95. Kohn AD, Moon RT: **Wnt and calcium signaling: β-catenin-independent pathways**. *Cell calcium* 2005, **38**(3-4):439-446.
96. Fodde R: **The APC gene in colorectal cancer**. *European journal of cancer* 2002, **38**(7):867-871.

97. Lin S-Y, Xia W, Wang JC, Kwong KY, Spohn B, Wen Y, Pestell RG, Hung M-C: **β-catenin, a novel prognostic marker for breast cancer: its roles in cyclin D1 expression and cancer progression**. *Proceedings of the National Academy of Sciences* 2000, **97**(8):4262-4266.
98. Guo Y, Zi X, Koontz Z, Kim A, Xie J, Gorlick R, Holcombe RF, Hoang BH: **Blocking Wnt/LRP5 signaling by a soluble receptor modulates the epithelial to mesenchymal transition and suppresses met and metalloproteinases in osteosarcoma Saos-2 cells**. *Journal of Orthopaedic Research* 2007, **25**(7):964-971.
99. Conacci-Sorrell M, Simcha I, Ben-Yedidia T, Blechman J, Savagner P, Ben-Ze'ev A: **Autoregulation of E-cadherin expression by cadherin–cadherin interactions: the roles of β-catenin signaling, Slug, and MAPK**. *The Journal of cell biology* 2003, **163**(4):847-857.
100. Onder TT, Gupta PB, Mani SA, Yang J, Lander ES, Weinberg RA: **Loss of E-cadherin promotes metastasis via multiple downstream transcriptional pathways**. *Cancer research* 2008, **68**(10):3645-3654.
101. Dissanayake SK, Wade M, Johnson CE, O'Connell MP, Leotlela PD, French AD, Shah KV, Hewitt KJ, Rosenthal DT, Indig FE: **The Wnt5A/protein kinase C pathway mediates motility in melanoma cells via the inhibition of metastasis suppressors and initiation of an epithelial to mesenchymal transition**. *Journal of Biological Chemistry* 2007, **282**(23):17259-17271.
102. Kanzawa M, Semba S, Hara S, Itoh T, Yokozaki H: **WNT5A is a key regulator of the epithelial-mesenchymal transition and cancer stem cell properties in human gastric carcinoma cells**. *Pathobiology* 2013, **80**(5):235-244.
103. Prasad CP, Manchanda M, Mohapatra P, Andersson T: **WNT5A as a therapeutic target in breast cancer**. *Cancer and Metastasis Reviews* 2018, **37**(4):767-778.
104. Angus-Hill ML, Elbert KM, Hidalgo J, Capecchi MR: **T-cell factor 4 functions as a tumor suppressor whose disruption modulates colon cell proliferation and tumorigenesis**. *Proceedings of the National Academy of Sciences* 2011, **108**(12):4914-4919.
105. Cadigan KM, Waterman ML: **TCF/LEFs and Wnt signaling in the nucleus**. *Cold Spring Harbor perspectives in biology* 2012, **4**(11):a007906.
106. Van De Wetering M, Sancho E, Verweij C, De Lau W, Oving I, Hurlstone A, Van Der Horn K, Batlle E, Coudreuse D, Haramis A-P: **The β-catenin/TCF-4 complex imposes a crypt progenitor phenotype on colorectal cancer cells**. *Cell* 2002, **111**(2):241-250.
107. Wang Z, Li Y, Kong D, H Sarkar F: **The role of Notch signaling pathway in epithelial-mesenchymal transition (EMT) during development and tumor aggressiveness**. *Current drug targets* 2010, **11**(6):745-751.
108. Miele L: **Notch signaling**. *Clinical Cancer Research* 2006, **12**(4):1074-1079.
109. Grego-Bessa J, Díez J, Pompa JLdl: **Notch and epithelial-mesenchyme transition in development and tumor progression: another turn of the screw**. *Cell cycle* 2004, **3**(6):716-719.
110. Miele L, Osborne B: **Arbiter of differentiation and death: Notch signaling meets apoptosis**. *Journal of cellular physiology* 1999, **181**(3):393-409.
111. Dickson BC, Mulligan AM, Zhang H, Lockwood G, O'Malley FP, Egan SE, Reedijk M: **High-level JAG1 mRNA and protein predict poor outcome in breast cancer**. *Modern pathology* 2007, **20**(6):685-693.
112. Santagata S, Demichelis F, Riva A, Varambally S, Hofer MD, Kutok JL, Kim R, Tang J, Montie JE, Chinnaiyan AM: **JAGGED1 expression is associated with prostate cancer metastasis and recurrence**. *Cancer research* 2004, **64**(19):6854-6857.
113. Shi T-p, Xu H, Wei J-f, Ai X, Ma X, Wang B-j, Ju Z-h, Zhang G-x, Wang C, Wu Z-q: **Association of low expression of notch-1 and jagged-1 in human papillary bladder cancer and shorter survival**. *The Journal of urology* 2008, **180**(1):361-366.

114. Zhu Y-M, Zhao W-L, Fu J-F, Shi J-Y, Pan Q, Hu J, Gao X-D, Chen B, Li J-M, Xiong S-M: **NOTCH1 mutations in T-cell acute lymphoblastic leukemia: prognostic significance and implication in multifactorial leukemogenesis**. *Clinical cancer research* 2006, **12**(10):3043-3049.
115. Dufraine J, Funahashi Y, Kitajewski J: **Notch signaling regulates tumor angiogenesis by diverse mechanisms**. *Oncogene* 2008, **27**(38):5132-5137.
116. Sahlgren C, Gustafsson MV, Jin S, Poellinger L, Lendahl U: **Notch signaling mediates hypoxia-induced tumor cell migration and invasion**. *Proceedings of the National Academy of Sciences* 2008, **105**(17):6392-6397.
117. Leong KG, Niessen K, Kulic I, Raouf A, Eaves C, Pollet I, Karsan A: **Jagged1-mediated Notch activation induces epithelial-to-mesenchymal transition through Slug-induced repression of E-cadherin**. *The Journal of experimental medicine* 2007, **204**(12):2935-2948.
118. Niimi H, Pardali K, Vanlandewijck M, Heldin C-H, Moustakas A: **Notch signaling is necessary for epithelial growth arrest by TGF-β**. *The Journal of cell biology* 2007, **176**(5):695-707.
119. Micalizzi DS, Farabaugh SM, Ford HL: **Epithelial-mesenchymal transition in cancer: parallels between normal development and tumor progression**. *Journal of mammary gland biology and neoplasia* 2010, **15**(2):117-134.
120. Taube JH, Herschkowitz JI, Komurov K, Zhou AY, Gupta S, Yang J, Hartwell K, Onder TT, Gupta PB, Evans KW: **Core epithelial-to-mesenchymal transition interactome gene-expression signature is associated with claudin-low and metaplastic breast cancer subtypes**. *Proceedings of the National Academy of Sciences* 2010, **107**(35):15449-15454.
121. Peinado H, Marin F, Cubillo E, Stark H-J, Fusenig N, Nieto MA, Cano A: **Snail and E47 repressors of E-cadherin induce distinct invasive and angiogenic properties in vivo**. *Journal of cell science* 2004, **117**(13):2827-2839.
122. Perl A-K, Wilgenbus P, Dahl U, Semb H, Christofori G: **A causal role for E-cadherin in the transition from adenoma to carcinoma**. *Nature* 1998, **392**(6672):190-193.
123. Peinado H, Olmeda D, Cano A: **Snail, Zeb and bHLH factors in tumour progression: an alliance against the epithelial phenotype?** *Nature reviews cancer* 2007, **7**(6):415-428.
124. Mrozik KM, Blaschuk OW, Cheong CM, Zannettino ACW, Vandyke K: **N-cadherin in cancer metastasis, its emerging role in haematological malignancies and potential as a therapeutic target in cancer**. *BMC cancer* 2018, **18**(1):1-16.
125. Hulit J, Suyama K, Chung S, Keren R, Agiostratidou G, Shan W, Dong X, Williams TM, Lisanti MP, Knudsen K: **N-cadherin signaling potentiates mammary tumor metastasis via enhanced extracellular signal-regulated kinase activation**. *Cancer research* 2007, **67**(7):3106-3116.
126. Wu S, Du Y, Beckford J, Alachkar H: **Upregulation of the EMT marker vimentin is associated with poor clinical outcome in acute myeloid leukemia**. *Journal of translational medicine* 2018, **16**(1):1-9.
127. Ni T, Li X-Y, Lu N, An T, Liu Z-P, Fu R, Lv W-C, Zhang Y-W, Xu X-J, Grant Rowe R: **Snail1-dependent p53 repression regulates expansion and activity of tumour-initiating cells in breast cancer**. *Nature cell biology* 2016, **18**(11):1221-1232.
128. Krebs AM, Mitschke J, Lasierra Losada M, Schmalhofer O, Boerries M, Busch H, Boettcher M, Mougiakakos D, Reichardt W, Bronsert P: **The EMT-activator Zeb1 is a key factor for cell plasticity and promotes metastasis in pancreatic cancer**. *Nature cell biology* 2017, **19**(5):518-529.
129. Xu Y, Lee D-K, Feng Z, Xu Y, Bu W, Li Y, Liao L, Xu J: **Breast tumor cell-specific knockout of Twist1 inhibits cancer cell plasticity, dissemination, and lung metastasis in mice**. *Proceedings of the National Academy of Sciences* 2017, **114**(43):11494-11499.
130. Noë V, Fingleton B, Jacobs K, Crawford HC, Vermeulen S, Steelant W, Bruyneel E, Matrisian LM, Mareel M: **Release of an invasion promoter E-cadherin fragment by matrilysin and stromelysin-1**. *Journal of cell science* 2001, **114**(1):111-118.

131. De Las Rivas J, Brozovic A, Izraely S, Casas-Pais A, Witz IP, Figueroa A: **Cancer drug resistance induced by EMT: Novel therapeutic strategies**. *Archives of Toxicology* 2021, **95**(7):2279-2297.
132. Sommers CL, Heckford SE, Skerker JM, Worland P, Torri JA, Thompson EW, Byers SW, Gelmann EP: **Loss of epithelial markers and acquisition of vimentin expression in adriamycin-and vinblastine-resistant human breast cancer cell lines**. *Cancer research* 1992, **52**(19):5190-5197.
133. Huang J, Li H, Ren G: **Epithelial-mesenchymal transition and drug resistance in breast cancer**. *International journal of oncology* 2015, **47**(3):840-848.
134. McConkey DJ, Choi W, Marquis L, Martin F, Williams MB, Shah J, Svatek R, Das A, Adam L, Kamat A: **Role of epithelial-to-mesenchymal transition (EMT) in drug sensitivity and metastasis in bladder cancer**. *Cancer and Metastasis Reviews* 2009, **28**(3):335-344.
135. Fischer KR, Durrans A, Lee S, Sheng J, Li F, Wong ST, Choi H, El Rayes T, Ryu S, Troeger J: **Epithelial-to-mesenchymal transition is not required for lung metastasis but contributes to chemoresistance**. *Nature* 2015, **527**(7579):472-476.
136. Zheng X, Carstens JL, Kim J, Scheible M, Kaye J, Sugimoto H, Wu C-C, LeBleu VS, Kalluri R: **Epithelial-to-mesenchymal transition is dispensable for metastasis but induces chemoresistance in pancreatic cancer**. *Nature* 2015, **527**(7579):525-530.
137. Teicher BA, Holden SA, Ara G, Chen G: **Transforming growth factor-β in in vivo resistance**. *Cancer chemotherapy and pharmacology* 1996, **37**(6):601-609.
138. Li J, Liu H, Yu J, Yu H: **Chemoresistance to doxorubicin induces epithelial-mesenchymal transition via upregulation of transforming growth factor β signaling in HCT116 colon cancer cells**. *Molecular medicine reports* 2015, **12**(1):192-198.
139. Deng J-J, Zhang W, Xu X-M, Zhang F, Tao W-P, Ye J-J, Ge W: **Twist mediates an aggressive phenotype in human colorectal cancer cells**. *International journal of oncology* 2016, **48**(3):1117-1124.
140. Haslehurst AM, Koti M, Dharsee M, Nuin P, Evans K, Geraci J, Childs T, Chen J, Li J, Weberpals J: **EMT transcription factors snail and slug directly contribute to cisplatin resistance in ovarian cancer**. *BMC cancer* 2012, **12**(1):1-10.
141. Siebzehnrubl FA, Silver DJ, Tugertimur B, Deleyrolle LP, Siebzehnrubl D, Sarkisian MR, Devers KG, Yachnis AT, Kupper MD, Neal D: **The ZEB1 pathway links glioblastoma initiation, invasion and chemoresistance**. *EMBO molecular medicine* 2013, **5**(8):1196-1212.
142. Wu Y, Ginther C, Kim J, Mosher N, Chung S, Slamon D, Vadgama JV: **Expression of Wnt3 Activates Wnt/β-Catenin Pathway and Promotes EMT-like Phenotype in Trastuzumab-Resistant HER2-Overexpressing Breast Cancer CellsWnt3 Promotes EMT and Acquired Resistance to Trastuzumab**. *Molecular Cancer Research* 2012, **10**(12):1597-1606.
143. Della Corte CM, Bellevicine C, Vicidomini G, Vitagliano D, Malapelle U, Accardo M, Fabozzi A, Fiorelli A, Fasano M, Papaccio F: **SMO Gene Amplification and Activation of the Hedgehog Pathway as Novel Mechanisms of Resistance to Anti-Epidermal Growth Factor Receptor Drugs in Human Lung CancerRole of the Hedgehog Pathway in EGFR-TKI–Resistant Lung Cancer**. *Clinical cancer research* 2015, **21**(20):4686-4697.
144. Mani SA, Guo W, Liao M-J, Eaton EN, Ayyanan A, Zhou AY, Brooks M, Reinhard F, Zhang CC, Shipitsin M: **The epithelial-mesenchymal transition generates cells with properties of stem cells**. *Cell* 2008, **133**(4):704-715.
145. Gottesman MM, Fojo T, Bates SE: **Multidrug resistance in cancer: role of ATP–dependent transporters**. *Nature reviews cancer* 2002, **2**(1):48-58.
146. Saxena M, Stephens MA, Pathak H, Rangarajan A: **Transcription factors that mediate epithelial–mesenchymal transition lead to multidrug resistance by upregulating ABC transporters**. *Cell death & disease* 2011, **2**(7):e179-e179.

147. Wang N, Westerterp M: **ABC transporters, cholesterol efflux, and implications for cardiovascular diseases**. *Lipid Transfer in Lipoprotein Metabolism and Cardiovascular Disease* 2020:67-83.
148. Cortes VA, Busso D, Maiz A, Arteaga A, Nervi F, Rigotti A: **Physiological and pathological implications of cholesterol**. *Frontiers in bioscience* 2014, **19**:416-428.
149. Zhang J, Li Q, Wu Y, Wang D, Xu L, Zhang Y, Wang S, Wang T, Liu F, Zaky MY: **Cholesterol content in cell membrane maintains surface levels of ErbB2 and confers a therapeutic vulnerability in ErbB2-positive breast cancer**. *Cell Communication and Signaling* 2019, **17**(1):1-12.
150. Silvente-Poirot S, Poirot M: **Cholesterol metabolism and cancer: the good, the bad and the ugly**. *Current opinion in pharmacology* 2012, **6**(12):673-676.
151. Simons K, Toomre D: **Lipid rafts and signal transduction**. *Nature reviews Molecular cell biology* 2000, **1**(1):31-39.
152. Sheng R, Chen Y, Gee HY, Stec E, Melowic HR, Blatner NR, Tun MP, Kim Y, Källberg M, Fujiwara TK: **Cholesterol modulates cell signaling and protein networking by specifically interacting with PDZ domain-containing scaffold proteins**. *Nature communications* 2012, **3**:1249.
153. Berg J, Tymoczko J, Stryer L: **Section 26.4, important derivatives of cholesterol include bile salts and steroid hormones**. *Biochemistry, 5th edn WH Freeman, New York* 2002.
154. Porter JA, Young KE, Beachy PA: **Cholesterol modification of hedgehog signaling proteins in animal development**. *Science* 1996, **274**(5285):255-259.
155. Repa JJ, Mangelsdorf DJ: **The role of orphan nuclear receptors in the regulation of cholesterol homeostasis**. *Annual review of cell and developmental biology* 2000, **16**(1):459-481.
156. Buhaescu I, Izzedine H: **Mevalonate pathway: a review of clinical and therapeutical implications**. *Clinical biochemistry* 2007, **40**(9-10):575-584.
157. Goldstein JL, Brown MS: **Regulation of the mevalonate pathway**. *Nature* 1990, **343**(6257):425.
158. Hinson D, Chambliss K, Toth M, Tanaka R, Gibson K: **Post-translational regulation of mevalonate kinase by intermediates of the cholesterol and nonsterol isoprene biosynthetic pathways**. *Journal of lipid research* 1997, **38**(11):2216-2223.
159. Risley JM: **Cholesterol biosynthesis: Lanosterol to cholesterol**. *Journal of chemical education* 2002, **79**(3):377.
160. Guengerich FP: **Cytochrome p450 and chemical toxicology**. *Chemical research in toxicology* 2007, **21**(1):70-83.
161. Wadhera RK, Steen DL, Khan I, Giugliano RP, Foody JM: **A review of low-density lipoprotein cholesterol, treatment strategies, and its impact on cardiovascular disease morbidity and mortality**. *Journal of clinical lipidology* 2016, **10**(3):472-489.
162. Tosi MR, Tugnoli V: **Cholesteryl esters in malignancy**. *Clinica chimica acta* 2005, **359**(1-2):27-45.
163. Hua X, Wu J, Goldstein JL, Brown MS, Hobbs HH: **Structure of the human gene encoding sterol regulatory element binding protein-1 (SREBF1) and localization of SREBF1 and SREBF2 to chromosomes 17p11. 2 and 22q13**. *Genomics* 1995, **25**(3):667-673.
164. Nelson ER, Chang C-y, McDonnell DP: **Cholesterol and breast cancer pathophysiology**. *Trends in Endocrinology Metabolism* 2014, **25**(12):649-655.
165. Altmann SW, Davis Jr HR, Zhu L-j, Yao X, Hoos LM, Tetzloff G, Iyer SPN, Maguire M, Golovko A, Zeng M: **Niemann-Pick C1 Like 1 protein is critical for intestinal cholesterol absorption**. *Science* 2004, **303**(5661):1201-1204.

166. Zhang J-H, Ge L, Qi W, Zhang L, Miao H-H, Li B-L, Yang M, Song B-L: **The N-terminal domain of NPC1L1 protein binds cholesterol and plays essential roles in cholesterol uptake**. *Journal of Biological Chemistry* 2011, **286**(28):25088-25097.
167. Ge L, Wang J, Qi W, Miao H-H, Cao J, Qu Y-X, Li B-L, Song B-L: **The cholesterol absorption inhibitor ezetimibe acts by blocking the sterol-induced internalization of NPC1L1**. *Cell metabolism* 2008, **7**(6):508-519.
168. Goldstein JL, Brown MS: **The LDL receptor**. *Arteriosclerosis, thrombosis, and vascular biology* 2009, **29**(4):431-438.
169. Luo J, Jiang L, Yang H, Song BL: **Routes and mechanisms of post-endosomal cholesterol trafficking: A story that never ends**. *Traffic* 2017, **18**(4):209-217.
170. Zelcer N, Hong C, Boyadjian R, Tontonoz P: **LXR regulates cholesterol uptake through Idol-dependent ubiquitination of the LDL receptor**. *Science* 2009, **325**(5936):100-104.
171. Lagace TA: **PCSK9 and LDLR degradation: regulatory mechanisms in circulation and in cells**. *Current opinion in lipidology* 2014, **25**(5):387.
172. Miller N: **HDL metabolism and its role in lipid transport**. *European heart journal* 1990, **11**(suppl_H):1-3.
173. Gelissen IC, Harris M, Rye K-A, Quinn C, Brown AJ, Kockx M, Cartland S, Packianathan M, Kritharides L, Jessup W: **ABCA1 and ABCG1 synergize to mediate cholesterol export to apoA-I**. *Arteriosclerosis, thrombosis, and vascular biology* 2006, **26**(3):534-540.
174. Graf GA, Yu L, Li W-P, Gerard R, Tuma PL, Cohen JC, Hobbs HH: **ABCG5 and ABCG8 are obligate heterodimers for protein trafficking and biliary cholesterol excretion**. *Journal of Biological Chemistry* 2003, **278**(48):48275-48282.
175. Zhu M, Zhao X, Chen J, Xu J, Hu G, Guo D, Li Q, Zhang X, Chang CC, Song B: **ACAT1 regulates the dynamics of free cholesterols in plasma membrane which leads to the APP-α-processing alteration**. *Acta biochimica et biophysica Sinica* 2015, **47**(12):951-959.
176. Nguyen TM, Sawyer JK, Kelley KL, Davis MA, Rudel LL: **Cholesterol esterification by ACAT2 is essential for efficient intestinal cholesterol absorption: evidence from thoracic lymph duct cannulation [S]**. *Journal of lipid research* 2012, **53**(1):95-104.
177. Ding X, Zhang W, Li S, Yang H: **The role of cholesterol metabolism in cancer**. *American journal of cancer research* 2019, **9**(2):219.
178. Li C, Yang L, Zhang D, Jiang W: **Systematic review and meta-analysis suggest that dietary cholesterol intake increases risk of breast cancer**. *Nutrition Research* 2016, **36**(7):627-635.
179. Jamnagerwalla J, Howard LE, Allott EH, Vidal AC, Moreira DM, Castro-Santamaria R, Andriole GL, Freeman MR, Freedland SJ: **Serum cholesterol and risk of high-grade prostate cancer: results from the REDUCE study**. *Prostate cancer and prostatic diseases* 2018, **21**(2):252-259.
180. Furberg A-S, Veierød MB, Wilsgaard T, Bernstein L, Thune I: **Serum high-density lipoprotein cholesterol, metabolic profile, and breast cancer risk**. *Journal of the National Cancer Institute* 2004, **96**(15):1152-1160.
181. Wu J, Lei X, Pan X, Zeng X, Li W: **Association between serum lipids and breast cancer risk in premenopausal women: systematic review and meta-analysis**. *Journal of International Medical Research* 2021, **49**(11):03000605211061033.
182. Llaverias G, Danilo C, Mercier I, Daumer K, Capozza F, Williams TM, Sotgia F, Lisanti MP, Frank PG: **Role of cholesterol in the development and progression of breast cancer**. *The American journal of pathology* 2011, **178**(1):402-412.
183. Clendening JW, Pandyra A, Boutros PC, Ghamrasni SE, Khosravi F, Trentin GA, Martirosyan A, Hakem A, Hakem R, Jurisica I: **Dysregulation of the mevalonate pathway promotes transformation**. *Proceedings of the National Academy of Sciences* 2010, **107**(34):15051-15056.
184. Sorrentino G, Ruggeri N, Specchia V, Cordenonsi M, Mano M, Dupont S, Manfrin A, Ingallina E, Sommaggio R, Piazza S: **Metabolic control of YAP and TAZ by the mevalonate pathway**. *Nature cell biology* 2014, **16**(4):357-366.

185. Brown DN, Caffa I, Cirmena G, Piras D, Garuti A, Gallo M, Alberti S, Nencioni A, Ballestrero A, Zoppoli G: **Squalene epoxidase is a bona fide oncogene by amplification with clinical relevance in breast cancer**. *Scientific reports* 2016, **6**(1):1-13.
186. Scully T, Kase N, Gallagher EJ, LeRoith D: **Regulation of low-density lipoprotein receptor expression in triple negative breast cancer by EGFR-MAPK signaling**. *Scientific reports* 2021, **11**(1):1-13.
187. He J, Shin H, Wei X, Kadegowda AKG, Chen R, Xie SK: **NPC1L1 knockout protects against colitis-associated tumorigenesis in mice**. *BMC cancer* 2015, **15**(1):1-9.
188. Smith B, Land H: **Anticancer activity of the cholesterol exporter ABCA1 gene**. *Cell reports* 2012, **2**(3):580-590.
189. Lee BH, Taylor MG, Robinet P, Smith JD, Schweitzer J, Sehayek E, Falzarano SM, Magi-Galluzzi C, Klein EA, Ting AH: **Dysregulation of Cholesterol Homeostasis in Human Prostate Cancer through Loss of ABCA1Loss of ABCA1 Promotes Prostate Cancer**. *Cancer research* 2013, **73**(3):1211-1218.
190. Luchetti G, Sircar R, Kong JH, Nachtergaele S, Sagner A, Byrne EF, Covey DF, Siebold C, Rohatgi R: **Cholesterol activates the G-protein coupled receptor Smoothened to promote Hedgehog signaling**. *Elife* 2016, **5**.
191. Yeganeh B, Wiechec E, Ande SR, Sharma P, Moghadam AR, Post M, Freed DH, Hashemi M, Shojaei S, Zeki AA: **Targeting the mevalonate cascade as a new therapeutic approach in heart disease, cancer and pulmonary disease**. *Pharmacology & therapeutics* 2014, **143**(1):87-110.
192. Nelson ER, Wardell SE, Jasper JS, Park S, Suchindran S, Howe MK, Carver NJ, Pillai RV, Sullivan PM, Sondhi V: **27-Hydroxycholesterol links hypercholesterolemia and breast cancer pathophysiology**. *Science* 2013, **342**(6162):1094-1098.
193. Umetani M, Shaul PW: **27-Hydroxycholesterol: the first identified endogenous SERM**. *Trends in Endocrinology & Metabolism* 2011, **22**(4):130-135.
194. Mast N, Lin JB, Pikuleva IA: **Marketed drugs can inhibit cytochrome P450 27A1, a potential new target for breast cancer adjuvant therapy**. *Molecular pharmacology* 2015, **88**(3):428-436.
195. Simigdala N, Gao Q, Pancholi S, Roberg-Larsen H, Zvelebil M, Ribas R, Folkerd E, Thompson A, Bhamra A, Dowsett M: **Cholesterol biosynthesis pathway as a novel mechanism of resistance to estrogen deprivation in estrogen receptor-positive breast cancer**. *Breast Cancer Research* 2016, **18**(1):58.
196. Bachmeier BE, Iancu CM, Killian PH, Kronski E, Mirisola V, Angelini G, Jochum M, Nerlich AG, Pfeffer U: **Overexpression of the ATP binding cassette gene ABCA1 determines resistance to Curcumin in M14 melanoma cells**. *Molecular cancer* 2009, **8**(1):1-12.
197. Wang W, Lokman NA, Noye TM, Macpherson AM, Oehler MK, Ricciardelli C: **ABCA1 is associated with the development of acquired chemotherapy resistance and predicts poor ovarian cancer outcome**. *Cancer Drug Resistance* 2021, **4**(2):485.
198. Liao X, Song G, Xu Z, Bu Y, Chang F, Jia F, Xiao X, Ren X, Zhang M, Jia Q: **Oxaliplatin resistance is enhanced by saracatinib via upregulation Wnt-ABCG1 signaling in hepatocellular carcinoma**. *BMC cancer* 2020, **20**(1):1-12.
199. Namba Y, Sogawa C, Okusha Y, Kawai H, Itagaki M, Ono K, Murakami J, Aoyama E, Ohyama K, Asaumi J-i: **Depletion of lipid efflux pump ABCG1 triggers the intracellular accumulation of extracellular vesicles and reduces aggregation and tumorigenesis of metastatic cancer cells**. *Frontiers in Oncology* 2018, **8**:376.
200. Wang C-W, Huang C-C, Chou P-H, Chang Y-P, Wei S, Guengerich FP, Chou Y-C, Wang S-F, Lai P-S, Souček P: **7-ketocholesterol and 27-hydroxycholesterol decreased doxorubicin sensitivity in breast cancer cells: estrogenic activity and mTOR pathway**. *Oncotarget* 2017, **8**(39):66033.

201. Shibata M-A, Ito Y, Morimoto J, Otsuki Y: **Lovastatin inhibits tumor growth and lung metastasis in mouse mammary carcinoma model: a p53-independent mitochondrial-mediated apoptotic mechanism**. *Carcinogenesis* 2004, **25**(10):1887-1898.
202. Horiguchi A, Sumitomo M, Asakuma J, Asano T, Asano T, Hayakawa M: **3-hydroxy-3-methylglutaryl-coenzyme a reductase inhibitor, fluvastatin, as a novel agent for prophylaxis of renal cancer metastasis**. *Clinical cancer research* 2004, **10**(24):8648-8655.
203. Taras D, Blanc J-F, Rullier A, Dugot-Senant N, Laurendeau I, Vidaud M, Rosenbaum J: **Pravastatin reduces lung metastasis of rat hepatocellular carcinoma via a coordinated decrease of MMP expression and activity**. *Journal of hepatology* 2007, **46**(1):69-76.
204. Sun X, Essalmani R, Day R, Khatib AM, Seidah NG, Prat A: **Proprotein convertase subtilisin/kexin type 9 deficiency reduces melanoma metastasis in liver**. *Neoplasia* 2012, **14**(12):1122-IN1125.
205. Chen Z, Chen L, Sun B, Liu D, He Y, Qi L, Li G, Han Z, Zhan L, Zhang S: **LDLR inhibition promotes hepatocellular carcinoma proliferation and metastasis by elevating intracellular cholesterol synthesis through the MEK/ERK signaling pathway**. *Molecular metabolism* 2021, **51**:101230.
206. Torres CG, Ramírez ME, Cruz P, Epuñan MJ, Valladares LE, Sierralta WD: **27-hydroxycholesterol induces the transition of MCF7 cells into a mesenchymal phenotype**. *Oncology reports* 2011, **26**(2):389-397.
207. Wu Q, Ishikawa T, Sirianni R, Tang H, McDonald JG, Yuhanna IS, Thompson B, Girard L, Mineo C, Brekken RA: **27-Hydroxycholesterol promotes cell-autonomous, ER-positive breast cancer growth**. *Cell reports* 2013, **5**(3):637-645.
208. Sheng R, Kim H, Lee H, Xin Y, Chen Y, Tian W, Cui Y, Choi J-C, Doh J, Han J-K: **Cholesterol selectively activates canonical Wnt signalling over non-canonical Wnt signalling**. *Nature communications* 2014, **5**(1):1-13.
209. Sezgin E, Azbazdar Y, Ng XW, Teh C, Simons K, Weidinger G, Wohland T, Eggeling C, Ozhan G: **Binding of canonical Wnt ligands to their receptor complexes occurs in ordered plasma membrane environments**. *The FEBS journal* 2017, **284**(15):2513-2526.
210. Wang F, Ma L, Zhang Z, Liu X, Gao H, Zhuang Y, Yang P, Kornmann M, Tian X, Yang Y: **Hedgehog signaling regulates epithelial-mesenchymal transition in pancreatic cancer stem-like cells**. *Journal of Cancer* 2016, **7**(4):408.
211. Ma X, Wang Q, Jiang Y, Xiao Z, Fang X, Chen Y-G: **Lateral diffusion of TGF-β type I receptor studied by single-molecule imaging**. *Biochemical and biophysical research communications* 2007, **356**(1):67-71.
212. Shapira KE, Ehrlich M, Henis YI: **Cholesterol depletion enhances TGF-β Smad signaling by increasing c-Jun expression through a PKR-dependent mechanism**. *Molecular biology of the cell* 2018, **29**(20):2494-2507.
213. Gabitova-Cornell L, Surumbayeva A, Peri S, Franco-Barraza J, Restifo D, Weitz N, Ogier C, Goldman AR, Hartman TR, Francescone R: **Cholesterol pathway inhibition induces TGF-β signaling to promote basal differentiation in pancreatic cancer**. *Cancer Cell* 2020, **38**(4):567-583. e511.
214. Zhao Z, Hao D, Wang L, Li J, Meng Y, Li P, Wang Y, Zhang C, Zhou H, Gardner K: **CtBP promotes metastasis of breast cancer through repressing cholesterol and activating TGF-β signaling**. *Oncogene* 2019, **38**(12):2076-2091.
215. Sirtori CR: **The pharmacology of statins**. *Pharmacological research* 2014, **88**:3-11.
216. Patel M, Kothari C: **Critical review of statins: A bio-analytical perspective for therapeutic drug monitoring**. *TrAC Trends in Analytical Chemistry* 2017, **86**:206-221.
217. Menter DG, Ramsauer VP, Harirforoosh S, Chakraborty K, Yang P, Hsi L, Newman RA, Krishnan K: **Differential effects of pravastatin and simvastatin on the growth of tumor cells from different organ sites**. *PloS one* 2011, **6**(12):e28813.

218. Jiang W, Hu J-W, He X-R, Jin W-L, He X-Y: **Statins: A repurposed drug to fight cancer**. *Journal of Experimental & Clinical Cancer Research* 2021, **40**(1):1-33.
219. Sivaprasad U, Abbas T, Dutta A: **Differential efficacy of 3-hydroxy-3-methylglutaryl CoA reductase inhibitors on the cell cycle of prostate cancer cells**. *Molecular cancer therapeutics* 2006, **5**(9):2310-2316.
220. Denoyelle C, Vasse M, Körner M, Mishal Z, Ganné F, Vannier J-P, Soria J, Soria C: **Cerivastatin, an inhibitor of HMG-CoA reductase, inhibits the signaling pathways involved in the invasiveness and metastatic properties of highly invasive breast cancer cell lines: an in vitro study**. *Carcinogenesis* 2001, **22**(8):1139-1148.
221. Spampanato C, De Maria S, Sarnataro M, Giordano E, Zanfardino M, Baiano S, Cartenì M, Morelli F: **Simvastatin inhibits cancer cell growth by inducing apoptosis correlated to activation of Bax and down-regulation of BCL-2 gene expression**. *International journal of oncology* 2012, **40**(4):935-941.
222. Warita K, Warita T, Beckwitt CH, Schurdak ME, Vazquez A, Wells A, Oltvai ZN: **Statin-induced mevalonate pathway inhibition attenuates the growth of mesenchymal-like cancer cells that lack functional E-cadherin mediated cell cohesion**. *Scientific reports* 2014, **4**(1):1-8.
223. Campbell MJ, Esserman LJ, Zhou Y, Shoemaker M, Lobo M, Borman E, Baehner F, Kumar AS, Adduci K, Marx C: **Breast cancer growth prevention by statins**. *Cancer research* 2006, **66**(17):8707-8714.
224. Cauley JA, McTiernan A, Rodabough RJ, LaCroix A, Bauer DC, Margolis KL, Paskett ED, Vitolins MZ, Furberg CD, Chlebowski RT: **Statin use and breast cancer: prospective results from the Women's Health Initiative**. *Journal of the National Cancer Institute* 2006, **98**(10):700-707.
225. Kodach LL, Jacobs RJ, Voorneveld PW, Wildenberg ME, Verspaget HW, van Wezel T, Morreau H, Hommes DW, Peppelenbosch MP, van den Brink GR: **Statins augment the chemosensitivity of colorectal cancer cells inducing epigenetic reprogramming and reducing colorectal cancer cell 'stemness' via the bone morphogenetic protein pathway**. *Gut* 2011, **60**(11):1544-1553.
226. Auer J, Sinzinger H, Franklin B, Berent R: **Muscle-and skeletal-related side-effects of statins: tip of the iceberg?** *European journal of preventive cardiology* 2016, **23**(1):88-110.
227. Strom BL, Schinnar R, Karlawish J, Hennessy S, Teal V, Bilker WB: **Statin therapy and risk of acute memory impairment**. *JAMA internal medicine* 2015, **175**(8):1399-1405.
228. Bonovas S, Filioussi K, Tsavaris N, Sitaras NM: **Use of statins and breast cancer: a meta-analysis of seven randomized clinical trials and nine observational studies**. *Journal of Clinical Oncology* 2005, **23**(34):8606-8612.
229. Setoguchi S, Glynn RJ, Avorn J, Mogun H, Schneeweiss S: **Statins and the risk of lung, breast, and colorectal cancer in the elderly**. *Circulation* 2007, **115**(1):27-33.
230. Vinogradova Y, Coupland C, Hippisley-Cox J: **Exposure to statins and risk of common cancers: a series of nested case-control studies**. *BMC cancer* 2011, **11**(1):1-12.
231. Bytyçi I, Penson PE, Mikhailidis DP, Wong ND, Hernandez AV, Sahebkar A, Thompson PD, Mazidi M, Rysz J, Pella D: **Prevalence of statin intolerance: a meta-analysis**. *European heart journal* 2022, **43**(34):3213-3223.
232. Farahat MG: **Enhancement of β-cyclodextrin production and fabrication of edible antimicrobial films incorporated with clove essential oil/β-cyclodextrin inclusion complex**. *Microbiology and Biotechnology Letters* 2020, **48**(1):12-23.
233. Crumling MA, King KA, Duncan RK: **Cyclodextrins and iatrogenic hearing loss: new drugs with significant risk**. *Frontiers in cellular neuroscience* 2017, **11**:355.
234. Mahammad S, Parmryd I: **Cholesterol depletion using methyl-β-cyclodextrin**. In: *Methods in Membrane Lipids.* edn.: Springer; 2015: 91-102.
235. Klein U, Gimpl G, Fahrenholz F: **Alteration of the Myometrial Plasma Membrane Cholesterol Content with. beta.-Cyclodextrin Modulates the Binding Affinity of the Oxytocin Receptor**. *Biochemistry* 1995, **34**(42):13784-13793.

236. Rodal SK, Skretting G, Garred Ø, Vilhardt F, Van Deurs B, Sandvig K: **Extraction of cholesterol with methyl-β-cyclodextrin perturbs formation of clathrin-coated endocytic vesicles**. *Molecular biology of the cell* 1999, **10**(4):961-974.
237. Zidovetzki R, Levitan I: **Use of cyclodextrins to manipulate plasma membrane cholesterol content: evidence, misconceptions and control strategies**. *Biochimica et Biophysica Acta (BBA)-Biomembranes* 2007, **1768**(6):1311-1324.
238. Ohno Y, Toshino M, Mohammed AF, Fujiwara Y, Komohara Y, Onodera R, Higashi T, Motoyama K: **Mannose-methyl-β-cyclodextrin suppresses tumor growth by targeting both colon cancer cells and tumor-associated macrophages**. *Carbohydrate Polymers* 2023:120551.
239. Mohammad N, Malvi P, Meena AS, Singh SV, Chaube B, Vannuruswamy G, Kulkarni MJ, Bhat MK: **Cholesterol depletion by methyl-β-cyclodextrin augments tamoxifen induced cell death by enhancing its uptake in melanoma**. *Molecular cancer* 2014, **13**(1):1-13.
240. Upadhyay AK, Singh S, Chhipa RR, Vijayakumar MV, Ajay AK, Bhat MK: **Methyl-β-cyclodextrin enhances the susceptibility of human breast cancer cells to carboplatin and 5-fluorouracil: Involvement of Akt, NF-κB and Bcl-2**. *Toxicology and applied pharmacology* 2006, **216**(2):177-185.
241. Ulloth JE, Almaguel FG, Padilla A, Bu L, Liu J-W, De Leon M: **Characterization of methyl-β-cyclodextrin toxicity in NGF-differentiated PC12 cell death**. *Neurotoxicology* 2007, **28**(3):613-621.
242. Gould S, Scott RC: **2-Hydroxypropyl-β-cyclodextrin (HP-β-CD): A toxicology review**. *Food and Chemical Toxicology* 2005, **43**(10):1451-1459.
243. Zimmer S, Grebe A, Bakke SS, Bode N, Halvorsen B, Ulas T, Skjelland M, De Nardo D, Labzin LI, Kerksiek A: **Cyclodextrin promotes atherosclerosis regression via macrophage reprogramming**. *Science translational medicine* 2016, **8**(333):333ra350-333ra350.
244. Yao J, Ho D, Calingasan NY, Pipalia NH, Lin MT, Beal MF: **Neuroprotection by cyclodextrin in cell and mouse models of Alzheimer disease**. *Journal of Experimental Medicine* 2012, **209**(13):2501-2513.
245. Davidson CD, Ali NF, Micsenyi MC, Stephney G, Renault S, Dobrenis K, Ory DS, Vanier MT, Walkley SU: **Chronic cyclodextrin treatment of murine Niemann-Pick C disease ameliorates neuronal cholesterol and glycosphingolipid storage and disease progression**. *PloS one* 2009, **4**(9):e6951.
246. Megías-Vericat JE, García-Robles AA, Poveda JL: **Use of 2-Hydroxypropyl-Beta-Cyclodextrin for Niemann-Pick Type C Disease**. In: *Cyclodextrin-A Versatile Ingredient.* edn.: IntechOpen; 2017.
247. Jamal MS, Parveen S, Beg MA, Suhail M, Chaudhary AG, Damanhouri GA, Abuzenadah AM, Rehan MJPO: **Anticancer compound plumbagin and its molecular targets: a structural insight into the inhibitory mechanisms using computational approaches**. 2014, **9**(2):e87309.
248. Sagar S, Esau L, Moosa B, Khashab NM, Bajic VB, Kaur MJA-CAiMC: **Cytotoxicity and apoptosis induced by a plumbagin derivative in estrogen positive MCF-7 breast cancer cells**. 2014, **14**(1):170-180.
249. Esau L, Sagar S, Bangarusamy D, Kaur MJG, cancer: **Identification of CETP as a molecular target for estrogen positive breast cancer cell death by cholesterol depleting agents**. 2016, **7**(9-10):309.
250. Du B, Shim JS: **Targeting epithelial–mesenchymal transition (EMT) to overcome drug resistance in cancer**. *Molecules* 2016, **21**(7):965.
251. Abdulla N, Vincent CT, Kaur M: **Mechanistic insights delineating the role of cholesterol in epithelial mesenchymal transition and drug resistance in cancer**. *Frontiers in Cell and Developmental Biology* 2021:3282.

252. Xie L, Law BK, Aakre ME, Edgerton M, Shyr Y, Bhowmick NA, Moses HL: **Transforming growth factor beta-regulated gene expression in a mouse mammary gland epithelial cell line**. *Breast Cancer Research* 2003, **5**(6):1-12.
253. Stine JE, Guo H, Sheng X, Han X, Schointuch MN, Gilliam TP, Gehrig PA, Zhou C, Bae-Jump VL: **The HMG-CoA reductase inhibitor, simvastatin, exhibits anti-metastatic and anti-tumorigenic effects in ovarian cancer**. *Oncotarget* 2016, **7**(1):946.
254. Fox CH, Johnson FB, Whiting J, Roller PP: **Formaldehyde fixation**. *Journal of Histochemistry & Cytochemistry* 1985, **33**(8):845-853.
255. Thavarajah R, Mudimbaimannar VK, Elizabeth J, Rao UK, Ranganathan K: **Chemical and physical basics of routine formaldehyde fixation**. *Journal of oral and maxillofacial pathology: JOMFP* 2012, **16**(3):400.
256. Im K, Mareninov S, Diaz MFP, Yong WH: **An introduction to performing immunofluorescence staining**. *Biobanking: methods and protocols* 2019:299-311.
257. Srokowski E, Woodhouse K: **2.20 Decellularized Scaffolds**. 2017.
258. Maxfield FR, Wüstner D: **Analysis of cholesterol trafficking with fluorescent probes**. In: *Methods in cell biology. Volume 108*, edn.: Elsevier; 2012: 367-393.
259. Qin C, Nagao T, Grosheva I, Maxfield FR, Pierini LM: **Elevated plasma membrane cholesterol content alters macrophage signaling and function**. *Arteriosclerosis, thrombosis, and vascular biology* 2006, **26**(2):372-378.
260. Van Tonder A, Joubert AM, Cromarty AD: **Limitations of the 3-(4, 5-dimethylthiazol-2-yl)-2, 5-diphenyl-2H-tetrazolium bromide (MTT) assay when compared to three commonly used cell enumeration assays**. *BMC research notes* 2015, **8**:1-10.
261. Li LT, Jiang G, Chen Q, Zheng JN: **Ki67 is a promising molecular target in the diagnosis of cancer**. *Molecular medicine reports* 2015, **11**(3):1566-1572.
262. Krycer JR, Brown AJ: **Cholesterol accumulation in prostate cancer: a classic observation from a modern perspective**. *Biochimica et Biophysica Acta (BBA)-Reviews on Cancer* 2013, **1835**(2):219-229.
263. Rodrigues dos Santos C, Domingues G, Matias I, Matos J, Fonseca I, de Almeida JM, Dias S: **LDL-cholesterol signaling induces breast cancer proliferation and invasion**. *Lipids in health and disease* 2014, **13**(1):1-9.
264. Murtola TJ, Visvanathan K, Artama M, Vainio H, Pukkala E: **Statin use and breast cancer survival: a nationwide cohort study from Finland**. *PloS one* 2014, **9**(10):e110231.
265. Ahern TP, Pedersen L, Tarp M, Cronin-Fenton DP, Garne JP, Silliman RA, Sørensen HT, Lash TL: **Statin prescriptions and breast cancer recurrence risk: a Danish nationwide prospective cohort study**. *Journal of the National Cancer Institute* 2011, **103**(19):1461-1468.
266. Baigent C, Blackwell L, Emberson J, Holland L, Reith C, Bhala N, Peto R, Barnes E, Keech A, Simes J: **Efficacy and safety of more intensive lowering of LDL cholesterol: a meta-analysis of data from 170,000 participants in 26 randomised trials**. *Lancet (London, England)* 2010, **376**(9753):1670-1681.
267. Carter P, Uppal H, Chandran S, Bainey K, Potluri R, Algorithm for Comorbidities A, Length of Stay, Unit MR: **3106 Patients with a diagnosis of hyperlipidaemia have a reduced risk of developing breast cancer and lower mortality rates: a large retrospective longitudinal cohort study from the UK ACALM registry**. *European Heart Journal* 2017, **38**(suppl_1):ehx504. 3106.
268. Hao Y, Baker D, Ten Dijke P: **TGF-β-mediated epithelial-mesenchymal transition and cancer metastasis**. *International journal of molecular sciences* 2019, **20**(11):2767.
269. Peinado H, Quintanilla M, Cano A: **Transforming growth factor β-1 induces snail transcription factor in epithelial cell lines: mechanisms for epithelial mesenchymal transitions**. *Journal of Biological Chemistry* 2003, **278**(23):21113-21123.

270. Wang X, Dong B, Zhang K, Ji Z, Cheng C, Zhao H, Sheng Y, Li X, Fan L, Xue W: **E-cadherin bridges cell polarity and spindle orientation to ensure prostate epithelial integrity and prevent carcinogenesis in vivo**. *PLoS genetics* 2018, **14**(8):e1007609.
271. Handschuh G, Candidus S, Luber B, Reich U, Schott C, Oswald S, Becke H, Hutzler P, Birchmeier W, Höfler H: **Tumour-associated E-cadherin mutations alter cellular morphology, decrease cellular adhesion and increase cellular motility**. *Oncogene* 1999, **18**(30):4301-4312.
272. Araki K, Shimura T, Suzuki H, Tsutsumi S, Wada W, Yajima T, Kobayahi T, Kubo N, Kuwano H: **E/N-cadherin switch mediates cancer progression via TGF-β-induced epithelial-to-mesenchymal transition in extrahepatic cholangiocarcinoma**. *British journal of cancer* 2011, **105**(12):1885-1893.
273. Alimperti S, Mirabella T, Bajaj V, Polacheck W, Pirone DM, Duffield J, Eyckmans J, Assoian RK, Chen CS: **Three-dimensional biomimetic vascular model reveals a RhoA, Rac1, and N-cadherin balance in mural cell–endothelial cell-regulated barrier function**. *Proceedings of the National Academy of Sciences* 2017, **114**(33):8758-8763.
274. Tanaka H, Shan W, Phillips GR, Arndt K, Bozdagi O, Shapiro L, Huntley GW, Benson DL, Colman DR: **Molecular modification of N-cadherin in response to synaptic activity**. *Neuron* 2000, **25**(1):93-107.
275. Ramis-Conde I, Chaplain MA, Anderson AR, Drasdo D: **Multi-scale modelling of cancer cell intravasation: the role of cadherins in metastasis**. *Physical biology* 2009, **6**(1):016008.
276. Nieman MT, Prudoff RS, Johnson KR, Wheelock MJ: **N-cadherin promotes motility in human breast cancer cells regardless of their E-cadherin expression**. *The Journal of cell biology* 1999, **147**(3):631-644.
277. Zhang B, Li M, McDonald T, Holyoake TL, Moon RT, Campana D, Shultz L, Bhatia R: **Microenvironmental protection of CML stem and progenitor cells from tyrosine kinase inhibitors through N-cadherin and Wnt–β-catenin signaling**. *Blood, The Journal of the American Society of Hematology* 2013, **121**(10):1824-1838.
278. Usman S, Waseem NH, Nguyen TKN, Mohsin S, Jamal A, Teh M-T, Waseem A: **Vimentin is at the heart of epithelial mesenchymal transition (EMT) mediated metastasis**. *Cancers* 2021, **13**(19):4985.
279. Sommers CL, Walker-Jones D, Heckford SE, Worland P, Valverius E, Clark R, McCormick F, Stampfer M, Abularach S, Gelmann EP: **Vimentin rather than keratin expression in some hormone-independent breast cancer cell lines and in oncogene-transformed mammary epithelial cells**. *Cancer research* 1989, **49**(15):4258-4263.
280. Liu C-Y, Lin H-H, Tang M-J, Wang Y-K: **Vimentin contributes to epithelial-mesenchymal transition cancer cell mechanics by mediating cytoskeletal organization and focal adhesion maturation**. *Oncotarget* 2015, **6**(18):15966.
281. Costigliola N, Ding L, Burckhardt CJ, Han SJ, Gutierrez E, Mota A, Groisman A, Mitchison TJ, Danuser G: **Vimentin fibers orient traction stress**. *Proceedings of the National Academy of Sciences* 2017, **114**(20):5195-5200.
282. Wu Y, Zhang X, Salmon M, Lin X, Zehner ZE: **TGFβ1 regulation of vimentin gene expression during differentiation of the C2C12 skeletal myogenic cell line requires Smads, AP-1 and Sp1 family members**. *Biochimica et Biophysica Acta (BBA)-Molecular Cell Research* 2007, **1773**(3):427-439.
283. Gilles C, Polette M, Mestdagt M, Nawrocki-Raby B, Ruggeri P, Birembaut P, Foidart J-M: **Transactivation of vimentin by β-catenin in human breast cancer cells**. *Cancer research* 2003, **63**(10):2658-2664.
284. Meng J, Chen S, Han J-X, Qian B, Wang X-R, Zhong W-L, Qin Y, Zhang H, Gao W-F, Lei Y-Y: **Twist1 Regulates Vimentin through Cul2 Circular RNA to Promote EMT in Hepatocellular CarcinomaTwist1 Regulates Vimentin through circRNA-Cul2 in HCC**. *Cancer research* 2018, **78**(15):4150-4162.

285. Messica Y, Laser-Azogui A, Volberg T, Elisha Y, Lysakovskaia K, Eils R, Gladilin E, Geiger B, Beck R: **The role of vimentin in regulating cell invasive migration in dense cultures of breast carcinoma cells**. *Nano letters* 2017, **17**(11):6941-6948.
286. Virtakoivu R, Mai A, Mattila E, De Franceschi N, Imanishi SY, Corthals G, Kaukonen R, Saari M, Cheng F, Torvaldson E: **Vimentin–ERK Signaling Uncouples Slug Gene Regulatory FunctionSlug Phosphorylation Induces Vimentin**. *Cancer research* 2015, **75**(11):2349-2362.
287. Joseph JV, Conroy S, Tomar T, Eggens-Meijer E, Bhat K, Copray S, Walenkamp AM, Boddeke E, Balasubramanyian V, Wagemakers M: **TGF-β is an inducer of ZEB1-dependent mesenchymal transdifferentiation in glioblastoma that is associated with tumor invasion**. *Cell death & disease* 2014, **5**(10):e1443-e1443.
288. Birts CN, Harding R, Soosaipillai G, Halder T, Azim-Araghi A, Darley M, Cutress RI, Bateman AC, Blaydes JP: **Expression of CtBP family protein isoforms in breast cancer and their role in chemoresistance**. *Biology of the Cell* 2011, **103**(1):1-19.
289. Di L-J, Byun JS, Wong MM, Wakano C, Taylor T, Bilke S, Baek S, Hunter K, Yang H, Lee M: **Genome-wide profiles of CtBP link metabolism with genome stability and epithelial reprogramming in breast cancer**. *Nature communications* 2013, **4**(1):1449.
290. Zheng X, Song T, Dou C, Jia Y, Liu Q: **CtBP2 is an independent prognostic marker that promotes GLI1 induced epithelial-mesenchymal transition in hepatocellular carcinoma**. *Oncotarget* 2015, **6**(6):3752.
291. Chinnadurai G: **The transcriptional corepressor CtBP: a foe of multiple tumor suppressors**. *Cancer research* 2009, **69**(3):731-734.
292. Zhang Y, Alexander PB, Wang X-F: **TGF-β family signaling in the control of cell proliferation and survival**. *Cold Spring Harbor perspectives in biology* 2017, **9**(4):a022145.
293. Azar R, Alard A, Susini C, Bousquet C, Pyronnet S: **4E-BP1 is a target of Smad4 essential for TGFβ-mediated inhibition of cell proliferation**. *The EMBO journal* 2009, **28**(22):3514-3522.
294. Baghdassarian N, Ffrench M: **Cyclin-dependent kinase inhibitors (CKIs) and hematological malignancies**. *Hematology and cell therapy* 1996, **38**:313-323.
295. Miller I, Min M, Yang C, Tian C, Gookin S, Carter D, Spencer SL: **Ki67 is a graded rather than a binary marker of proliferation versus quiescence**. *Cell reports* 2018, **24**(5):1105-1112. e1105.
296. Nieto MA, Huang RY-J, Jackson RA, Thiery JP: **EMT: 2016**. *Cell* 2016, **166**(1):21-45.
297. Jolly MK, Ware KE, Gilja S, Somarelli JA, Levine H: **EMT and MET: necessary or permissive for metastasis?** *Molecular oncology* 2017, **11**(7):755-769.
298. Aulas A, Liberatoscioli ML, Finetti P, Cabaud O, Birnbaum DJ, Birnbaum D, Bertucci F, Mamessier E: **Epithelial-to-mesenchymal transition lowers the cholesterol pathway, wich influences colon tumors differentiation**. *medRxiv* 2021:2021.2010. 2013.21264887.
299. Jiang S, Wang X, Song D, Liu X, Gu Y, Xu Z, Wang X, Zhang X, Ye Q, Tong Z: **Cholesterol induces epithelial-to-mesenchymal transition of prostate cancer cells by suppressing degradation of EGFR through APMAP**. *Cancer research* 2019, **79**(12):3063-3075.
300. Chen Y-G: **Endocytic regulation of TGF-β signaling**. *Cell research* 2009, **19**(1):58-70.
301. Warita K, Ishikawa T, Sugiura A, Tashiro J, Shimakura H, Hosaka YZ, Ohta K-i, Warita T, Oltvai ZN: **Concomitant attenuation of HMGCR expression and activity enhances the growth inhibitory effect of atorvastatin on TGF-β-treated epithelial cancer cells**. *Scientific reports* 2021, **11**(1):1-11.
302. Kim JH, Kim CN, Kang DW: **Squalene epoxidase correlates E-cadherin expression and overall survival in colorectal cancer patients: the impact on prognosis and correlation to clinicopathologic features**. *Journal of Clinical Medicine* 2019, **8**(5):632.
303. Jiao K, Zhen J, Wu M, Teng M, Yang K, Zhou Q, Hu C, Zhou M, Li Y, Li Z: **27-Hydroxycholesterol-induced EndMT acts via STAT3 signaling to promote breast cancer cell migration by altering the tumor microenvironment**. *Cancer Biology & Medicine* 2020, **17**(1):88.

304. Matsuo M: **ABCA1 and ABCG1 as potential therapeutic targets for the prevention of atherosclerosis**. *Journal of Pharmacological Sciences* 2022, **148**(2):197-203.
305. Prijic S, Chang JT: **ABCA1 expression is upregulated in an EMT in breast cancer cell lines via MYC-mediated de-repression of its proximal Ebox element**. *Biomedicines* 2022, **10**(3):581.
306. Revilla G, Pons MdP, Baila-Rueda L, García-León A, Santos D, Cenarro A, Magalhaes M, Blanco R, Moral A, Ignacio Pérez J: **Cholesterol and 27-hydroxycholesterol promote thyroid carcinoma aggressiveness**. *Scientific Reports* 2019, **9**(1):10260.
307. Özmen HK, Askın S: **Lecithin: cholesterol acyltransferase and Na+-K+-ATPase activity in patients with breast cancer**. *Journal of breast cancer* 2013, **16**(2):159-163.
308. Czarnecka H, Yokoyama S: **Regulation of Cellular Cholesterol Efflux by Lecithin: Cholesterol Acyltransferase Reaction through Nonspecific Lipid Exchange (∗)**. *Journal of Biological Chemistry* 1996, **271**(4):2023-2028.
309. Caliceti C, Zambonin L, Prata C, Vieceli Dalla Sega F, Hakim G, Hrelia S, Fiorentini D: **Effect of plasma membrane cholesterol depletion on glucose transport regulation in leukemia cells**. 2012.
310. Han J, Zhang L, Guo H, Wysham WZ, Roque DR, Willson AK, Sheng X, Zhou C, Bae-Jump VL: **Glucose promotes cell proliferation, glucose uptake and invasion in endometrial cancer cells via AMPK/mTOR/S6 and MAPK signaling**. *Gynecologic oncology* 2015, **138**(3):668-675.
311. Oh S, Kim H, Nam K, Shin I: **Glut1 promotes cell proliferation, migration and invasion by regulating epidermal growth factor receptor and integrin signaling in triple-negative breast cancer cells**. *BMB reports* 2017, **50**(3):132.
312. Murai T, Maruyama Y, Mio K, Nishiyama H, Suga M, Sato C: **Low cholesterol triggers membrane microdomain-dependent CD44 shedding and suppresses tumor cell migration**. *Journal of Biological Chemistry* 2011, **286**(3):1999-2007.
313. Collisson EA, Kleer C, Wu M, De A, Gambhir SS, Merajver SD, Kolodney MS: **Atorvastatin prevents RhoC isoprenylation, invasion, and metastasis in human melanoma cells**. *Molecular cancer therapeutics* 2003, **2**(10):941-948.
314. Brown M, Hart C, Tawadros T, Ramani V, Sangar V, Lau M, Clarke N: **The differential effects of statins on the metastatic behaviour of prostate cancer**. *British journal of cancer* 2012, **106**(10):1689-1696.
315. Farina HG, Bublik DR, Alonso DF, Gomez DE: **Lovastatin alters cytoskeleton organization and inhibits experimental metastasis of mammary carcinoma cells**. *Clinical & experimental metastasis* 2002, **19**:551-560.
316. Canel M, Serrels A, Frame MC, Brunton VG: **E-cadherin–integrin crosstalk in cancer invasion and metastasis**. *Journal of cell science* 2013, **126**(2):393-401.
317. McInroy L, Määttä A: **Down-regulation of vimentin expression inhibits carcinoma cell migration and adhesion**. *Biochemical and biophysical research communications* 2007, **360**(1):109-114.
318. Mendez MG, Kojima S-I, Goldman RD: **Vimentin induces changes in cell shape, motility, and adhesion during the epithelial to mesenchymal transition**. *The FASEB Journal* 2010, **24**(6):1838.
319. Cho HJ, Baek KE, Saika S, Jeong M-J, Yoo J: **Snail is required for transforming growth factor-β-induced epithelial–mesenchymal transition by activating PI3 kinase/Akt signal pathway**. *Biochemical and biophysical research communications* 2007, **353**(2):337-343.
320. Steck TL, Lange Y: **Cell cholesterol homeostasis: mediation by active cholesterol**. *Trends in cell biology* 2010, **20**(11):680-687.
321. Shen Z, Zhu D, Liu J, Chen J, Liu Y, Hu C, Li Z, Li Y: **27-Hydroxycholesterol induces invasion and migration of breast cancer cells by increasing MMP9 and generating EMT through activation of STAT-3**. *Environmental toxicology and pharmacology* 2017, **51**:1-8.

322. Zhan J, Wang P, Li S, Song J, He H, Wang Y, Liu Z, Wang F, Bai H, Fang W: **HOXB13 networking with ABCG1/EZH2/Slug mediates metastasis and confers resistance to cisplatin in lung adenocarcinoma patients**. *Theranostics* 2019, **9**(7):2084.
323. Taulet N, Comunale F, Favard C, Charrasse S, Bodin S, Gauthier-Rouvière C: **N-cadherin/p120 catenin association at cell-cell contacts occurs in cholesterol-rich membrane domains and is required for RhoA activation and myogenesis**. *Journal of Biological Chemistry* 2009, **284**(34):23137-23145.
324. Zhao Y, He L, Wang T, Zhu L, Yan N: **2-Hydroxypropyl-β-cyclodextrin regulates the epithelial to mesenchymal transition in breast cancer cells by modulating cholesterol homeostasis and endoplasmic reticulum stress**. *Metabolites* 2021, **11**(8):562.
325. Zampelas A, Magriplis E: **New insights into cholesterol functions: a friend or an enemy?** In., vol. 11: MDPI; 2019: 1645.
326. Li X, Wu JB, Li Q, Shigemura K, Chung LW, Huang W-C: **SREBP-2 promotes stem cell-like properties and metastasis by transcriptional activation of c-Myc in prostate cancer**. *Oncotarget* 2016, **7**(11):12869.
327. Wang K, Xu T, Ruan H, Xiao H, Liu J, Song Z, Cao Q, Bao L, Liu D, Wang C: **LXRα promotes cell metastasis by regulating the NLRP3 inflammasome in renal cell carcinoma**. *Cell death & disease* 2019, **10**(3):159.

SUPPLEMENTARY MATERIAL

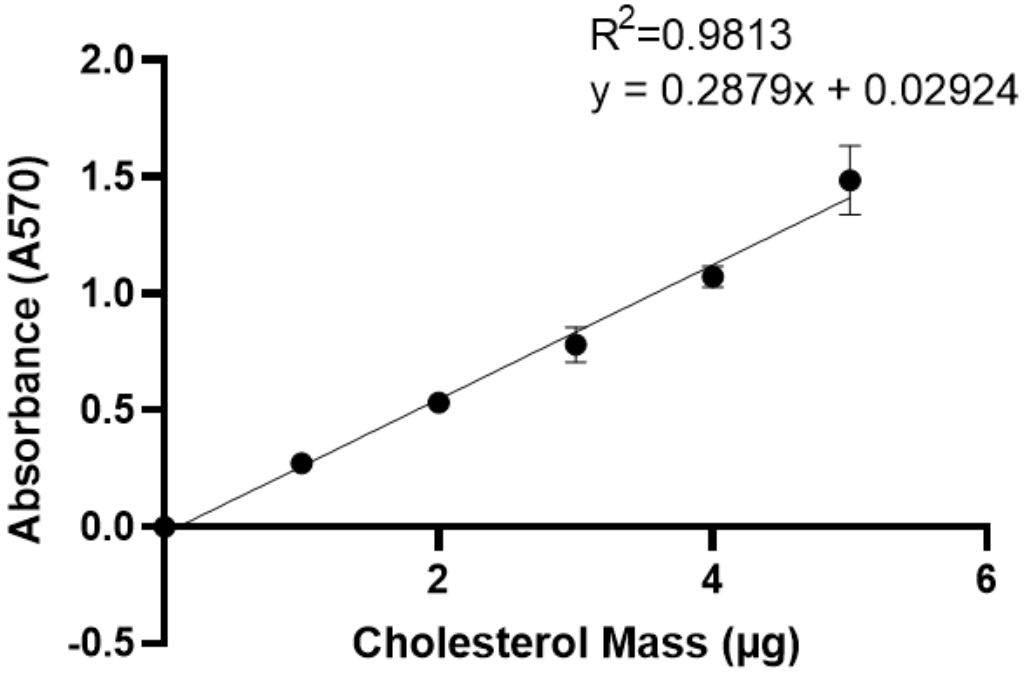

Figure S1: Cholesterol assay standard curve. Standard curve based on the absorbance of cholesterol standards of known mass at 570 nm, where y = 0.2879x + 0.02924 and R^2 = 0.9813. Data shown represents mean ± standard deviation; n=3

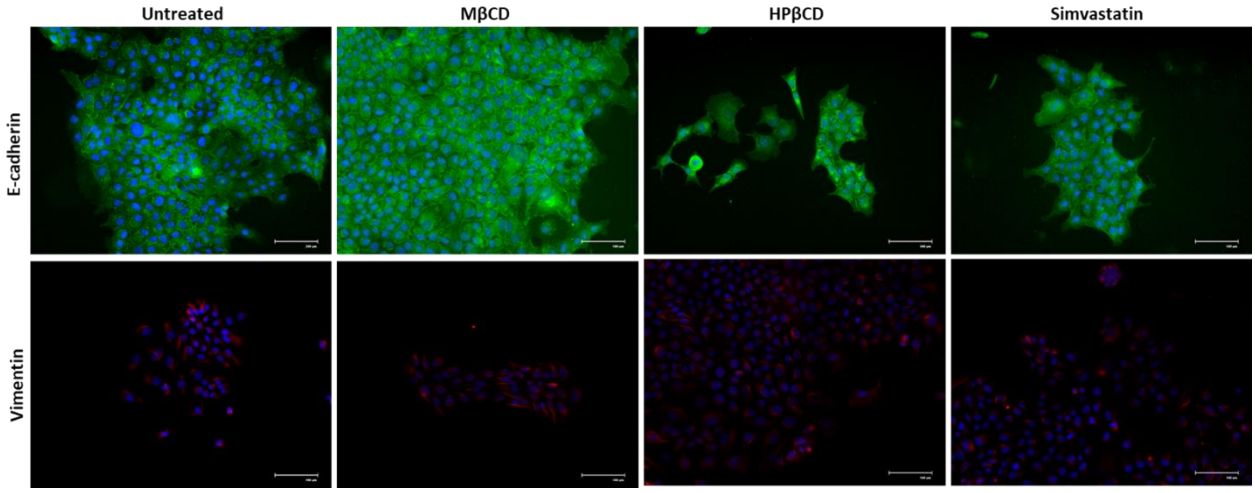

Figure S1: Changes in E-cadherin and Vimentin fluorescence in response to cholesterol depletion in NMuMG cells pre-EMT. (a) Representative micrograph images showing fluorescent labelling of E-cadherin and Vimentin following treatment with 1 mM MβCD, 10 mM HPβCD, and 10 μM simvastatin for 2 hours in NMuMG cells pre-EMT. E-cadherin staining is depicted in green with nuclei stained blue with DAPI. Vimentin staining is depicted in red with nuclei stained blue with DAPI. The scale bar represents 100 μm. Micrographs were generated using the Floid™ Cell Imaging System